

**BIOTRIBOLOGY : ARTICULAR CARTILAGE
FRICTION, WEAR, AND LUBRICATION**

by

Matthew O. Schroeder

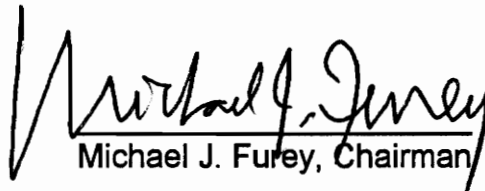
Thesis submitted to the Faculty of
Virginia Polytechnic Institute and State University
in partial fulfillment of the requirements for the degree of

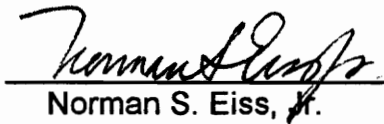
MASTER OF SCIENCE

in

Mechanical Engineering

APPROVED:


Michael J. Furey, Chairman


Norman S. Eiss, Jr.


Hugo P. Veit

July 1995

Blacksburg, Virginia

C.2

LD
5655
V855
1995
S376
C.2

BIOTRIBOLOGY : ARTICULAR CARTILAGE FRICTION, WEAR, AND LUBRICATION

by
Matthew O. Schroeder
Michael J. Furey, Chairman
(Mechanical Engineering Department)

(ABSTRACT)

This study developed, explored, and refined techniques for the *in vitro* study of cartilage-on-cartilage friction, deformation, and wear. Preliminary results of *in vitro* cartilage-on-cartilage experiments with emphasis on wear and biochemistry are presented. Cartilage-bone specimens were obtained from the stifle joints of steers from a separate controlled study. The load, sliding speed, and traverse of the lower specimens were held constant as lubricant and test length were varied. Lubricants tested consisted of a phosphate buffered saline solution, bovine serum, and bovine synovial fluid.

Synovial fluid as a lubricant produced the least amount of damage to the cartilage. Serum produced more wear and damage than synovial fluid, but less than buffered saline (which produced the most damage). Three-hour tests produced more wear than one-hour tests, with severe damage to the lower plug in several of the three-hour tests.

Analysis of the results was possible through: data acquisition of normal load, tangential load, and LVDT displacement; photomacrographs; ESEM and SEM surface studies; stained cross-sectional slides of cartilage; and hydroxyproline analysis of cartilage wear.

Detailed procedures and discussion of results are presented along with recommended changes for future biotribology research.

ACKNOWLEDGMENTS

I am indebted to many people for their help and support during my work on this project at Virginia Tech. I would especially like to thank Dr. Michael J. Furey who served as my advisor. He interested me in the fascinating topic of biotribology and provided guidance, support, advice, and direction throughout the entire project. Thanks also to Dr. Norman Eiss, Jr. and Dr. Hugo Veit for serving on my graduate committee. Without the help of Dr. Veit in collecting specimens and his insightful discussions, this project could not have been completed.

I extend my sincere thanks to the Office of Naval Research for providing my graduate funding. Without this fellowship I would not have been able to continue my education.

I also give my thanks to Dr. E. T. Kornegay for his support at several meetings and Dr. E. M. Gregory for all of the time spent in meetings and helping me learn hydroxyproline analysis. This research could not have been carried out without the use of Dr. Gregory's biochemistry lab. Several others I would like to thank include: Ms. Heather Hughes for her tremendous help with the literature search, specimen preparation, and microscopy work (both optical and SEM); Mr. Mark Freeman for his assistance in designing new machine components, and his

help in collecting test specimens; Mr. Michael Owellen for his aid with the computer data acquisition system; Ms. Amy Diegleman for her help in learning biochemistry and biochemical techniques; the Mechanical Engineering machine shop for all of the work on machine parts and cutters; Mr. Ben Poe for his support with computer problems; and Ms. June Mullins, Ms. Kathy Hayman, Ms. Virginia Viers, and Ms. Traci Sachs for their help with the SEM and cross-sectional slide preparation.

I also thank the tribology students Mr. Ben Tritt, Mr. Doug Patterson, Mr. Mark Freeman and Mr. Ed Lee for their friendship and support over the last two years.

My final thanks goes to God, my parents, and Ms. Melanie Thompson. Without their loving support and encouragement I could never have completed this project.

TABLE OF CONTENTS

ABSTRACT	ii
ACKNOWLEDGMENTS	iii
TABLE OF CONTENTS	v
LIST OF FIGURES	viii
LIST OF TABLES	xiv
1. INTRODUCTION	1
1.1 Rationale	1
1.2 Objectives	3
2. LITERATURE REVIEW	7
2.1 Synovial Joints	7
2.2 Articular Cartilage Lubrication	12
2.3 Cartilage Wear	14
2.4 Cartilage Disease and Damage	19
3. EXPERIMENTAL TECHNIQUE	26
3.1 Cartilage Testing Device	26
3.2 Test Materials Acquisition	29
3.3 Lubricants	32
3.4 Procedure for <i>In Vitro</i> Cartilage-on-Cartilage Tests	33
3.5 Measurements and Observations	34
3.5.1 Data Acquisition	35
3.5.2 Examination of Cartilage Specimens	35
3.5.3 Analysis of Fluid	38

4.	RESULTS	41
4.1	Effects of Fluid Composition on Friction and Vertical Displacement	42
4.1.1	Saline Solution Tests.	42
4.1.2	Serum Tests.	48
4.1.3	Synovial Fluid Tests.	57
4.2	Cartilage Wear as Determined from Hydroxyproline Analysis	67
4.3	ESEM and SEM Results	70
4.4	Optical Microscope Findings.	78
4.4.1	Photomacrography.	78
4.4.2	Stained Slides	84
5.	DISCUSSION	97
5.1	Overview of Results.	97
5.2	Analytical Techniques.	108
5.2.1	Computer Data Acquisition	109
5.2.2	Hydroxyproline Analysis of Cartilage Wear.	111
5.2.3	Microscopic Surface Analysis	111
5.2.4	Slides of Cartilage Cross Sections	112
5.3	Wear and Damage.	113
5.4	Summary	114
6.	CONCLUSIONS	116
7.	RECOMMENDATIONS.	120
	REFERENCES	124

APPENDICES 128

 APPENDIX A Modifications Designed for Cartilage Testing Machine 128

 APPENDIX B BASIC Program Used in All Wear Tests. 134

 APPENDIX C Calibration of Instrumentation. 136

 APPENDIX D Listing of All Tests, Stored Joints, and Synovial Fluid . 140

 APPENDIX E Hydroxyproline Assay Results of Test Washings142

VITA 143

LIST OF FIGURES

Fig. 1.1	Overall Plan of Cartilage-on-Cartilage Research	6
Fig. 2.1	Simplified Synovial Joint	7
Fig. 2.2	Proteoglycan Subunit	9
Fig. 2.3	Proteoglycan Aggregate	9
Fig. 2.4	Articular Cartilage Zones	11
Fig. 2.5	Possible Osteoarthritis and Tribological Connections	20
Fig. 3.1	Diagram of Cartilage-on-Cartilage Test Device	26
Fig. 3.2	Microscopic Analysis of Surface and Subsurface Damage.	36
Fig. 3.3	Typical Hydroxyproline Standard Curve Showing Linearity	40
Fig. 4.1	Tangential Force at the Start of a Three-Hour Saline Test (test 18)	43
Fig. 4.2	Tangential Force at the End of a Three-Hour Saline Test (test 18)	43
Fig. 4.3	LVDT Displacement at the Start of a Three-Hour Saline Test (test 18)	44
Fig. 4.4	LVDT Displacement at the End of a Three-Hour Saline Test (test 18)	44
Fig. 4.5	Coefficient of Friction at the Start of a Three-Hour Saline Test (test 18)	45
Fig. 4.6	Coefficient of Friction at the End of a Three-Hour Saline Test (test 18)	45
Fig. 4.7	Average Maximum Coefficient of Friction for Buffered Saline Tests	47
Fig. 4.8	Tangential Force at the Start of a Low Damage Three-Hour Serum Test (test 17)	49

Fig. 4.9	Tangential Force at the End of a Low Damage Three-Hour Serum Test (test 17)	49
Fig. 4.10	Displacement at the Start of a Low Damage Three-Hour Serum Test (test 17)	50
Fig. 4.11	Displacement at the End of a Low Damage Three-Hour Serum Test (test 17)	50
Fig. 4.12	Coefficient of Friction at the Start of a Low Damage Three-Hour Serum Test (test 17)	51
Fig. 4.13	Coefficient of Friction at the End of a Low Damage Three-Hour Serum Test (test 17)	51
Fig. 4.14	Tangential Force Recorded at the Start of a High Damage Three-Hour Serum Test (test 16)	52
Fig. 4.15	Tangential Force Recorded at the End of a High Damage Three-Hour Serum Test (test 16)	52
Fig. 4.16	Displacement at the Start of a High Damage Three-Hour Serum Test (test 16)	53
Fig. 4.17	Displacement at the End of a High Damage Three-Hour Serum Test (test 16)	53
Fig. 4.18	Coefficient of Friction at the Start of a High Damage Three-Hour Serum Test (test 16)	54
Fig. 4.19	Coefficient of Friction at the End of a High Damage Three-Hour Serum Test (test 16)	54
Fig. 4.20	Average Maximum Coefficient of Friction for Serum Tests	56
Fig. 4.21	Tangential Force at the Start of a Low Wear Three-Hour Synovial Fluid Test (test 14).	58
Fig. 4.22	Tangential Force at the End of a Low Wear Three-Hour Synovial Fluid Test (test 14)	58
Fig. 4.23	LVDT Displacement at the Start of a Low Wear Three-Hour Synovial Fluid Test (test 14)	59

LIST OF FIGURES

Fig. 4.24	LVDT Displacement at the End of a Low Wear Three-Hour Synovial Fluid Test (test 14)	59
Fig. 4.25	Coefficient of Friction at the Start of a Low Wear Three-Hour Synovial Fluid Test (test 14)	60
Fig. 4.26	Coefficient of Friction at the End of a Low Wear Three-Hour Synovial Fluid Test (test 14)	60
Fig. 4.27	Tangential Force at the Start of a High Wear Three-Hour Synovial Fluid Test (test 15)	61
Fig. 4.28	Tangential Force at the End of a High Wear Three-Hour Synovial Fluid Test (test 15)	61
Fig. 4.29	LVDT Displacement at the Start of a High Wear Three-Hour Synovial Fluid Test (test 15)	63
Fig. 4.30	LVDT Displacement at the End of a High Wear Three-Hour Synovial Fluid Test (test 15)	63
Fig. 4.31	Coefficient of Friction at the Start of a High Wear Three-Hour Synovial Fluid Test (test 15)	64
Fig. 4.32	Coefficient of Friction at the End of a High Wear Three-Hour Synovial Fluid Test (test 15)	64
Fig. 4.33	Average Maximum Coefficient of Friction for Synovial Fluid Tests.	65
Fig. 4.34	Measurement of Cartilage Wear in One-Hour Tests	68
Fig. 4.35	Measurement of Cartilage Wear in Three-Hour Tests	69
Fig. 4.36	ESEM Photograph of an Unworn Surface Showing Cells (300X magnification)	71
Fig. 4.37	SEM Photograph of an Unworn Surface Showing Cells (300X magnification).	72
Fig. 4.38	SEM Photograph of a Top Plug from a Three-Hour Saline Test (test 9; 20X magnification)	73
Fig. 4.39	SEM Photograph of a Top Plug from a Three-Hour Serum Test (test 16; 20X magnification).	74

LIST OF FIGURES

Fig. 4.40	SEM Photograph of a Top Plug from a Three-Hour Serum Test (test 16; 150X magnification)	75
Fig. 4.41	SEM Photograph of a Top Plug from a Three-Hour Serum Test (test 16; 300X magnification)	76
Fig. 4.42	SEM Photograph of a Top Plug from the Three-Hour High Wear Synovial Fluid Test (test 15; 20X magnification)	77
Fig. 4.43	Photomacrograph of the Top Plug from a Three-Hour Saline Test (test 9; 16.25X magnification)	79
Fig. 4.44	Photomacrograph of the Top Plug from a Three-Hour Serum Test (test 17; 16.25X magnification)	80
Fig. 4.45	Photomacrograph of the Bottom Plug from a Three-Hour Saline Test (test 18; 16.25X magnification)	81
Fig. 4.46	Photomacrograph of the Bottom Plug from a One-Hour Synovial Fluid Test (test 10; 16.25X magnification).	82
Fig. 4.47	Photomacrograph of the Bottom Plug from a Three-Hour High Wear Synovial Fluid Test (test 15; 32.25X magnification).	83
Fig. 4.48	H&E Stained Section of Cartilage from Unworn Cartilage (500X magnification)	85
Fig. 4.49	Alcian Blue Stained Section of Cartilage Highlighting Zones (50X magnification)	86
Fig. 4.50	H&E Stained Section of Cartilage and Bone Showing Attachment to Subchondral Bone (50X magnification)	87
Fig. 4.51	Alcian Blue Stained Section of Cartilage Showing Worn and Unworn Areas (100X magnification)	88
Fig. 4.52	Alcian Blue Stained Section of Cartilage from a Worn Region of a One-Hour Saline Test Showing Pre-Flap Conditions (test 7; 500X magnification)	89

Fig. 4.53	H&E Stained Section of Cartilage from a Three-Hour Saline Test Showing a Loose Flap (test 9; 500X magnification) . . .	90
Fig. 4.54	Alcian Blue Stained Section of Cartilage from a Three-Hour Saline Test Showing a Very Large Flap (test 18; 100X magnification)	91
Fig. 4.55	Alcian Blue Stained Section of Cartilage from Within the Worn Region of a Three-Hour Saline Test (test 18; 500X magnification)	92
Fig. 4.56	Alcian Blue Stained Section of Cartilage from a Low Damage Three-Hour Serum Test (test 17; 500X magnification)	93
Fig. 4.57	H&E Stained Section of Cartilage from a Low Wear Three-Hour Synovial Fluid Test (test 14; 500X magnification)	94
Fig. 4.58	H&E Stained Section of Cartilage from a High Wear Three-Hour Synovial Fluid Test (test 15; 200X magnification)	95
Fig. 4.59	H&E Stained Section of Cartilage from an Unworn Region Showing a Rough Surface (500X magnification)	96
Fig. 5.1	Cartilage Wear in Three-Hour Tests as Measured by Hydroxyproline Assay	100
Fig. 5.2	LVDT Plot from the Start of Low and High Wear Synovial Fluid Tests (tests 14,15).	101
Fig. 5.3	LVDT Data from the Start and End of the High Wear Synovial Fluid Test (test 15)	101
Fig. 5.4	LVDT from Start and End of Low Damage Serum Test Showing Displacement (test 17).	102
Fig. 5.5	Elastic Deformation and Complete Recovery of Cartilage	103
Fig. 5.6	Plastic Deformation of Cartilage Surface	104
Fig. 5.7	Loss of Cartilage from Top Plug Only	105
Fig. 5.8	Loss of Cartilage from Bottom Plug Only	106

Fig. 5.9 Diagram of the Exaggerated Tilt of a Lower Specimen 107

Fig. 5.10 Combination of Elastic Deformation, Plastic Deformation,
Wear, and Damage. 108

Fig. 5.11 LVDT Change from Start to End of Each Test
(6.72 N shaft weight) 110

Fig. A1 New Shaft Attached to Redesigned Top Plate (by Mark Freeman) 129

Fig. A2 Redesigned Top Plate 130

Fig. A3 New Shaft Holder. 131

Fig. A4 Coupler Between Shaft and Strain Ring. 132

Fig. A5 Redesigned Cartilage Testing Machine (by Mark Freeman). 133

Fig. C1 LVDT Calibration Curve 136

Fig. C2 Tangential Calibration Curve 137

Fig. C3 Normal Calibration Using Weights 138

Fig. C4 Voltage vs. Pressure Calibration. 139

LIST OF TABLES

Table 3.1 Flexibility of Features of Cartilage Test Device 28

Table 3.2 Test Parameters Used in the Present Study 29

Table D.1 Test Listing 140

Table D.2 Joint and Synovial Fluid Listing 141

Table E.1 Hydroxyproline Assay Results of Test Washings 142

CHAPTER 1

INTRODUCTION

1.1 RATIONALE

Articular cartilage is an amazing natural material that allows synovial joints to function throughout a lifetime with extremely low friction and wear. Biotribology may be defined as a study of this biological lubrication phenomenon [1]. While healthy joints can maintain low friction and wear even under high loads, millions of people suffer pain and immobility due to joint disease, injury, and aging.

Although joints have been studied extensively, very little is known about the mechanisms of wear and lubrication of articular cartilage. Researchers have proposed over two dozen theories of joint lubrication [2]. Most of their work was focused on the study of friction, not wear or damage. Of the studies that involved carrying out actual tests, the contact areas and pressures were rarely known, and often the tests were conducted with artificial materials. Biochemistry and articular cartilage structure have usually been disregarded in joint lubrication theories. The ongoing biotribology research at the Virginia Polytechnic Institute and State University is an effort to further the understanding of possible connections between joint lubrication and tribology.

Studies have rarely mixed theories governing normal, healthy cartilage with those concerning damaged or diseased cartilage. Damage can be produced or accelerated by sports injuries, degenerative aging, arthritis, or natural cartilage flaws. Arthritis is a general term that is used to describe over 100 types of joint and connective tissue diseases. Of these, rheumatoid arthritis and osteoarthritis are the most common. Osteoarthritis is sometimes referred to as the wear and tear form of arthritis and often leads to joint pain and loss of use. The specific mechanisms and causes of this cartilage wear and damage are virtually unknown.

One way to acquire more information about joint lubrication and damage is to carry out controlled *in vitro* cartilage-on-cartilage tests. This research is part of a continuing study begun by Furey [1,2,3,4,5] and involves the use of a cartilage testing machine designed by Burkhardt [6]. Emphasis in this study is on the importance of the biochemistry of synovial fluid on cartilage damage and wear. It is hoped that this research can provide some insight into the complex mechanism of synovial joint lubrication and possibly begin to answer questions about the significance of cartilage lubricant biochemistry.

1.2 OBJECTIVES

The primary goal of this research – as part of our broader, long-range objectives in the study of biotribology – is to develop, use, refine, and explore techniques for the *in vitro* study of cartilage-on-cartilage friction, deformation, and wear. A secondary goal is to observe the behavior of three fluids as lubricants in preliminary cartilage-on-cartilage experiments, namely a buffered saline solution, bovine serum, and bovine synovial fluid. An important part of this entire study consisted of the frequent discussions, cooperation, and feedback from the various members of the group in biotribology including professors as well as graduate and undergraduate students.

The specific objectives of this research were:

1. To acquire suitable bovine joints and synovial fluid for this and future research; to decide on ways of handling and storing these specimens before use.
2. To develop and refine procedures for cutting small and large cartilage-bone test specimens.
3. To ensure that the cartilage test device and instrumentation are working properly.
4. Using this device, to conduct the first *in vitro* tribological study of cartilage-on-cartilage – measuring friction, deformation, and wear.

5. To make measurements during a test of deformation, displacement, and friction under controlled normal load, frequency, and amplitude of oscillatory motion; to use data acquisition and analysis to examine the detailed changes in displacement, load, and friction occurring within a single cycle.
6. To develop and refine procedures for collecting used test fluids and wear debris for detailed studies of cartilage wear.
7. To use hydroxyproline analysis of the test fluids to give a quantitative measurement of cartilage wear; this also includes analysis of the original fluid. (This biochemical research would be carried out under the guidance of Dr. E. M. Gregory in his laboratory.)
8. To explore the use of photomacrography, scanning electron microscopy (SEM), and environmental scanning electron microscopy (ESEM) to examine cartilage specimens before and after sliding contact.
9. To work with Dr. Hugo Veit and Ms. Heather Hughes in exploring the application of cartilage sectioning and staining techniques used in histology for light microscopy studies.
10. To carry out preliminary cartilage-on-cartilage experiments using lubricants of buffered saline solution, bovine serum, and bovine synovial fluid.
11. Throughout all of this work, (a) to observe any unusual phenomena occurring as a result of tribological contact, and (b) to describe special problems that occur in carrying out cartilage-on-cartilage tests.

12. To modify the test device to reduce friction and play of the vertical shaft holding the upper test specimen.
13. To make recommendations for further studies in the light of the findings made in the present research and new information reported in the literature. This includes participating in discussions of the long-range plans of research in biotribology at Virginia Tech.
14. To assist in the training of undergraduate and graduate students who are or will be carrying out research in the area of biotribology.

Figure 1.1 gives an overview of the project objectives. Some of these objectives will be met in the future after the ground work has been laid with this project. It is hoped that this work will continue on and eventually lead to *in vivo* experiments involving specific biochemical constituents.

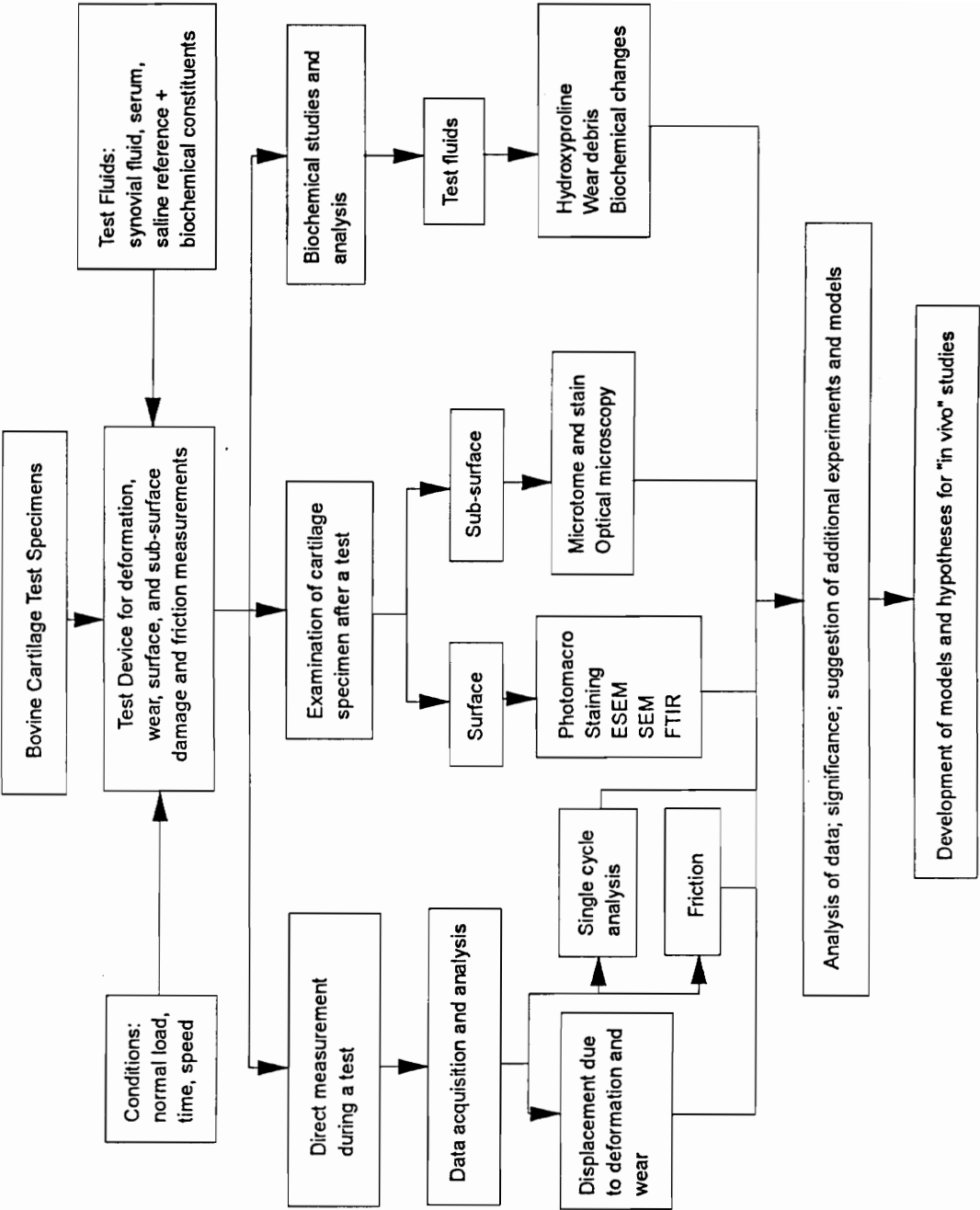


Figure 1.1 Overall Plan of Cartilage-on-Cartilage Research [7]

CHAPTER 2

LITERATURE REVIEW

2.1 SYNOVIAL JOINTS

Synovial joints are incredibly complex structures consisting of a joint capsule containing a synovial membrane which encloses the two articulating joint surfaces. This membrane produces synovial fluid, a viscous lubricant that both protects and provides nutrients to the articular cartilage [8]. Figure 2.1 depicts a simplified synovial joint.

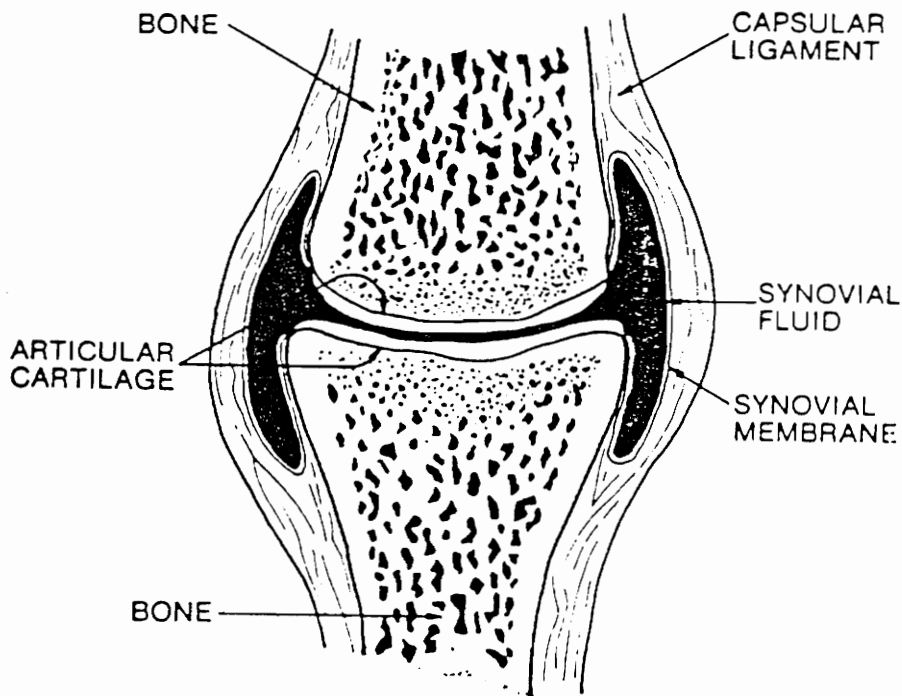


Figure 2.1 Simplified Synovial Joint (Furey [2])

The bone ends of a synovial joint are covered with protective layers of articular cartilage. These layers enable the bone ends to articulate on one another with very low friction and wear. Sharp impacts are absorbed by this natural composite which serves to cushion the joint surfaces. Articular cartilage is composed of approximately 75% water, collagen fibers, and macromolecules such as proteoglycans [8]. There are relatively few cells (chondrocytes) in cartilage, but their role is vital in maintaining the health, normal repair, and replacement of cartilage components. Collagen fibers are very strong and resist tensile forces on the joint surface during use. The proteoglycans combine with water to form a gel which is trapped within the collagen lattice. This gel enables the cartilage layer to resist deformation during loading by becoming pressurized as load increases [9].

Proteoglycan subunits are formed from long chain polysaccharides (glycosaminoglycans) attached at regular intervals to a core protein in a “test tube brush” fashion [10] as shown in Figure 2.2. This subunit is combined with others along a hyaluronic acid molecule to form the proteoglycan aggregate shown in Figure 2.3.

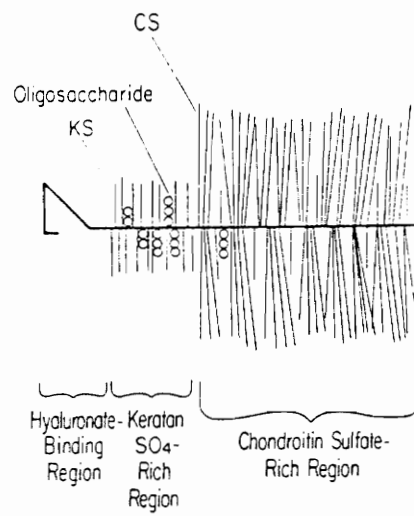


Figure 2.2 Proteoglycan Subunit (Mankin and Brandt [10])

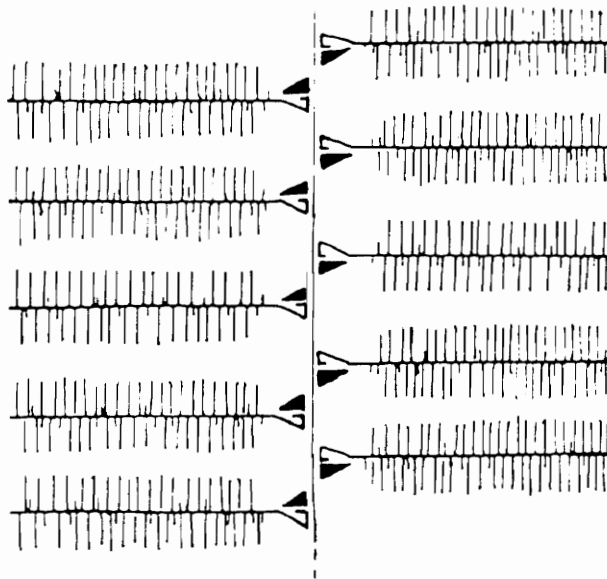


Figure 2.3 Proteoglycan Aggregate (Muir [9])

One can see from this description that articular cartilage is not the simple material that it first appears to be. Its composite composition is even further complicated by the fact that the arrangement and distribution of the cartilage components changes with depth within the cartilage layer. Four distinct regions can be described in this complex layer. Each region has a separate function in maintaining a healthy, functioning, low friction, low wear articulating surface. Figure 2.4 depicts each of these regions [9]. Zone 1 is a superficial layer that is resistant to wear due to collagen fibers lying tangential to the articular surface. Chondrocytes in this region are flattened in shape with their flat sides tangential to the surface. Below the superficial zone is the intermediate or transitional zone. This region contains spherical chondrocytes and collagen fibers randomly oriented in a mesh-like structure. Zone 3 is the deep or radiate zone. Here, chondrocytes form in columns of four to eight cells and the collagen fibers are arranged perpendicularly to the cartilage surface. The bottom region or zone 4 is labeled the calcified zone because of its high concentration of calcium salt crystals. This region has an irregular bottom surface in order to attach to the pitted subchondral bone to form a strong joint. The distinction between zone 3 and zone 4 is easily seen in stained cross-sectional slides. This separation of regions is termed the tide mark [9].

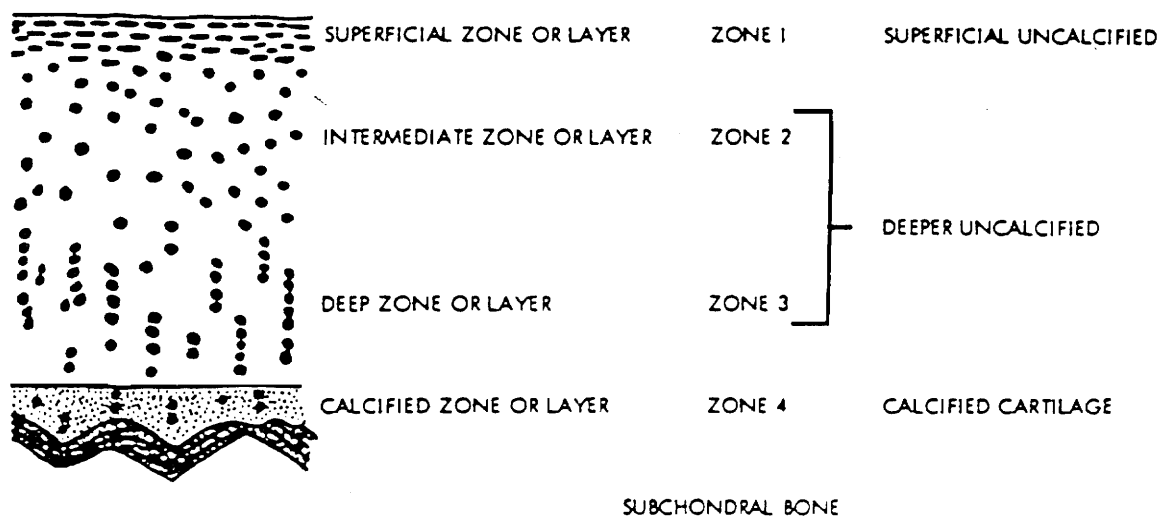


Figure 2.4 Articular Cartilage Zones (Meachim and Stockwell [9])

Collagen fibers are protein molecules made of helical amino acid chains. Articular cartilage collagen is Type II collagen and has a different molecular structure from the Type I collagen found in skin and bone. Tropocollagen molecules are the most basic units of collagen. They are grouped together to form fibrils which in turn form collagen fibers 10 to 100 nanometers in diameter [11]. Type IX collagen links collagen fibers together to form a somewhat elastic mesh which makes up 40-70% of the dry weight of cartilage [12]. One component of collagen is hydroxyproline, an amino acid, that makes up approximately 8% of the mass of collagen [13]. One way to determine cartilage wear is to determine the amount of hydroxyproline (using a procedure developed by Lipshitz et al. [14,15]) in the lubricant after a test and then calculate the

corresponding mass of cartilage worn. Various studies have employed this wear measurement method including Lipshitz, Etheredge, and Glimcher [14,15], Furey [4], and the present study.

Synovial fluid is a viscous, pale yellow fluid produced by the synovial membrane surrounding the joint (see Figure 2.1). The fluid is non-Newtonian, its viscosity varying inversely with the rate of shear. Damaged or deteriorating joints are often found to contain less viscous synovial fluid [9]. Synovial fluid is mainly composed of water (ca. 85%) and is a dialysate of blood plasma with additional proteins, polysaccharides, and hyaluronic acid. Cartilage cells receive their nutrients from synovial fluid which also carries away waste products [2].

2.2 ARTICULAR CARTILAGE LUBRICATION

Synovial joints have the amazing ability to function smoothly over a wide range of loads and speeds. For example, joints such as the human hip can operate with coefficients of friction as low as 0.001 and withstand compressive stresses as high as 18 MPa [16]. Joint lubrication has been studied extensively over the past 60 years with over thirty theories proposed [6]. Most of these theories concentrate on friction, not wear. Several authors have compiled excellent reviews of cartilage lubrication theories. Further detail on these numerous theories can be found in articles by Swanson [17], Higginson and Unsworth [18], Furey [2], and theses by Droogendijk [19] and Burkhardt [6].

Some researchers invoked the possibility of more traditional types of lubrication such as hydrodynamic, elastohydrodynamic, and squeeze film lubrication. These each have some merit with the squeeze film carrying the load during little or no joint movement and hydrodynamic lubrication occurring during relatively high velocity joint motion. Other scientists investigated completely new ideas such as the theory of weeping lubrication proposed by McCutchen. This theory was based on the idea that as cartilage compressed, lubricating fluid was squeezed from the porous matrix into pools on the dimpled cartilage surface. Then, as the load was released, excess fluid was absorbed by the cartilage. A related theory called boosted lubrication was later proposed by Walker. This involved the possibility of the dimpled cartilage surface holding pockets of enriched synovial fluid that carried the load. In the opinion of Higginson and Unsworth [18], it is very likely that cartilage uses both weeping and boosted lubrication along with possibly several other methods of lubrication to achieve such low friction and wear.

Many of the theories proposed in the last decade consist of computer models with very little actual experimental data. Researchers such as V. C. Mow [16] have proposed elaborate sets of rheological equations governing the flow of lubricant both within and on the surface of articular cartilage. These computer models have lent some support to the squeeze film, boundary, weeping, and boosted lubrication theories [16]. A study of recent synovial joint lubrication

papers failed to uncover any totally new theories of lubrication. However, work within the past ten years by Furey [2], Hayes et al. [20], and Stachowiak et al. [21] has started to focus more on wear as an important factor when discussing joint lubrication.

2.3 CARTILAGE WEAR

The inclusion of cartilage wear in the study of joint lubrication is vital, especially when one considers the implications of excessive joint wear. Cartilage wear and damage can be studied by a variety of methods including biochemical markers, physical measurements, and microscopy. Each of these methods adds another dimension to the understanding of joint function.

Analysis of the biochemistry of cartilage and synovial fluid has been used to help evaluate joint lubrication in several studies. Hydroxyproline, an amino acid found in collagen, has been used successfully to measure cartilage wear in a number of *in vitro* tests. Lipshitz, Etheredge, and Glimcher [15] found that the hydroxyproline content of cartilage is relatively constant throughout the cartilage layer and can be used to measure the actual quantity of cartilage removed from a joint surface during a test. Other research such as Furey's [2] and the present study have also used this method as one means of evaluating articular cartilage wear. Changes in proteoglycan concentration or proteoglycan degradation and alteration have been used as markers of joint disease and damage [12].

Collagen changes within the cartilage layer such as degradation or lower concentrations have also been shown to be a sign of joint wear and degeneration [22].

Other measurements of wear and damage can be made using X-ray techniques, magnetic resonance imaging (MRI), and for *in vitro* tests, a linear variable differential transducer (LVDT) can be used. X-rays can be used to measure the distance between bone ends within a joint; the cartilage is not visible. This means that X-rays are most useful in determining changes that occur over time within a joint as it deteriorates, since the bone ends become closer as the cartilage wears. MRI scans of synovial joints are very detailed and can show fat, muscles, tendons, bone, and cartilage [23]. With this level of detail it is even possible to determine the difference between fibrous and hyaline cartilage. Minor changes in cartilage thickness are possible to detect along with natural repair to damaged regions. The quality of cartilage is possible to assess to a certain extent, leading to the early detection of some types of joint disease and damage. The MRI observations are much more detailed than X-ray examinations. Other than using invasive procedures such as arthroscopic techniques, an MRI is the only way to view the tissue health and type of cartilage growing on the bone ends. Wear transducers are commonly used with *in vitro* tests to record the deformation, surface contour, and damage to a joint. An LVDT was used in the present work and in other studies such as those carried

out by Stachowiak et al. [21]. Hayes et al. [20] used displacement transducers to measure changes as small as 1 μ m during *in vitro* tests.

VIRGINIA TECH RESEARCH

Recent work in which cartilage wear and damage was stressed includes ongoing research by Furey [2] at the Virginia Polytechnic Institute and State University. Furey's work involves not only the wear of cartilage but also takes into account the biochemistry of the cartilage--synovial fluid system. This study recognizes that measurement and analysis of the damage to the joint surface was an extremely important factor, rather than simply focusing on friction measurements. This research is the basis of the present study and other biotribology research at Virginia Tech such as that by Burkhardt [6]. Techniques for working with cartilage-bone plugs were developed and biochemical cartilage wear measurement procedures were studied and carried out. Working at The Children's Hospital Medical Center, Harvard Medical School in Boston, Furey's research involved sliding bovine articular cartilage against an oscillating polished stainless steel plate. Test fluids included a buffered saline reference fluid, synovial fluid, and several constituents added to the reference fluid: two forms of hyaluronic acid, a lubricating glycoprotein isolated by Swann (LGP-I), and a protein complex from synovial fluid. Cartilage wear was measured using hydroxyproline assays. Furey found that distilled water and the buffered saline

LITERATURE REVIEW

reference fluid both produced similarly high amounts of wear. Synovial fluid produced significantly less (e.g., 90%) wear. Another interesting finding was that Swann's LGP-I did not reduce cartilage wear. The protein complex isolated from synovial fluid by Swann was very effective in reducing wear. This complex (when added to the reference fluid) produced similar wear results to those obtained in synovial fluid tests. This could indicate that this protein complex (and possibly others) has the specific function of helping to reduce wear in synovial joints. Wear reduction was also found using hyaluronic acid, but this synovial fluid constituent was not as effective as the protein complex or synovial fluid. This work demonstrated the importance of wear measurements when testing cartilage lubrication – friction measurements alone are not enough to determine the lubricating ability of a test fluid. SEM photographs helped to emphasize the fact that the type of lubricant significantly affects the type and amount of cartilage damage in this form of *in vitro* testing. Karen Hodgens of Children's Hospital carried out the complex SEM sample fixation procedure. The SEM photographs indicated that significant changes take place on the surface of the cartilage under these conditions of sliding contact and each lubricant produced a characteristic change on the cartilage surface. The study also found that a lack of lubricant causes rapid development of severe damage. The continuing work at Virginia Tech in biotribology builds on these findings by using

some of these same analytical techniques and test fluids with *in vitro* cartilage-on-cartilage tests.

OTHER RESEARCH ON CARTILAGE WEAR

Other researchers have investigated the effects of third body wear on joint lubrication and damage. Hayes et al. [20,24] have been interested in the role played by crystal deposits in joints. In one study, equine cartilage plugs were worn against a stainless steel plate in a pin-on-disk apparatus. Lubricants containing crystals such as those found in some arthritic joints were added and cartilage wear was measured. Two techniques were incorporated to determine cartilage wear – ion chromatography of bound sulfate and spectrophotometric assay of the sulfated glycosaminoglycans. Photographs were also taken with an SEM to give further detail of surface damage to the cartilage. This study found that complex wear mechanisms and increased wear are produced by adding crystals to the test lubricant. Comparison with arthritic articular cartilage that was worn *in vivo* showed that this test procedure produced similar damage.

Stachowiak et al. measured friction and wear changes using a pin-on-disk apparatus with an adult rat femur running against a stainless steel plate. These tests were run dry and with lubricants consisting of synovial fluid or saline solution. The authors found much lower friction with synovial fluid and a poor lubricating effect with saline solution. An environmental scanning electron

microscope was used to take photographs of the specimens after testing. This microscopic examination showed that lower levels of damage corresponded with the lower friction of synovial fluid tests. Stachowiak et al. concluded that there is a thin lipid layer covering the articular cartilage that protects the surface from damage. Even without synovial fluid, this layer was able to protect the cartilage for a short time. However, once the protective layer wears away or is removed, damage and friction increase rapidly.

2.4 CARTILAGE DISEASE AND DAMAGE

Arthritis is a term used to describe over 100 types of joint and connective tissue diseases. Rheumatoid arthritis and osteoarthritis are two of the most widespread forms of joint disease. Rheumatoid arthritis involves damage to articular cartilage by enzymes released by joint inflammation, especially of the synovial membrane. This disease usually causes joint swelling, pain, and can eventually lead to loss of joint function. Osteoarthritis is also known as the wear and tear form of arthritis due to the characteristic wearing away of articular cartilage [2]. This wear can lead to exposed subchondral bone and cause bony growths to form within the joint [25].

Degenerative joint disease may have tribological connections as discussed by Furey [3,5]. Two of the possible factors which may increase joint wear are changes in the wear resistance of cartilage and reduced anti-wear

properties of the lubricating synovial fluid. Both of these factors are related to tribology and biochemistry. Osteoarthritis may be caused by a number of pathways [26] and each case must be treated according to the primary cause of the disease. Figure 2.5 is a schematic diagram suggesting possible mechanisms leading to osteoarthritis and how tribology may be a factor involved in this process. This disease is difficult to diagnose until the later stages because initially there is no pain or noticeable swelling of the joint. Later stages are recognized by loss of mobility and progressive thinning of the cartilage layers as seen by x-ray examination or arthroscopic surgery.

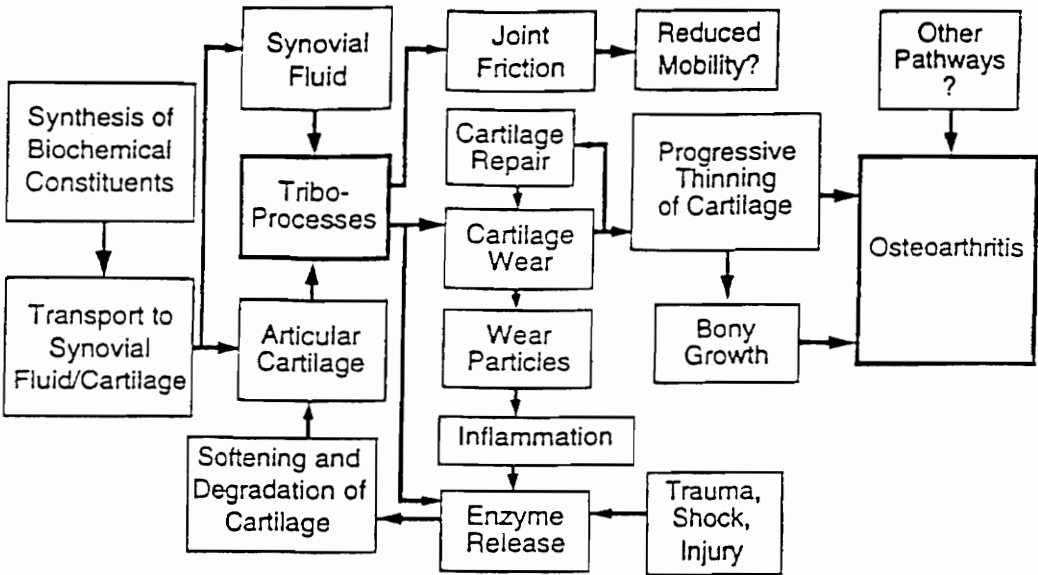


Figure 2.5 Possible Osteoarthritis and Tribological Connections (Furey [3])

Severe osteoarthritis, rheumatoid arthritis and cartilage defects may cause pain and at least a partial loss of joint function often requiring surgery to return joint mobility. Full thickness defects in articular cartilage are regions in the joint where injury or abnormality has exposed the underlying bone. Defects of this type usually do not heal on their own, and any healing that does occur creates an inferior cartilage surface [27].

Several treatments exist for the various joint problems. In the case of a tear or rip in the cartilage due to a sports injury, the surgeon may decide that removing the loose cartilage will reduce joint pain. A rip in the cartilage in a non-load bearing area could be stopped by cutting out the section, thus stopping further crack growth. Joints that have deteriorated further may require partial or total replacement. Hip joint replacement usually involves removing the femoral head and acetabulum and replacing these with a ball-in-socket joint prosthesis. The femoral head is made from Co-Cr-Mo alloy, stainless steel, titanium alloy, or even a ceramic such as alumina or zirconia. The acetabular cup is nearly always made of ultra-high molecular weight polyethylene (UHMWPE) [28]. A more recent idea in cartilage repair is in the area of implantation of replacement plugs of material in the defect region. Work in Sweden by Brittberg and others has focused on repair of defects using the patient's own cartilage cells grown in culture and transplanted into the damaged area [27]. Other researchers such as

Tighe have considered the possibility of synthetic hydrogels as a cartilage replacement [29].

Each of these solutions has a variety of problems that have led researchers to continue the search for the best material and method of articular cartilage repair. Cutting away the cartilage defect can lead to further degradation and eventually require partial or total joint replacement. Articular cartilage does not repair itself easily [27], especially in load bearing regions or in relatively large areas of damage. In a non-critical area, the defective cartilage can be removed and a partial healing of the affected area can take place. This means that the option of cutting away the cartilage defect is only possible in a limited number of cases and will most likely never allow the joint to return to full mobility.

Partial and total joint replacement is the most common option for older patients with arthritic joints. This requires major surgery, and in active patients more than one operation may be necessary as the prosthetic joint wears over a period of use. There is no chance for natural repair after this operation takes place since at least one entire surface of the joint is removed. Partial joint replacements carry the risk of damage to the cartilage surface by the artificial surface and may require future surgery to perform a total joint replacement [30]. The femoral head of a hip joint often loosens and requires a second operation. The body may respond to an implant and its wear products by eroding the bone

around the implant, thus causing loosening and increased wear. Bulk UHMWPE has excellent biocompatibility and low wear characteristics. It is stable in the body and even absorbs some of the load carried by the joint. This shock absorption is far less than that offered by natural cartilage and in older people brittle bones can break more easily if loaded suddenly. Wear is a significant concern in these artificial joints. The UHMWPE wear particles can cause a biological reaction that involves irritation of the surrounding tissues, leading to further joint and nearby bone erosion and infection [28].

Implantation of cartilage cells into a damaged area has been suggested in the past, but successful tests have only been recently completed. Brittberg and others carried out a study involving 23 patients with serious cartilage defects [27]. The study involved transplanting the patients' own cultured cartilage cells (chondrocytes) from an undamaged region to the defect in order to repair the articulating surface. Animal studies were carried out in 1984 by Peterson et al. [31] that indicated successful cartilage repair could be accomplished using transplanted cultured cartilage cells. The recent human trial has confirmed these earlier results. Cartilage slices were obtained from an undamaged, low load area of the patient's own knee. After isolating the cells (180,000 to 455,000 cells), the chondrocytes were placed in a culture medium and grown for 14 to 21 days to obtain 2.6 to 5 million cells. Patients were given antibiotics, and their cartilage defects were operated on to remove all of the affected tissue. A

periosteal flap (membrane of tough, fibrous connective tissue covering the bone) was sewn over the cartilage defect and the chondrocytes were injected under the flap. Weight was gradually added over the eight weeks following surgery.

The condition of the patients' knees was watched closely over the months following surgery to determine the success of the transplantation. An arthroscopy was performed three months after surgery to check on the repair of the defect. The study found that after three months the damaged area was filled in with cartilage, but this regrown tissue was not attached firmly to the underlying bone and was still soft in the middle of the defect. After 12 to 14 months, the cartilage was firmly attached to the bone just as normal cartilage appears. Also, the softer regions had disappeared. Patients with femoral defects (the part of the knee that the kneecap contacts) had great success while patients with patellar (kneecap) defects did not have as promising results. Of the 16 patients with femoral defects, 14 were found to have good to excellent results meaning they had no swelling and only mild aching with strenuous activity. The patients with patellar defects had much poorer results probably due to the high loads on the patella or the large variety of original injuries to the patellar cartilage.

This study found that transplanting cultured cartilage cells into a femoral cartilage defect will considerably reduce pain, knee locking, and swelling. A new cartilage surface can be created with similar properties to normal articular cartilage and is made of normal hyaline cartilage. When knees are injured and

cartilage is damaged, there is a possibility of a body reaction that leads to osteoarthritis. This method of cartilage repair may reduce the chances of the patient developing arthritis. Also, patients with arthritis due to a cartilage defect should be able to find relief by having the defective cartilage removed and new, healthy cartilage grown in place. Other forms of arthritis such as rheumatoid, in which the peripheral joint is being eroded away, will probably not be helped by this method of repair.

Some concerns with this method of treatment include the question of why the cartilage defect occurred in the first place? Will this new cartilage simply wear out again in a few more years since really long term studies have not taken place? Why is there such a problem with the patellar defects? Will taking a slice of cartilage from a healthy region eventually lead to problems in that area of the joint? Although there is still the question of exactly how this repair mechanism works, these research results are very promising and will likely lead to reduced suffering and increased mobility by many people with articular cartilage damage. This type of cartilage repair research provides even more motivation for understanding the wear and lubrication mechanisms of joints. Since natural repair is limited, and damage is difficult to fix surgically perhaps more work needs to be focused in the area of prevention or at least limiting joint damage in the first place.

CHAPTER 3

EXPERIMENTAL TECHNIQUE

3.1 CARTILAGE TESTING DEVICE

The cartilage-on-cartilage tests of this study were run on a modification of a test device originally designed by Bettina Burkhardt [6]. A diagram of this device is shown in Figure 3.1. The device consists of a pneumatic cylinder for application of the normal load, an octagonal strain ring for measuring forces, a motion controller, and an LVDT (linear variable differential transducer). Appendix A contains a description of modifications designed for this machine.

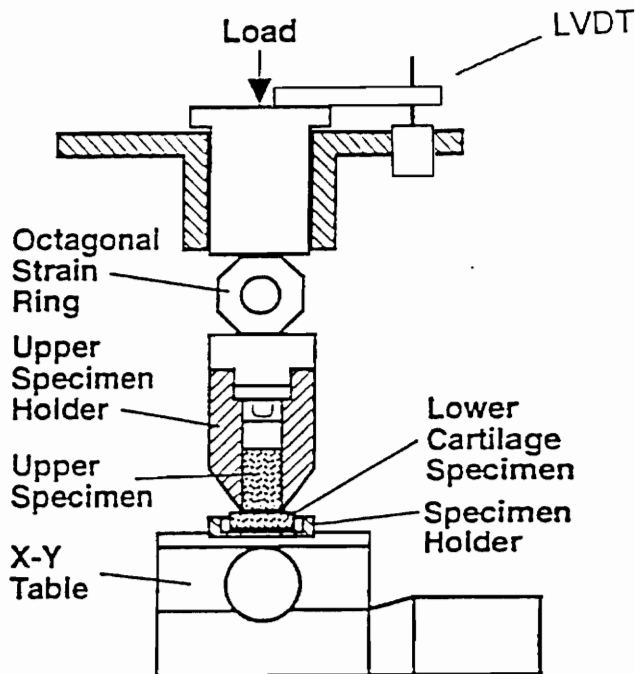


Figure 3.1 Diagram of Cartilage-on-Cartilage Test Device

The pneumatic cylinder pressurized by nitrogen allows the application of a wide range of normal loads (10-300 N). The cylinder is connected to a digital pressure gage for accurate pressure readings. Normal and tangential loads are measured using strain gages attached to the octagonal strain ring. Astro-Med Dash II chart recorders and a computer running the program Global Lab collect data from both strain gages and the LVDT. Wear, deformation, and gross surface topography are measured during testing using the LVDT. The computer data acquisition system allows the detailed analysis of a single test cycle. Therefore, it is possible to compare damage and wear measured after a test with changes in the behavior of the cartilage measured during a test. Another computer running a BASIC program (Appendix B) is connected to the NEAT-310 programmable motion controller. This allows the programming of the speed and sliding distance for each test. The lower specimen is mounted to an X-Y table driven by stepping motors. The flexibility of test parameters is shown in Table 3.1.

Table 3.1 Flexibility of Features of Cartilage Test Device [6,7]

Contact System:	Cartilage-on-cartilage
Contact Geometry:	Flat-on-flat, Convex-on-flat, Irregular-on-irregular
Cartilage Type:	Articular, any source (e.g., bovine, porcine)
Specimen Size:	Upper specimen, 4-6.35 mm diam.; Lower specimen, 15-25.4 mm diam.
Applied Load:	10 - 300 N
Average pressure:	0.08 - 2.4 MPa
Type of Motion:	Linear, oscillating; circular, constant velocity; more complex patterns
Sliding Velocity:	0 -20 mm/s
Fluid Temperature	Ambient (20°C)
Environment:	Ambient
Measurements:	Normal load, friction, displacement

The test parameters used in this study are listed in Table 3.2.

Table 3.2 Test Parameters Used in the Present Study

Contact System:	Cartilage-on-cartilage
Contact Geometry:	Flat-on-flat (macroscopically)
Cartilage Type:	Bovine
Specimen Size:	Upper specimen, 6.22 mm diam. Lower specimen, 25.4 mm diam.
Applied Load:	63.8 N
Average Pressure:	2.1 MPa
Type of Motion:	Linear, oscillating
Traverse Length:	6.26 mm
Sliding Velocity:	8 mm/s
Fluid Temperature:	Ambient (20°C)
Environment:	Ambient (20°C)

3.2 TEST MATERIALS ACQUISITION

Dr. Hugo Veit, Professor of Pathobiology in the College of Veterinary Medicine, made it possible to collect nearly 90 bovine shoulder and stifle joints from 24 steers involved in a separate controlled study. Synovial fluid was collected from the carpal and stifle joints of most of the animals. The joints were

immediately dissected and placed in labeled Ziploc bags with saline saturated gauze pads. Excess air was removed from the bags and they were placed in a freezer at -25°C. The literature generally reported that this storage procedure should not adversely affect the cartilage [32,33,34,35,36]. The synovial fluid was stored in separate vials for each joint, labeled, and frozen at -25°C.

Plugs for the wear tests were cut from the frozen joints using a 6.22 mm diameter plug cutter for the upper plug and a 25.4 mm diameter cutter for the lower sample. An initial cut was made through the cartilage using a cork borer. This cut ensured that the cartilage plugs had well finished edges with no extraneous collagen fibers. A variable speed, variable torque drill press was used at low speeds with high torque while de-ionized water was sprayed on the joint. This kept the joint cool and hydrated while also removing bone particles. After cutting the plugs from opposite joint surfaces, the plugs were rinsed clean with de-ionized water. For tests with a 25.4 mm diameter lower cartilage specimen, large joints (bovine) were required. However if a smaller lower specimen is used, tests could be performed using available equine or porcine cartilage. The following is a detailed list of all of the materials needed and steps for cutting bone-cartilage plugs used in the present cartilage-on-cartilage wear tests:

Materials and equipment needed:

bovine stifle joint (both tibial and femoral halves cut to approx. 4" length)
vise
stainless steel pan
de-ionized water
1 1/8" hole cutter (cuts 1" plugs)
1/4" plug cutter
hacksaw
paper towels
safety glasses
small screwdriver
small vials
plastic or glass jars
labels
rubber gloves
cork bores (1/4" and 3/8")
high torque, low speed drill press

Steps followed:

1. Remove stored joints from the freezer.
2. Choose a joint and cut it to fit in the vise if necessary.
3. Position the joint for lower (1" diameter) plug in the vise and clamp tightly in place.
4. Set the drill press for low speed and high torque. The speed should be adjusted to be low enough to keep from heating the cartilage plug.
5. Have one person hold the joint while the other sprays the joint surface with de-ionized water and begins cutting slowly.
6. Cut at least 1/2" into the joint while cooling with de-ionized water.
7. Repeat for the other 1" sample.
8. Check to be sure teeth of 1/4" cutter are clean.
9. Replace 1" cutter with 1/4" cutter and set speed slightly higher.

10. Score the femoral condyle in the desired location with the 1/4" and 3/8" cork borers. Remove this ring of cartilage to allow the 1/4" cutter to have clean bone to cut.
11. Have one person hold the joint while the other sprays the joint surface with de-ionized water and begins slowly cutting.
12. Cut about 3/4" into the joint, lifting the cutter several times to wash away debris.
13. After cutting is completed, snap off plug at the base by inserting a small screwdriver next to the plug and prying sideways.
14. Place 1/4" plug in labeled vial with a small amount of de-ionized water and freeze at -25°C for later use.
15. To remove the 1" plugs from the joint, cut with a hacksaw and then use a screwdriver to loosen.
16. Place 1" plug in a labeled jar with a small amount of de-ionized water and freeze at -25°C for later use.

The process described above takes approximately 45 minutes from start to finish. Two sets of upper and lower plugs can be obtained from each stifle.

3.3 LUBRICANTS

The test fluids used in this study consisted of a phosphate buffered saline solution (PBS), serum from a mature lactating Holstein, and synovial fluid from the same animal as the cartilage test specimens. 500 ml of the buffered saline was made following the procedure given by Sambrook et al. [37]. Add 4.0 g of NaCl, 0.1 g of KCl, 0.72 g of Na₂HPO₄, and 0.12 g of KH₂PO₄ to 400 ml of distilled water. Check the pH and adjust to 7.4 with HCl if necessary then add

distilled water to make 500 ml of solution. The solution should be sterilized by autoclaving for 20 minutes at 15 psi. on liquid cycle. Serum is a pale yellow fluid that is obtained by removing the cells and clotting factors from blood. This differs from plasma which still contains clotting factors such as fibrinogen [38].

3.4 PROCEDURE FOR *IN VITRO* CARTILAGE-ON-CARTILAGE TESTS

Cartilage-on-cartilage tests were designed to check on effects of lubricant composition and test length variation. Tests were run using lubricants of phosphate buffered saline, serum, and synovial fluid for periods of one and three hours. Before tests began, all instrumentation was calibrated as described in Appendix C. The following steps detail the procedure followed in all of the cartilage-on-cartilage tests undertaken in this study.

1. Remove pre-cut plugs from the freezer to thaw overnight in the refrigerator (approx. 40°C).
2. Rinse upper and lower plugs with de-ionized water to remove all loose particles.
3. View upper and lower plugs under the optical microscope and describe and photograph any abnormalities.
4. Turn on chart recorders, strain gages, and the LVDT instrumentation to let it warm up for at least 30 minutes.
5. Cut the lower plug to the correct height (approx. 0.5") and trim all loose fibers.
6. Place upper and lower plugs in sample holders and use spacers as needed.

7. Put the O-ring on the lower plug surface before threading the lower sample holder together. Check the lower plug seal for leaking using 1.5 ml of de-ionized water. If leaking does occur, use Teflon pipe tape to fill cracks in seal caused by irregular plug contours.
8. Check all settings on the chart recorders and computer for data acquisition. Settings of 0.5 V/minor div. for the LVDT, 50 mV/minor div. for the normal load, and 20 mV/minor div. for the tangential load worked well.
9. Add 1.5 ml of test fluid to the lower sample.
10. The strain gages must be balanced before each test. Decide on a value for the tangential and normal readouts and set this to the same value at the start of each test.
11. Check the location of the wear track on the lower specimen. Lower the upper sample holder and start the chart recorders. Apply pressure slowly until the full test load is reached (63.8 N).
12. Using the test program stored on the computer, run the test for the required time (1 or 3 hours). Use a stop watch to keep track of the test progress.
13. Record computer data at the start of the test and every half hour.
14. Stop the test and wash upper and lower plugs for hydroxyproline testing. First remove and save all fluid from the surface of the lower specimen. Then wash the lower specimen three times using 1 ml volumes of de-ionized water. Also rinse the upper specimen to free any wear particles.
15. View and photograph upper and lower plugs under the optical microscope and describe.
16. Store plugs and washings in the freezer for later analysis.

3.5 MEASUREMENTS AND OBSERVATIONS

Measurements and observations were made before, during, and after each test. Samples were viewed and photographed with a photomicroscope

before testing to check for natural cartilage damage or defects. During each test data was collected on normal and tangential loads and LVDT displacement. In order to determine the extent of damage and wear, photographs were taken using a variety of microscopes and sample treatments, and the test washings were analyzed for wear particles. Appendix D contains a listing of all joints and synovial fluid used and stored in this study.

3.5.1 Data Acquisition

Data was collected during the tests using a computer data acquisition system and with strip chart recorders. Tangential and normal load data were combined to calculate the changing coefficients of friction during a single cycle of a test. This information along with the LVDT readout gave insight to what was happening at specific locations along the wear track during a test as damage or other changes occurred. These results were later combined with the findings from microscopic techniques and fluid analysis to produce a more complete test analysis.

3.5.2 Examination of Cartilage Specimens

Cartilage specimens were viewed using and a scanning electron microscope (SEM) and light microscopes [39,40,41,42]. Figure 3.2 gives an

overview of the microscopic techniques used to determine effects of cartilage-on-cartilage tests in this study.

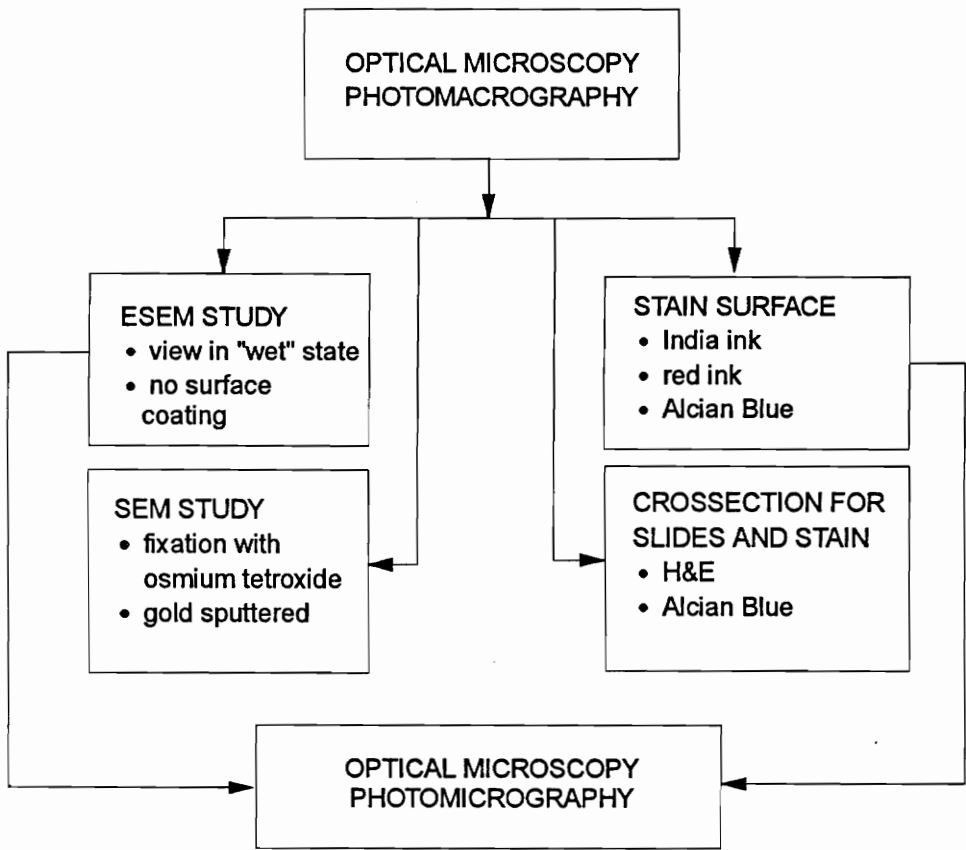


Figure 3.2 Microscopic Analysis of Surface and Subsurface Damage [7]

Scanning and Environmental Electron Microscopy

The Scanning Electron Microscope (SEM) proved to be a useful tool in examining surfaces of both worn and unworn cartilage samples. A lengthy Osmium Tetroxide fixation procedure carried out by Ms. June Mullins at the

College of Veterinary Medicine must take place in order to remove the water and preserve the natural features of the cartilage surface. After fixing and gold sputtering the samples, the SEM was used to reach high magnifications not possible with a light microscope.

The Environmental Scanning Electron Microscope (ESEM) was another tool used to view the cartilage surface at high magnifications. No complicated sample preparation is needed as with the SEM and gold coating is not necessary. The ESEM allowed samples to be viewed in their natural "wet" state. The ultra high vacuum (10^{-8} torr) of an SEM was eliminated and samples could be viewed at 10 torr. This allowed a hydrated sample such as cartilage to remain in its natural state by cooling the specimen stage and keeping the temperature near the point of condensation. These hydrated sample surfaces were difficult to focus on with the ESEM. Although magnifications are not as high as those with the SEM, features seen in the SEM could be verified by the ESEM and artifacts produced by SEM sample preparation eliminated.

Optical Microscopy

India ink and red ink were dripped onto worn and unworn cartilage surfaces to highlight scratches and wear patterns. These specimens and other unstained test specimens were washed in tap water and then viewed and photographed with a photomicroscope. Stained cracks and scratches were

much easier to see and clearly stood out from the undamaged areas. Alcian blue was also used to stain the surface of cartilage plugs. Samples were placed in fixative solution for at least 24 hours and then washed in 70% ethanol for three days. Alcian blue was dripped onto the surface and photomacroscopic pictures were taken. Section 4.5.1 details the results of the optical surface analysis.

In order to make cross-sectional slides, samples were cut in sections with dimensions no greater than 25.4 mm x 12.7 mm x 6.35 mm. After being placed in a fixative solution, they were dehydrated, embedded in paraffin wax, chilled, and cut into 5 μ m thick slices. Hemotoxylin and eosin (H&E) and alcian blue stains were used to highlight various tissue components. Alcian blue stains the proteoglycans dark blue. Section 4.5.2 contains photographs and analysis of the cross-sectional slide studies.

3.5.3 Analysis of Fluid

Cartilage wear was measured quantitatively using hydroxyproline analysis of the test washings. Hydroxyproline is an amino acid residue found almost exclusively in collagen. Therefore, the amount of collagen, and thus the amount of cartilage worn, can be determined. The procedure described by Bergman and Loxley [13] was followed in this analysis.

The frozen washings from the wear tests were thawed and lyophilized to remove the water. Hydrolysis in 1-2 ml of 6 M HCl overnight broke down the collagen fibers. The hydrolysates were neutralized with equal amounts of 6 M NaOH and 25 - 200 μ l were taken for colorimetric analysis. Distilled water was added to each sample to bring the total volume in each test tube to 200 μ l. 400 μ l of acetate-citrate buffer (57 g sodium acetate, 33.4 g citric acid, 435 ml 1 M NaOH, 385 ml 2-propanol, de-ionized water to 1 liter) was added to each tube along with 200 μ l of solution A(1:4 v/v Chloramine-T (7% w/v):acetate citrate buffer) and mixed. After room temperature incubation for 5 minutes, 2.5 ml of solution B (3:13 v/v DAB reagent (10 g p-dimethylaminobenzaldehyde in 15 ml 70% perchloric acid): 2-propanol) was added and mixed. This solution was held at 58°C for 25 minutes causing a color change in the tubes containing hydroxyproline. The absorbance at 558 nm was read on a spectrophotometer within 30 minutes and compared to hydroxyproline standards.

Commercial trans-hydroxyproline from Sigma was used in the standardization procedure. An example of a standard hydroxyproline curve is shown in Figure 3.3. This linear curve is typical of the standard curves produced. The extreme sensitivity of this assay is evident from the figure; it is possible to detect the presence of less than 0.1 μ g of hydroxyproline. Hydroxyproline analysis was also performed on bovine serum, synovial fluid, and unworn cartilage to determine pre-test hydroxyproline concentrations. The

hydroxyproline content of the test washings is listed in Appendix E. Section 4.2 contains the calculated cartilage wear results from the hydroxyproline analysis.

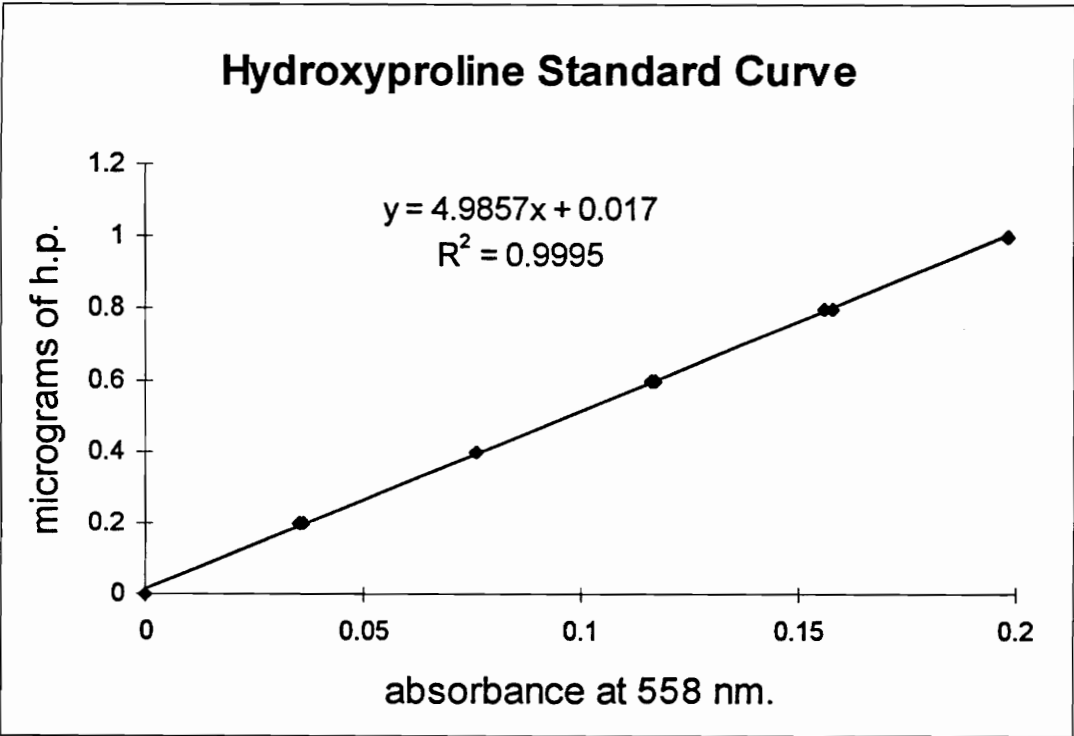


Figure 3.3 Typical Hydroxyproline Standard Curve Showing Linearity

CHAPTER 4

RESULTS

Friction, deformation, cartilage wear, SEM photographs, cross-sectional slide microscope photographs, and photomicroscope pictures are presented as examples of the effects of lubricant and test duration variation. Graphs of frictional forces, displacement, and coefficient of friction are included to portray differences between lubricants and also to show how the geometry of the cartilage plugs can affect test results. SEM and photomicroscope pictures of the plug surfaces before and after testing give insight into the type of surface damage resulting from these test conditions. Cross-sectional slide photographs are included to show the importance of subsurface damage that can lead to surface damage in some cases. Hydroxyproline assay results are presented as a means of measuring the cartilage removed from the test plugs. All figures are presented with their corresponding test number. Appendix D contains a list and description of these tests.

4.1 EFFECTS OF FLUID COMPOSITION ON FRICTION AND VERTICAL DISPLACEMENT

Tests were run with three different lubricants: buffered saline, bovine serum, and synovial fluid. Both frictional forces and displacement data are presented together because of their close interaction. Graphs shown here are included not only as examples of general results found, but also to demonstrate problems encountered and considered in analysis of these results.

4.1.1 Saline Solution Tests

Buffered saline solution tests were performed with 1.5 ml of lubricant following the procedure given in the experimental technique section (section 3.4). Three cartilage-on-cartilage tests were run for one hour (tests 6,7,8) and two tests were run for three hours (tests 9,18). The plots included here are typical of the results of saline tests where an area of cartilage was removed or at least partially detached from the wear track. Figure 4.1 is a graph of the tangential force recorded for three seconds at the start of a three-hour test. Three seconds of data corresponds to approximately two and a half cycles of sliding. This can be compared to the tangential force recorded at the end of the test as shown in Figure 4.2.

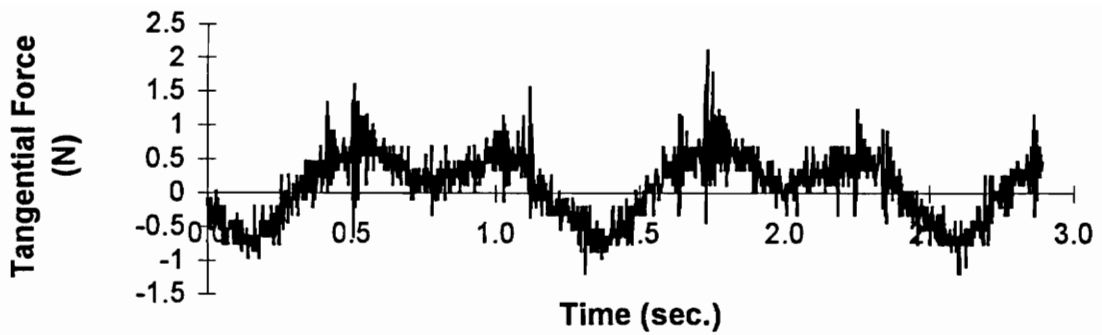


Figure 4.1 Tangential Force at the Start of a Three-Hour Saline Test (test 18)

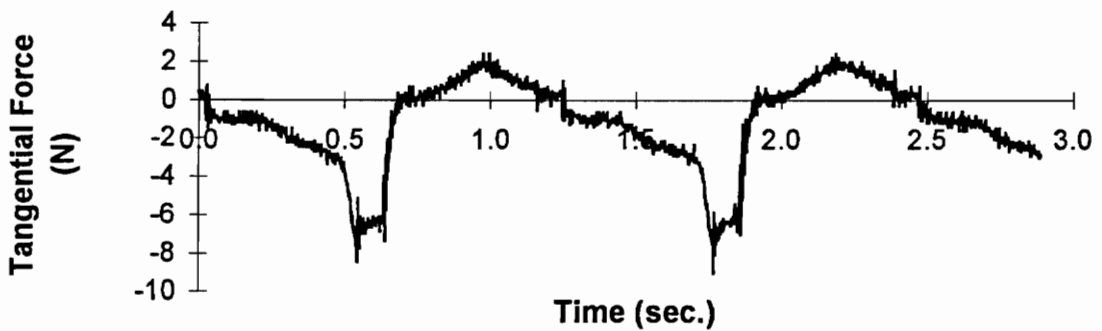


Figure 4.2 Tangential Force at the End of a Three-Hour Saline Test (test 18)

As shown in Figures 4.1 and 4.2, a drastic change in frictional (tangential) force occurred over the length of the test. It is important to note that the large peak in frictional force seen twice in Figure 4.2 is only in one direction of sliding and occurred near one end of the wear track. The positive and negative tangential force values correspond to the two directions of sliding.

Displacement measurements were also taken at the same time as the normal and tangential loads were recorded. Figures 4.3 and 4.4 are graphs of

vertical displacement of the LVDT at the start and end of the same three-hour saline test from Figures 4.1 and 4.2.

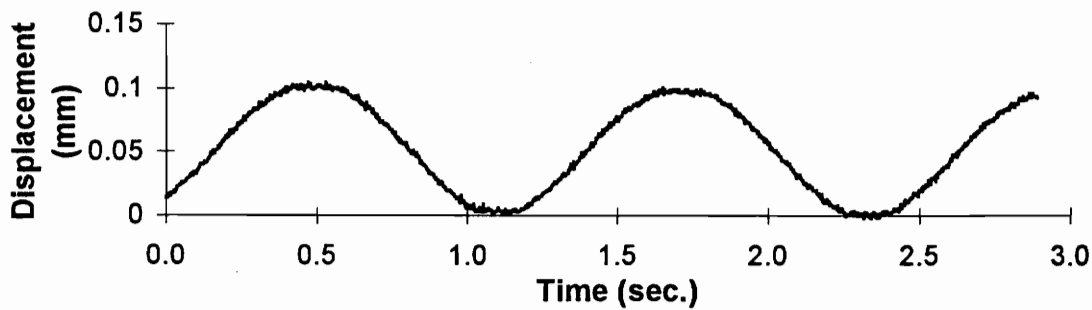


Figure 4.3 LVDT Displacement at the Start of a Three-Hour Saline Test (test 18)

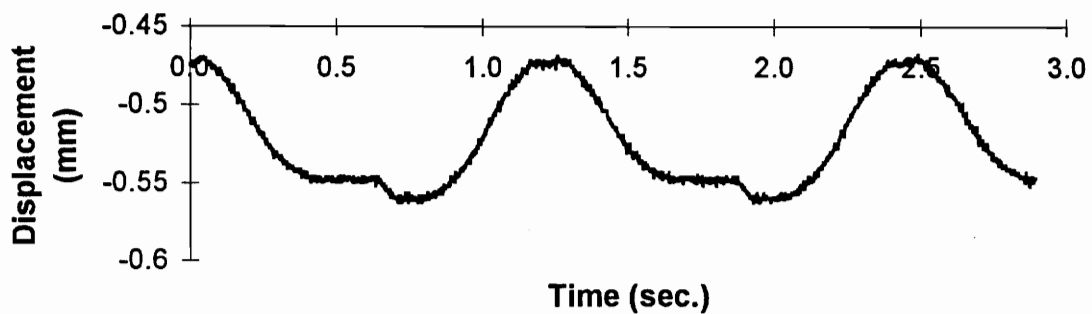


Figure 4.4 LVDT Displacement at the End of a Three-Hour Saline Test (test 18)

A comparison of these two displacement plots shows that over the length of the test, the cartilage contour changed. Overall LVDT displacement is also visible, but the most interesting feature is a reversal of the hills and valleys over the two and a half cycles recorded here. Figure 4.4 also contains a sudden change in displacement at the end of the wear track in the same location as the

high frictional force found in Figure 4.2. Chapter 5 will examine the LVDT data more closely and discuss the displacement and how it relates to wear and deformation of the cartilage.

The coefficient of friction over the length of two and a half cycles was calculated from the normal and tangential force measurements. Figures 4.5 and 4.6 are plots of the coefficient of friction at the start and end of the saline test in Figures 4.1 - 4.4.

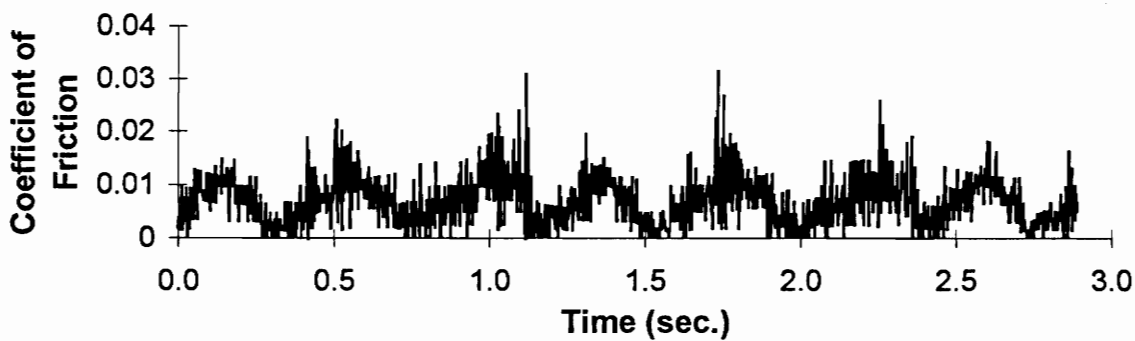


Figure 4.5 Coefficient of Friction at the Start of a Three-Hour Saline Test (test 18)

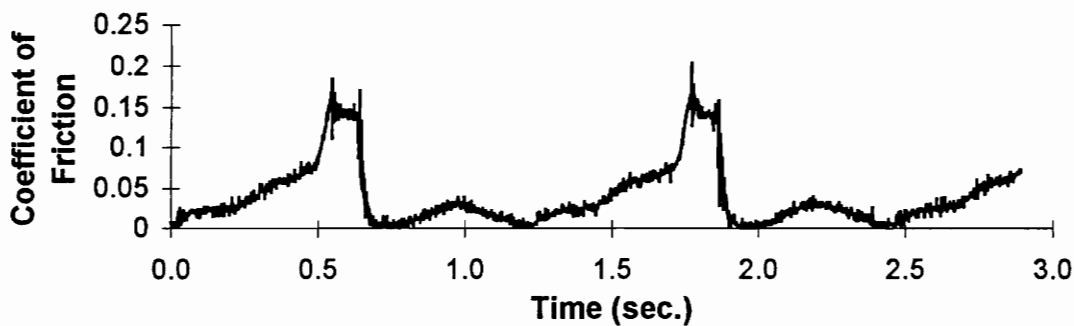


Figure 4.6 Coefficient of Friction at the End of a Three-Hour Saline Test (test 18)

Figure 4.5 shows that at the start of the test the coefficient of friction was quite low (0.02 or less) and relatively equal in both directions of sliding. Figure 4.6 indicates a drastic increase in friction near the end of one direction of sliding. The opposite direction of sliding produced a fairly low coefficient of friction that was similar in magnitude to that found at the start of the three-hour test.

All five of the saline tests showed an increase in friction over the length of the tests. Figure 4.7 is a graph of the average maximum coefficient of friction at various time periods during the buffered saline tests. This coefficient of friction represents the average of the highest frictional forces measured at the start of each test and again at one hour and three hours into the tests. Both three-hour tests produced the highest coefficients of friction and visible surface damage.

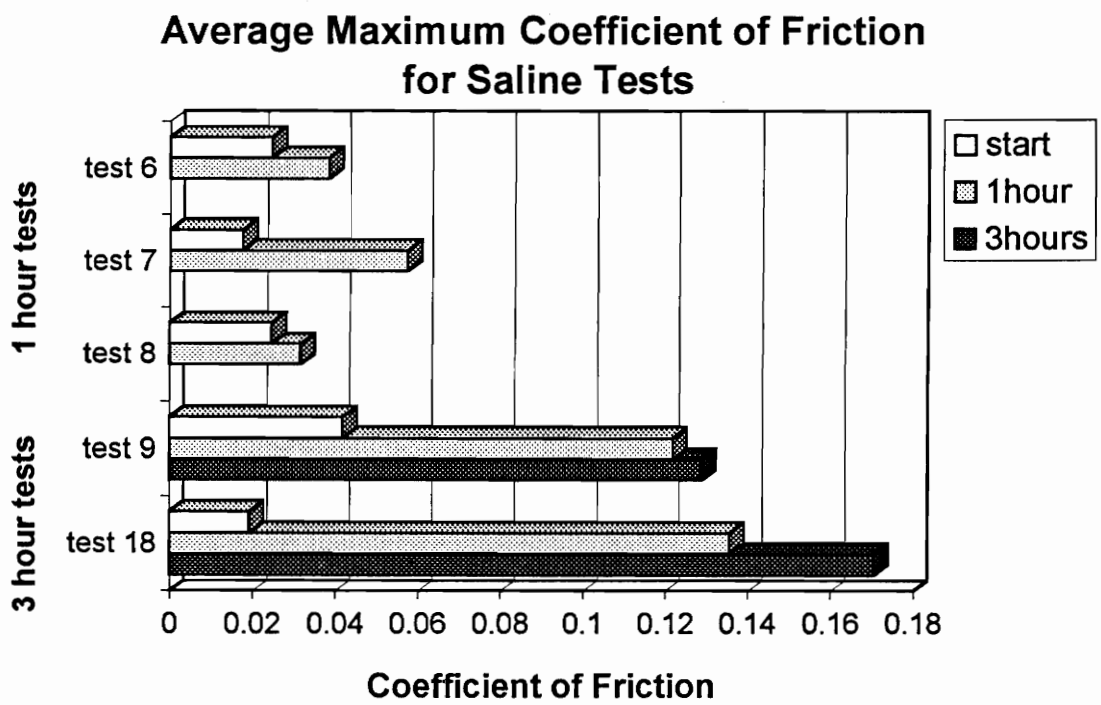


Figure 4.7 Average Maximum Coefficient of Friction for Buffered Saline Tests

4.1.2 Serum Tests

Four cartilage-on-cartilage tests were run using 1.5 ml of serum from a mature Holstein as the lubricant. Two tests were run for one hour (tests 12,13) and two were run for three hours (tests 16,17). The graphs presented below are from the three-hour tests. Results are presented from two tests to show the differences between a low and high damage test. Figures 4.8 - 4.13 are all from the same low damage three-hour serum test (test 17), and Figures 4.14 - 4.17 are from the high damage three-hour serum test (test 16). It is interesting to note that in the three-hour serum tests, severe damage did not produce high wear values. This is discussed further in Chapter 5. Each three second plot represents approximately two and a half cycles of sliding.

Figures 4.8 and 4.9 are plots of the tangential force recorded at the beginning and end of the three-hour low damage serum test.

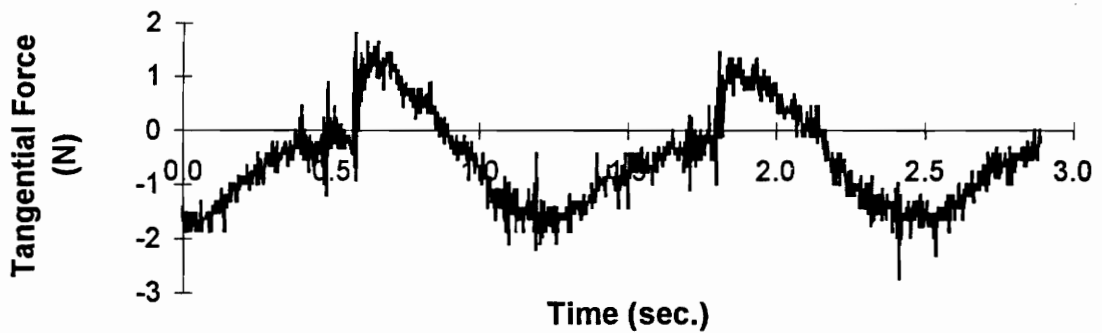


Figure 4.8 Tangential Force at the Start of a Low Damage Three-Hour Serum Test (test 17)

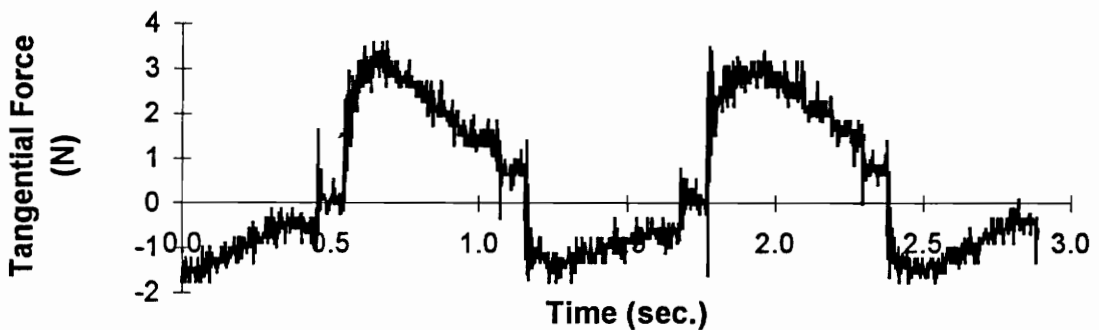


Figure 4.9 Tangential Force at the End of a Low Damage Three-Hour Serum Test (test 17)

From these two plots (Figures 4.8 and 4.9) it can be seen that the frictional forces remained low over the course of the three-hour test. However, it should be noted that the frictional force increased more in one direction of sliding (Figure 4.9).

Vertical displacement was recorded over the same time intervals as the tangential readings at the beginning and end of the three-hour test. Figures 4.10 and 4.11 below are plots of this displacement data.

RESULTS

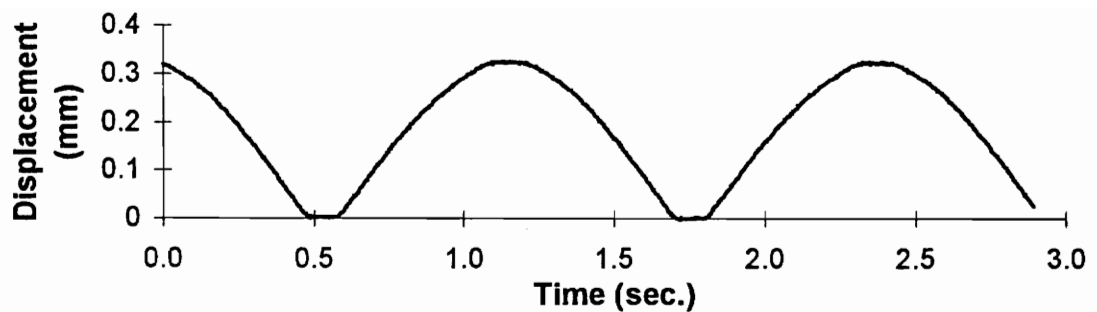


Figure 4.10 Displacement at the Start of a Low Damage Three Hour Serum Test (test 17)

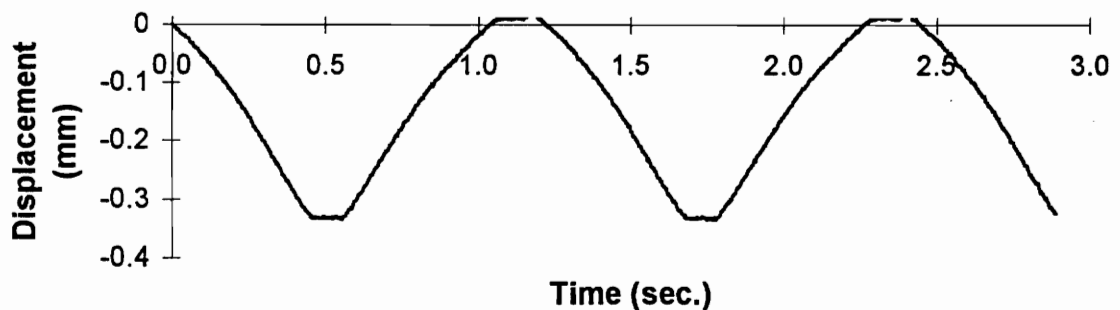


Figure 4.11 Displacement at the End of a Low Damage Three Hour Serum Test (test 17)

The displacement variation over the course of one cycle (0.35 mm from peak to valley) remained nearly the same throughout the test. The only major change in the LVDT reading was a general downward shift of the displacement curve (0.33 mm). This shift was commonly seen in all cartilage-on-cartilage tests, although the magnitude of the shift varied from test to test.

RESULTS

The coefficient of friction over the two and a half cycles was calculated and plotted in Figures 4.12 and 4.13. The maximum coefficients of friction recorded at the start and end of this test were quite low (0.03 at the start and 0.06 at the end). However, this is a doubling of the coefficient of friction.

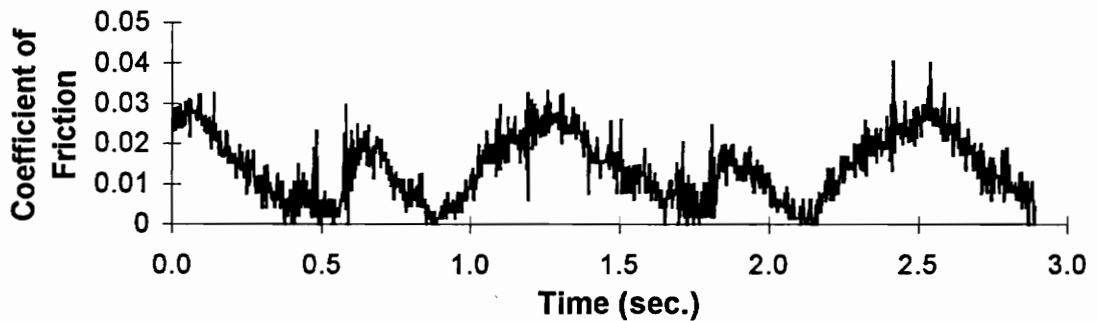


Figure 4.12 Coefficient of Friction at the Start of a Low Damage Three-Hour Serum Test (test 17)

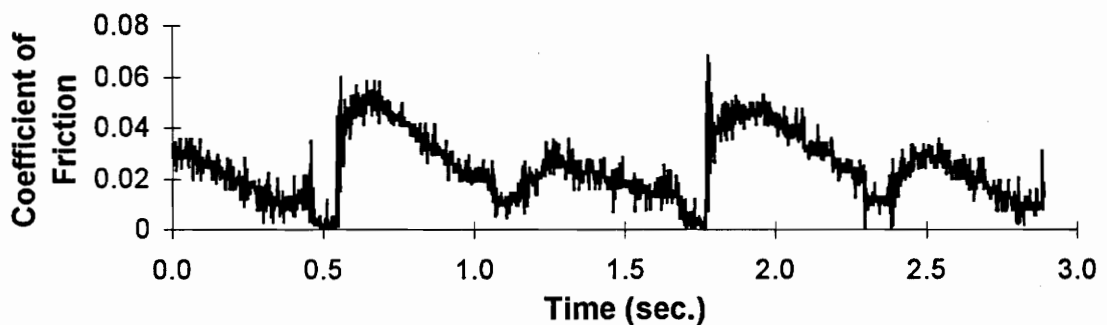


Figure 4.13 Coefficient of Friction at the End of a Low Damage Three-Hour Serum Test (test 17)

Figures 4.14 - 4.19 are from a three-hour high damage serum test (test 16). The tangential force at the start and end of this test is graphed in Figures 4.14 and 4.15.

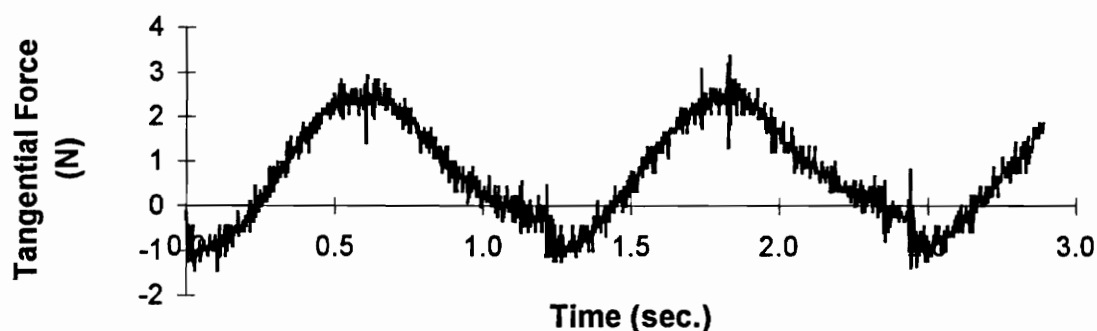


Figure 4.14 Tangential Force Recorded at the Start of a High Damage Three-Hour Serum Test (test 16)

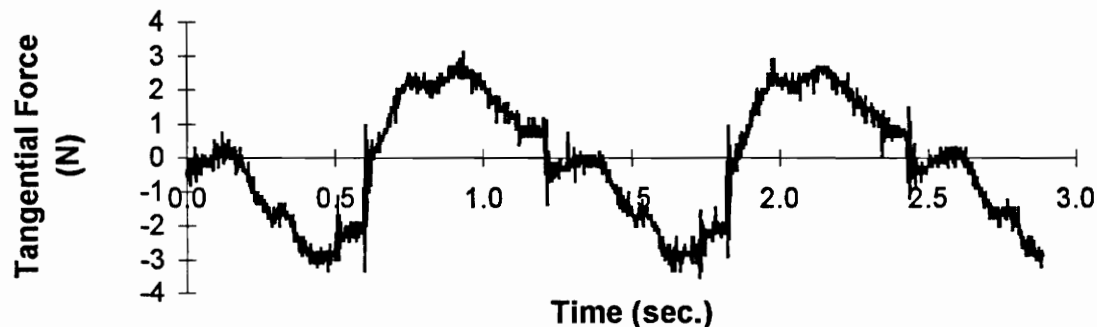


Figure 4.15 Tangential Force Recorded at the End of a High Damage Three-Hour Serum Test (test 16)

These two plots of the tangential force clearly show that although there was very little increase in force with time, there were significant changes in the smoothness of the curves. The test started out with a fairly smoothly fluctuating

tangential reading, but over the length of the test this output became quite rough with many sudden peaks.

The displacement at the beginning and end of the high damage serum test is shown in Figures 4.16 and 4.17. The scale has the same magnitude in both graphs.

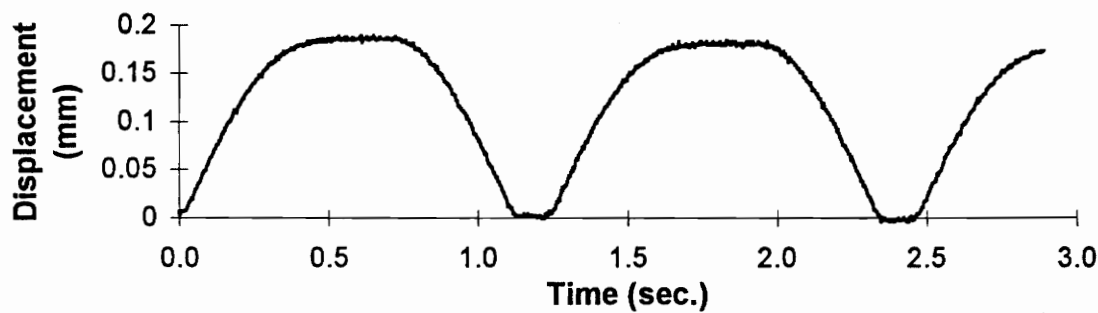


Figure 4.16 Displacement at the Start of a High Damage Three-Hour Serum Test (test 16)

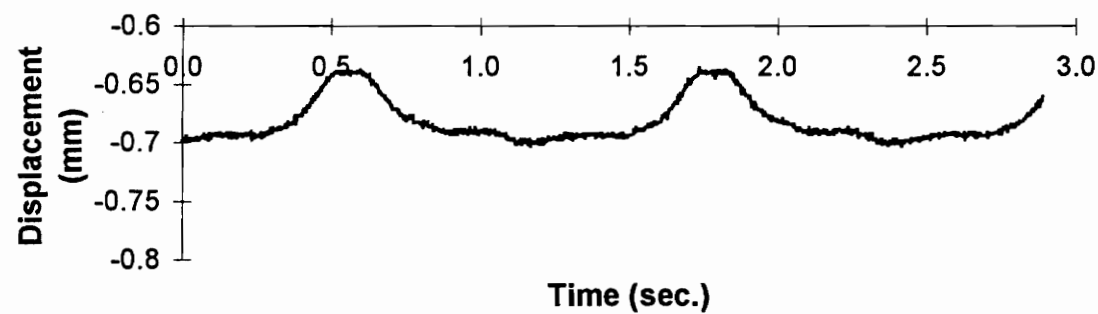


Figure 4.17 Displacement at the End of a High Damage Three-Hour Serum Test (test 16)

A comparison of the two displacement curves indicates that the original surface contour (Figure 4.16) was not simply displaced, but instead was modified during the test. The original distance from the high to low point on the displacement graph was 0.18 mm. At the end of the test, this value was much lower (0.06 mm).

The coefficient of friction over two and a half cycles at the start and end of the high damage serum test is shown in Figures 4.18 and 4.19.

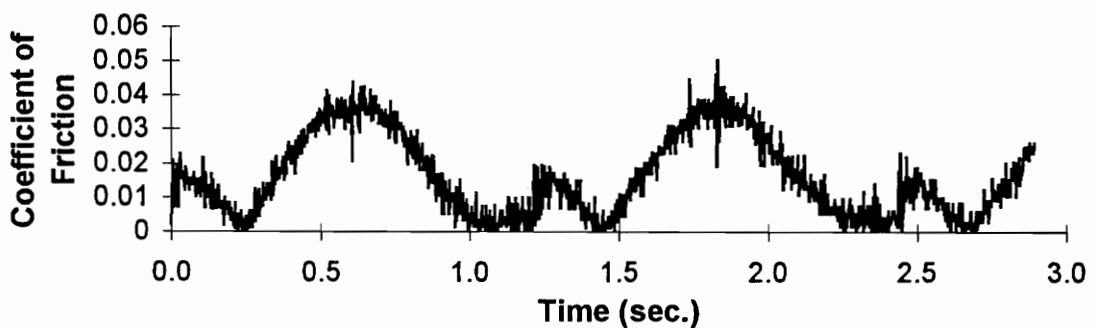


Figure 4.18 Coefficient of Friction at the Start of a High Damage Three-Hour Serum Test (test 16)

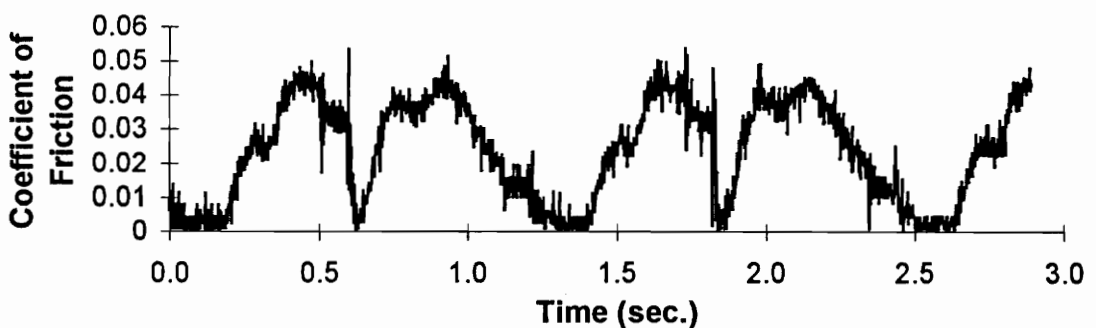


Figure 4.19 Coefficient of Friction at the End of a High Damage Three-Hour Serum Test (test 16)

As with the plots of tangential readings, the coefficient of friction became much more irregular and rough over the course of the test. This was accompanied by a very slight (0.01) increase in the maximum values of the coefficient of friction. This test was particularly interesting because it demonstrated that the presence of high amounts of damage does not necessarily mean that high values of friction will also be found. However, in other tests where significant damage was produced, the coefficient of friction also increased substantially, as will be shown later.

Average maximum values of the coefficient of friction from the serum tests were calculated and graphed in Figure 4.20. The relatively high value of friction seen in the second one-hour test (test 13) corresponded to a case of high wear. It is interesting to note that in two cases the coefficient of friction dropped during the first hour but then increased (in test 16) during the remainder of the test.

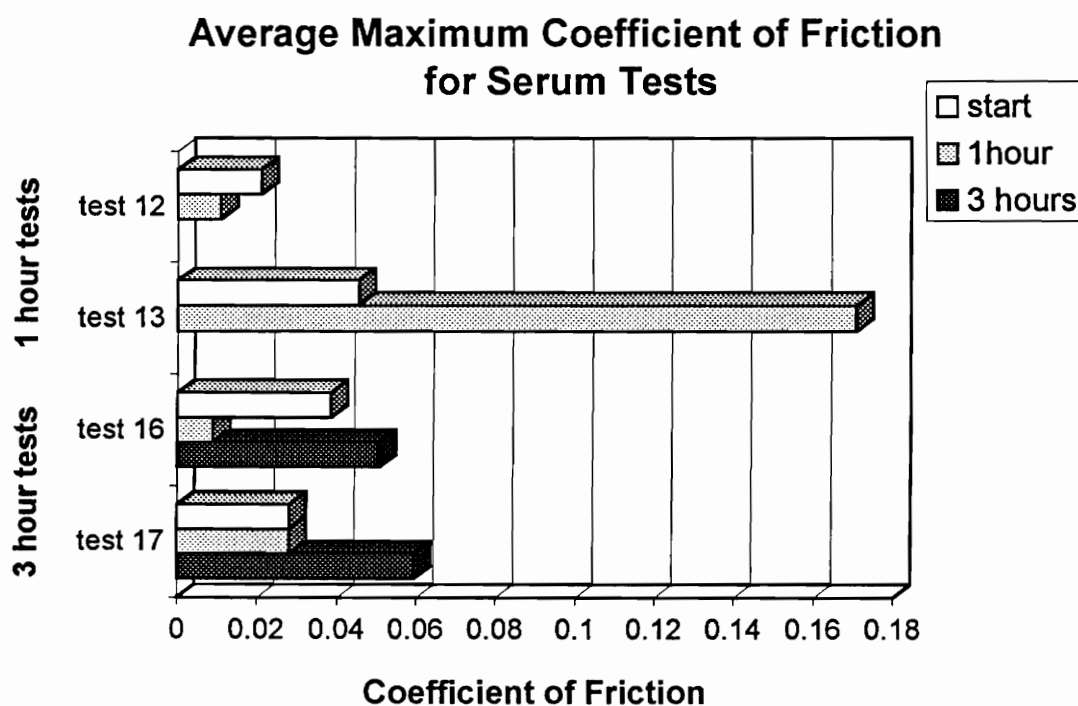


Figure 4.20 Average Maximum Coefficient of Friction for Serum Tests

4.1.3 Synovial Fluid Tests

Four synovial fluid cartilage-on-cartilage tests were conducted. Each test used the synovial fluid from the same joint that produced cartilage/bone plugs. These fluids were called A,B,C,D where fluids A and B were used in the two one-hour tests (tests 10,11) and fluids C and D were used in the three-hour tests (tests 14,15). Tangential force, displacement, and coefficient of friction data obtained from the three-hour tests are represented in Figures 4.21 - 4.33. The first set (Figures 4.21 - 4.26) of six plots is from a low wear three-hour test with synovial fluid C (test 14). The second set (Figures 4.27 - 4.32) is from a high wear three-hour test with synovial fluid D (test 15). Possible causes of this high wear are discussed in detail in Chapter 5.

The tangential force was graphed for two and a half cycles at the start and end of the low wear synovial test in Figures 4.21 and 4.22.

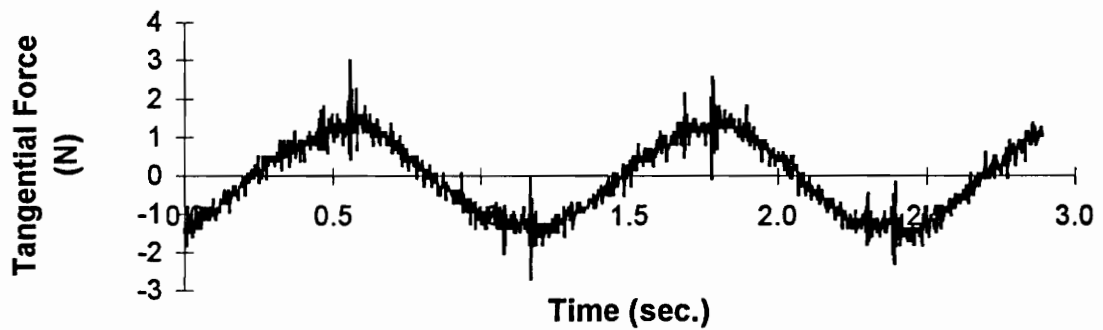


Figure 4.21 Tangential Force at the Start of a Low Wear Three-Hour Synovial Fluid Test (test 14)

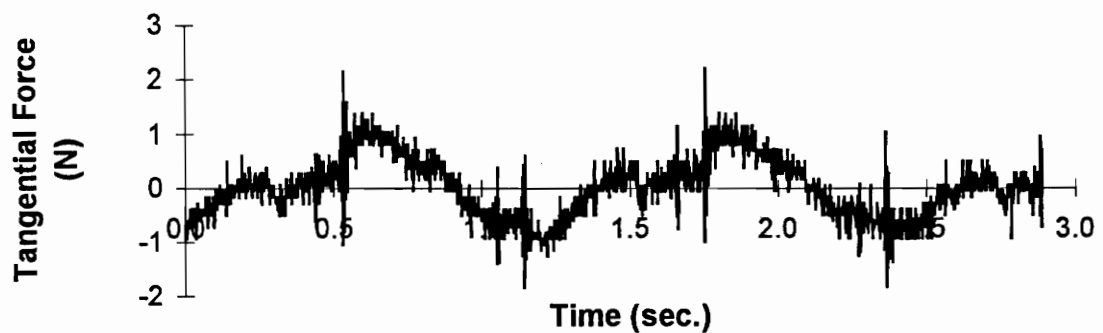


Figure 4.22 Tangential Force at the End of a Low Wear Three-Hour Synovial Fluid Test (test 14)

These plots of the frictional force show that there was actually a slight decrease in the maximum force over the length of the test. A comparison of Figures 4.21 and 4.22 shows that although the maximum force decreased by about 30%, the graph changed from a relatively smooth sine wave shape to a more irregular pattern.

The displacement at the start and end of the low wear synovial test is graphed in figures 4.23 and 4.24. The scale is the same in both plots to show the changes more clearly.

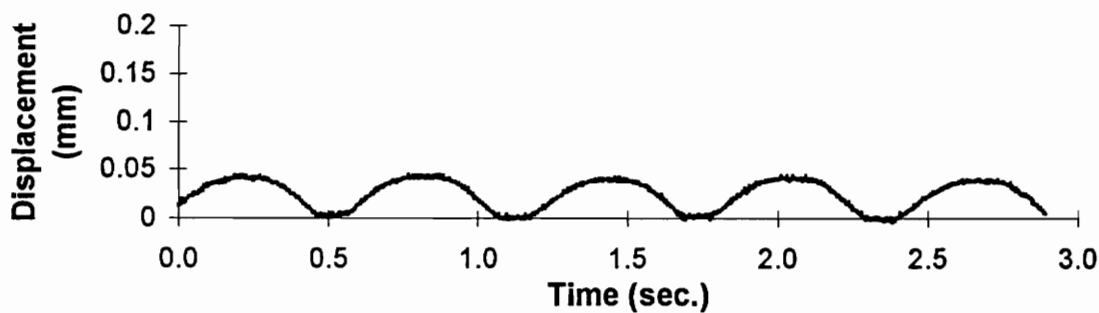


Figure 4.23 LVDT Displacement at the Start of a Low Wear Three-Hour Synovial Fluid Test (test 14)

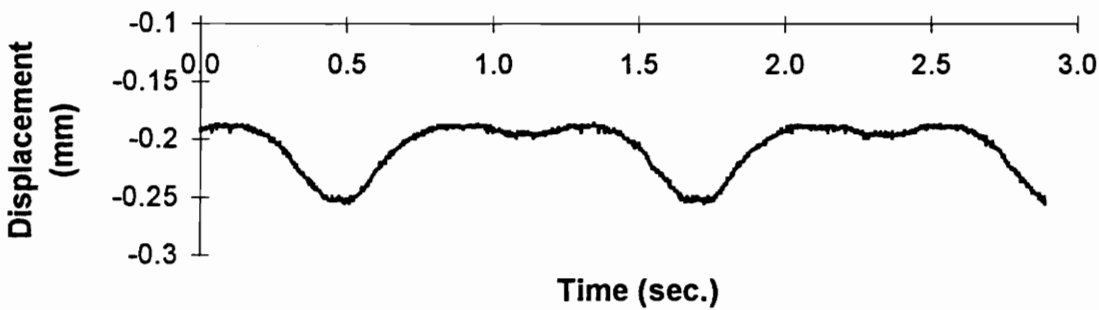


Figure 4.24 LVDT Displacement at the End of a Low Wear Three-Hour Synovial Fluid Test (test 14)

Figures 4.23 and 4.24 show that during this test, there was almost no change in the peak to valley distance (0.06 mm). However, 0.25 mm of LVDT displacement did occur. The curve also changed shape while remaining smooth, indicating that changes occurred during the test other than simple uniform LVDT displacement.

The coefficient of friction over two and a half cycles is shown in Figures 4.25 and 4.26.

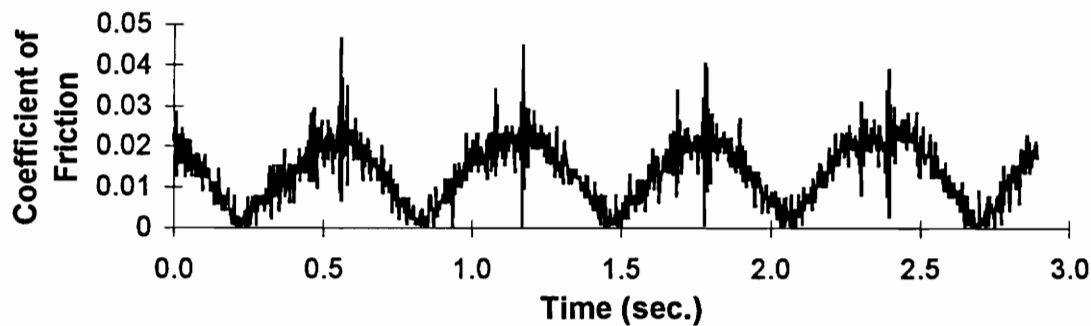


Figure 4.25 Coefficient of Friction at the Start of a Low Wear Three-Hour Synovial Fluid Test (test 14)

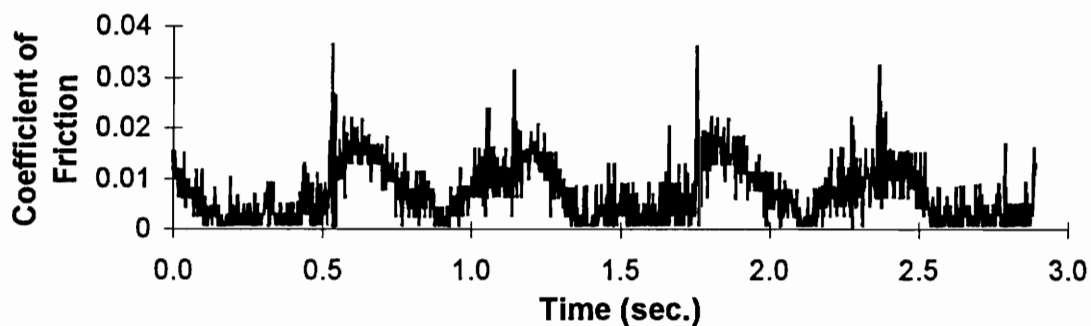


Figure 4.26 Coefficient of Friction at the End of a Low Wear Three-Hour Synovial Fluid Test (test 14)

A comparison of Figures 4.25 and 4.26 shows that the maximum coefficient of friction decreased over the length of the test. However, as with other low wear tests, the friction graph changed from a smooth, regular shape at the start of the test to a more irregular curve after three hours.

The three-hour test with synovial fluid D (test 15) produced high wear and damage to the lower specimen. Two and a half cycles of tangential, displacement, and coefficient of friction data are presented in Figures 4.27 - 4.32. Graphs of the tangential (frictional) force at the start and end of the test are shown in Figures 4.27 and 4.28. The possible causes of this abnormally high wear are discussed in detail in Chapter 5.

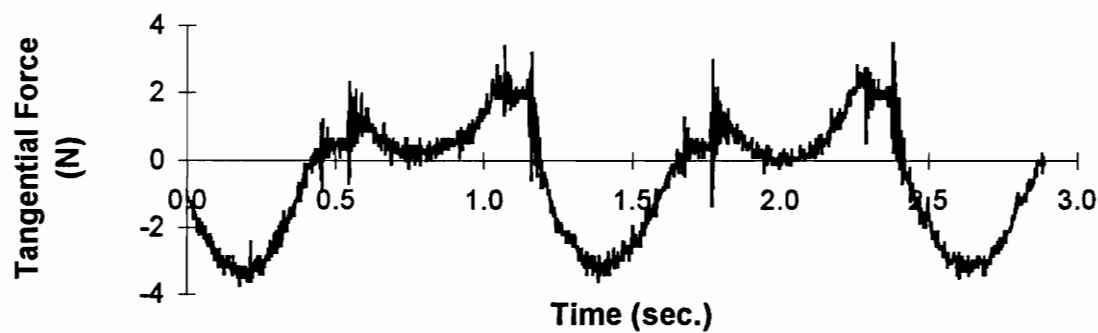


Figure 4.27 Tangential Force at the Start of a High Wear Three-Hour Synovial Fluid Test (test 15)

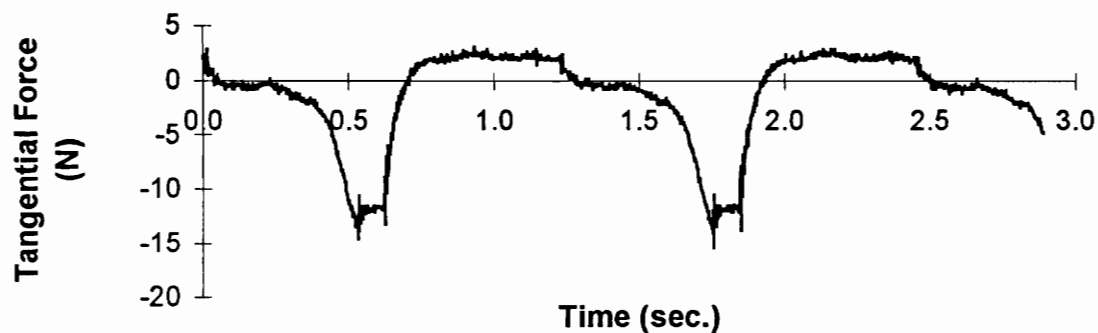


Figure 4.28 Tangential Force at the End of a High Wear Three-Hour Synovial Fluid Test (test 15)

The first item noted when running test 15 was the lack of a smooth sine wave-like plot even at the start of the test. The irregular graph of the tangential force in Figure 4.27 is clearly different from the other test beginnings. Figure 4.28 indicates that the frictional force increased drastically (nearly 15 N) in one direction of sliding while the other direction continued to produce relatively low frictional forces (2.5 N).

Vertical Displacement was measured at the start and end of the test and is graphed below in Figures 4.29 and 4.30. The scale is the same in both plots to show changes more clearly.

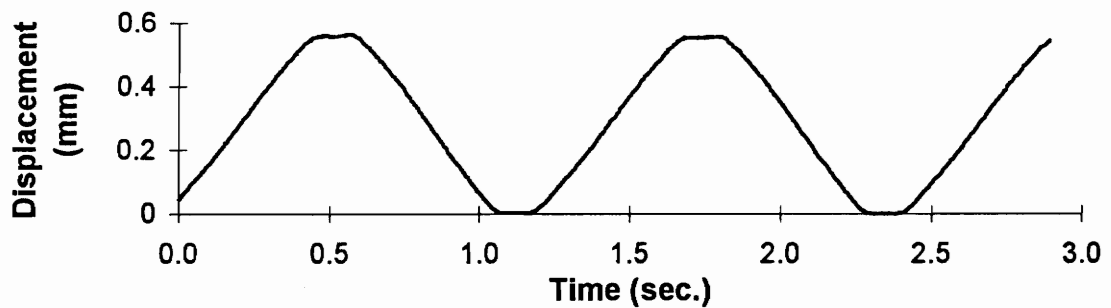


Figure 4.29 LVDT Displacement at the Start of a High Wear Three-Hour Synovial Fluid Test (test 15)

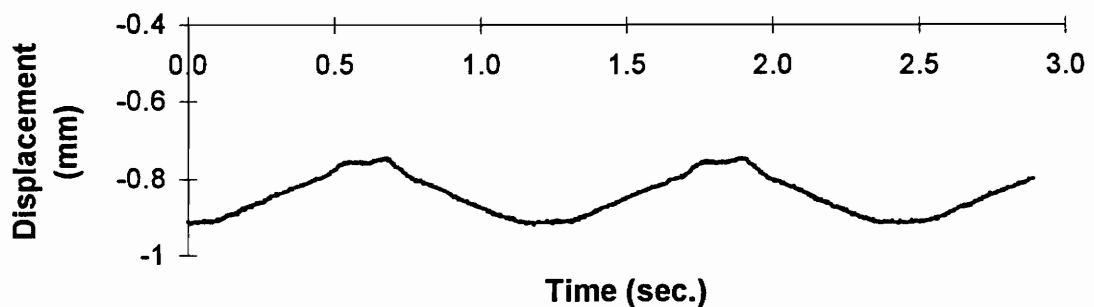


Figure 4.30 LVDT Displacement at the End of a High Wear Three-Hour Synovial Fluid Test (test 15)

By comparing the starting displacement shown in Figure 4.29 with other tests, it is evident that this test started with a larger peak to valley distance (nearly 0.6 mm). This large displacement over the course of a cycle meant that the upper cartilage plug was forced to climb these hills and remove or deform the surface. As Figure 4.30 shows, the peak to valley height was greatly lowered to less than 0.2 mm by the end of this three-hour test. The peaks in

displacement are still in the original locations. However, the curve is no longer smooth. Chapter 5 contains a detailed discussion of this test.

Figures 4.31 and 4.32 are graphs of the coefficient of friction at the beginning and end of the three-hour high wear synovial fluid test. Notice the vertical scale is not the same in these two plots.

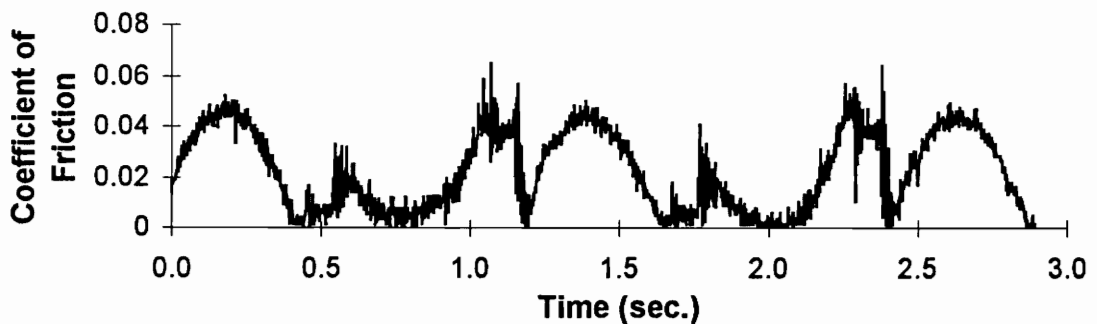


Figure 4.31 Coefficient of Friction at the Start of a High Wear Three-Hour Synovial Fluid Test (test 15)

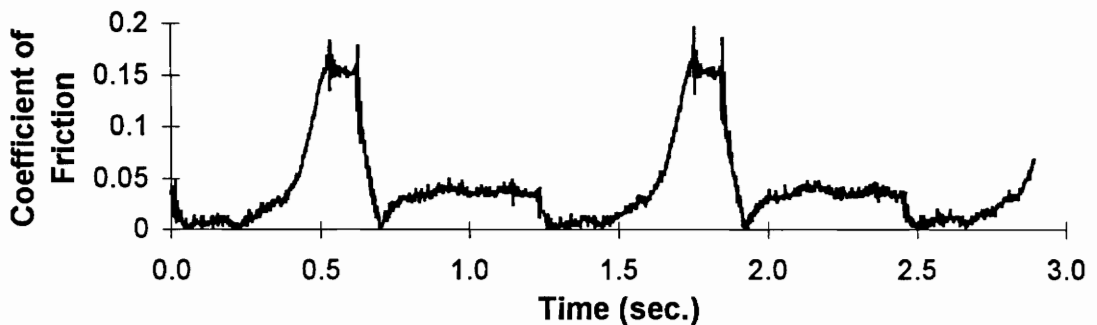


Figure 4.32 Coefficient of Friction at the End of a High Wear Three-Hour Synovial Fluid Test (test 15)

As with the frictional force plot at the start of the test (Figure 4.27), the irregular plot of the coefficient of friction (Figure 4.31) is in sharp contrast with

the normally smooth plots usually present at the beginning of tests. Figure 4.32 at the end of the test shows that over three hours there was an increase in the maximum value of the coefficient of friction from 0.02 to 0.16 (in one direction of sliding). While the other direction of sliding produced a relatively constant coefficient of friction of 0.05 over the entire test. The peak in Figure 4.32 corresponds with the peak in the displacement curves.

The average maximum coefficients of friction for all of the synovial tests are graphed in Figure 4.33.

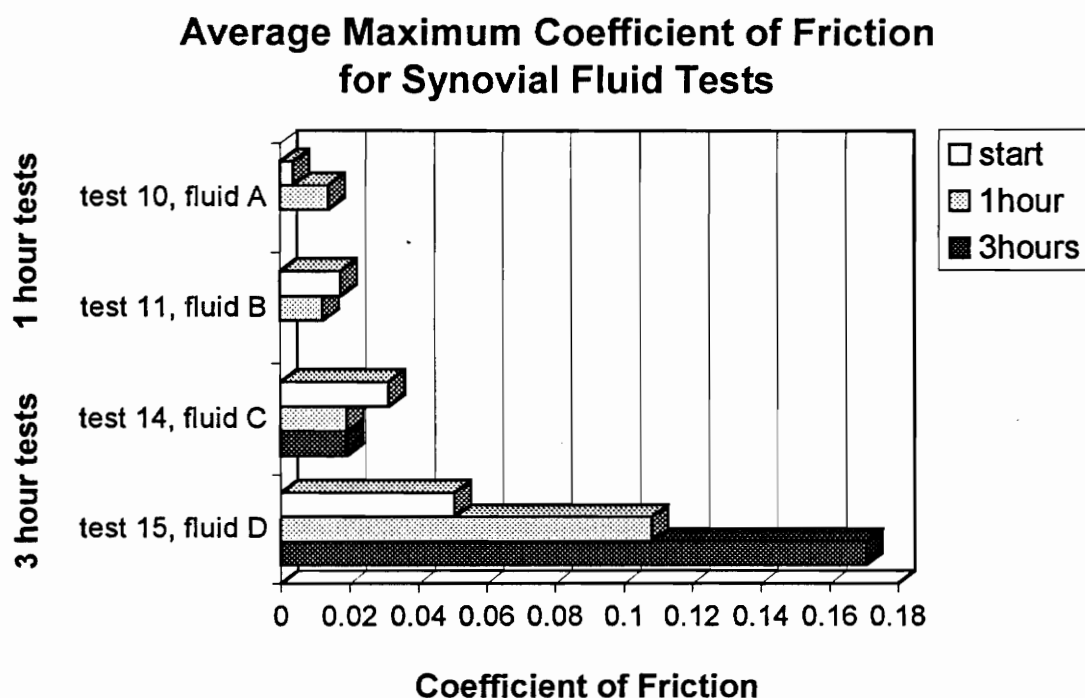


Figure 4.33 Average Maximum Coefficient of Friction for Synovial Fluid Tests

Synovial fluid tests A, B, and C all produced extremely low friction values. The test with fluid C showed that in synovial fluid tests, it is possible to have decreasing friction even over a three-hour test. This feature was never seen in any other tests with serum or saline solution. Synovial test D was the high wear test. The coefficient of friction started out relatively high (for a synovial fluid test) and continued to increase over the entire test. In general, all three test fluids started with coefficients of friction of approximately 0.02 or lower. The differences in friction showed up when looking at the change in friction over a test. By the end of the tests the buffered saline produced coefficients of friction of 0.04 or higher (up to 0.17). The serum coefficients of friction generally remained below 0.04. Synovial fluid showed coefficients of friction of 0.02 or less (except for test 15). This is at least 50% lower friction than either of the other fluids.

4.2 CARTILAGE WEAR AS DETERMINED FROM HYDROXYPROLINE ANALYSIS

Cartilage wear in each of the cartilage-on-cartilage tests was measured using the hydroxyproline assay as described in section 3.5.1. In order to convert from the mass of hydroxyproline detected to the amount of cartilage worn, unworn cartilage was analyzed for hydroxyproline content. A sample of cartilage was taken from one of the tested joints and dehydrated. This dried cartilage was weighed and subjected to acid hydrolysis. Hydroxyproline analysis was performed, and the percent of hydroxyproline in hydrated cartilage was calculated as 2.1% assuming a cartilage water content of 75% (water content can range from 65-80% [9]). This compares closely to the value of 2% found using hydroxyproline percentages in the literature [9,13]. Synovial fluids A, B, C, and D were tested for hydroxyproline content, and each was found to contain a significant amount (between 12 and 26 $\mu\text{g/ml}$) of hydroxyproline. This pre-test hydroxyproline was subtracted from the concentrations found in the assays of the test washings. Only one synovial fluid test produced visible damage and measurable hydroxyproline due to wear. Samples of the untested serum were also analyzed for hydroxyproline. This assay showed that the samples of serum used in this study contained 28.14 μg of hydroxyproline in 1.5 ml of fluid. As with the synovial fluid results, the serum hydroxyproline levels were subtracted from the test washing results to give actual cartilage wear.

RESULTS

Graphs of cartilage wear in the one and three-hour tests are presented in Figures 4.34 and 4.35.

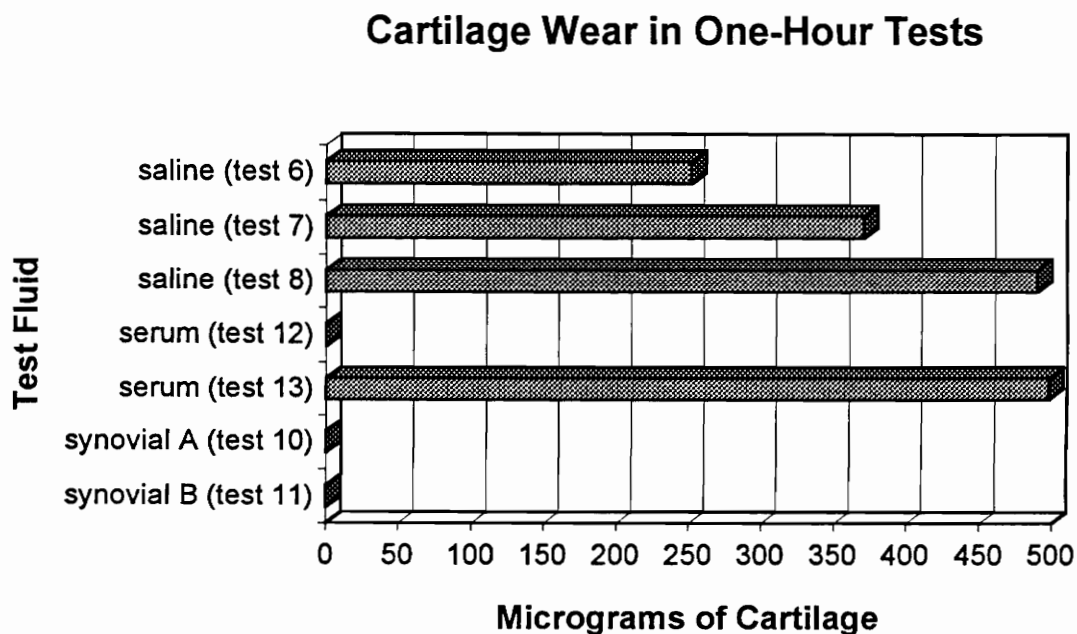


Figure 4.34 Measurement of Cartilage Wear in One-Hour Tests

As Figure 4.34 indicates, all three of the one-hour saline tests and the second serum test produced measurable and significant wear. The first serum test and the two synovial fluid tests (A and B) did not produce detectable wear. The hydroxyproline in these three tests (tests 10,11,12) was completely accounted for by the concentrations found in the pre-test fluids. The high wear of the second serum test (test 13) was also visible by eye when viewing the lower cartilage specimen after the test.

Cartilage wear for the three-hour tests is graphed in Figure 4.35.

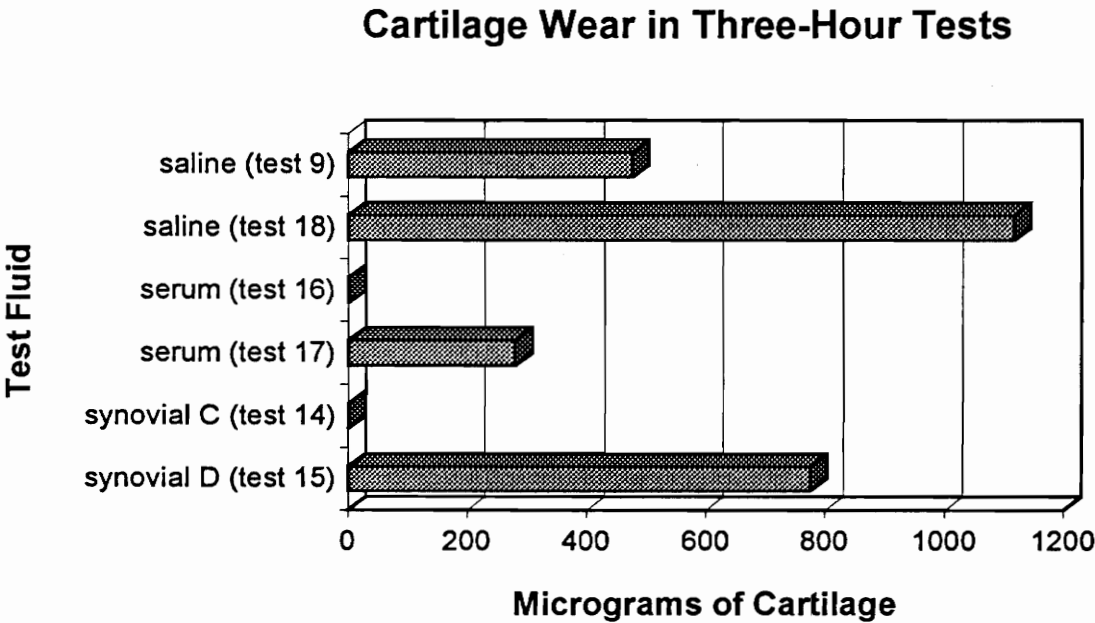


Figure 4.35 Measurement of Cartilage Wear in Three-Hour Tests

As with the one-hour tests, Figure 4.35 indicates that both saline tests (tests 9,18) and one serum test (test 17) produced measurable wear. No detectable increase in hydroxyproline concentrations due to wear were seen in the one serum test (test 16) and the synovial fluid C test. This meant that no wear was detected in the first three-hour serum test and synovial test C. However, cartilage wear was detected in one serum test (test 17) and in synovial fluid test D. Surface damage could be seen by eye in each of the tests that produced measurable wear.

4.3 ESEM AND SEM RESULTS

Environmental scanning electron microscopy and scanning electron microscopy were both used to view worn and unworn cartilage specimens at high magnifications. Sample preparation and instrument use are described in section 3.5.2. A selection of ESEM and SEM photographs is included here to show the application and value of electron microscopy in cartilage damage analysis. All wear tracks are horizontal and parallel to the direction of sliding in these photographs.

Figure 4.36 is an ESEM photograph of an unworn cartilage surface. The cartilage has begun to dry out and small circular indentations due to subsurface cells are visible. These cells are 10 to 15 μm in diameter.

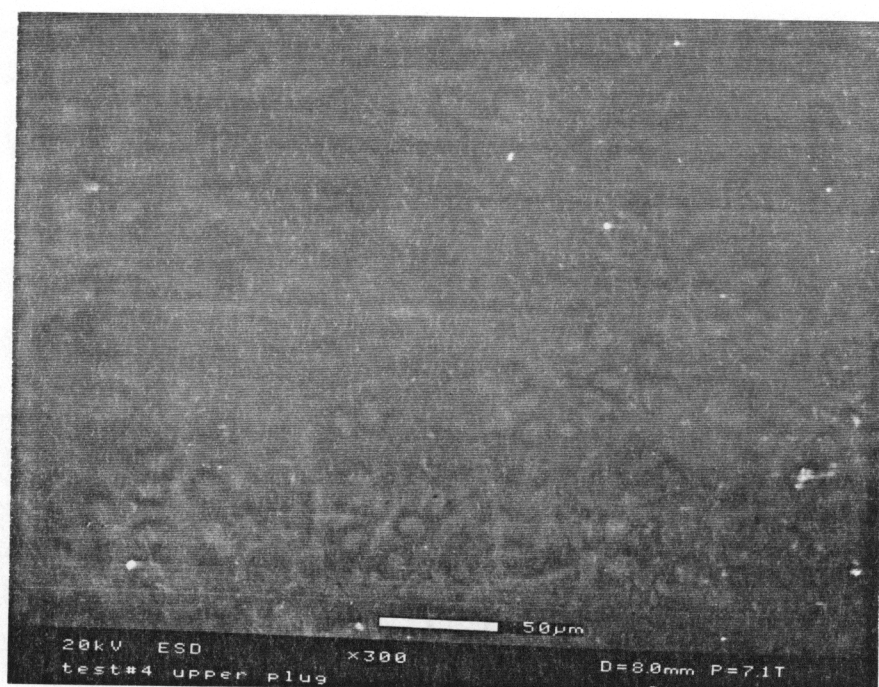


Figure 4.36 ESEM Photograph of an Unworn Surface Showing Cells (300X magnification)

Figure 4.37 is an SEM photograph of an unworn cartilage surface. Cell outlines are also visible in this picture. Contours on the cartilage surface and even some bundles of collagen fibers are visible. Higher magnifications are possible with SEM photographs than with the ESEM. Although the ESEM does not require sample preparation, it was difficult to keep the cartilage at its normal hydration level. A film of water was almost always present on the cartilage surface which created pictures that appear to be out of focus. The only way to overcome this was to allow the sample to become dehydrated. However, this changed the surface contours. Therefore, it was found that the SEM produced more reliable detailed photographs.

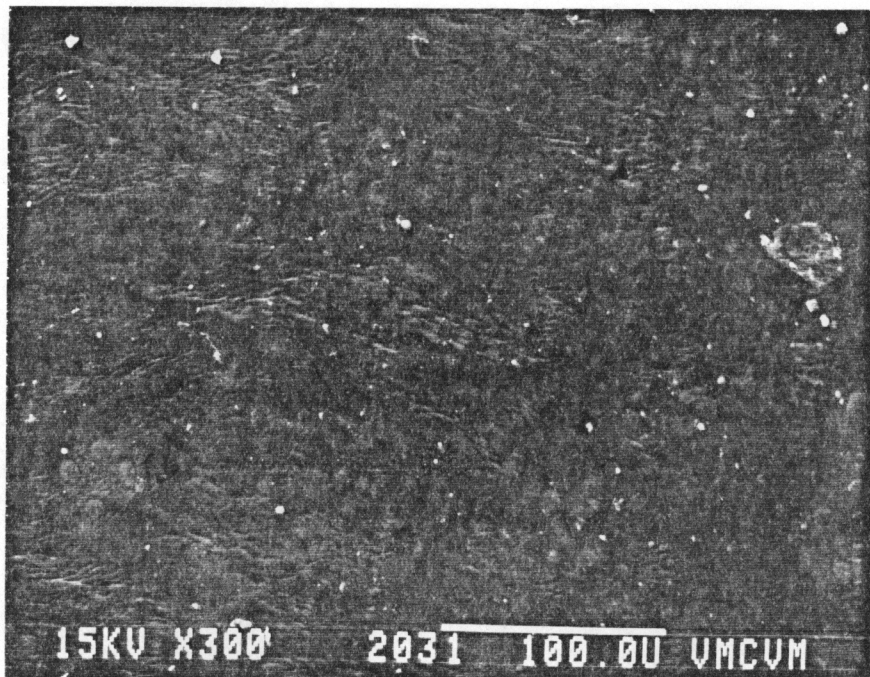


Figure 4.37 SEM Photograph of an Unworn Surface Showing Cells (300X magnification)

An SEM photograph of the top cartilage plug from a three-hour saline test is shown in Figure 4.38. There are two distinct horizontal wear tracks visible that coincide with the direction of sliding. These wear scratches were the largest seen in any of the tests. This top plug produced severe damage to the lower test specimen. All of the tests consistently showed much more surface damage to the lower specimens than to the upper test plugs (qualitative observation).

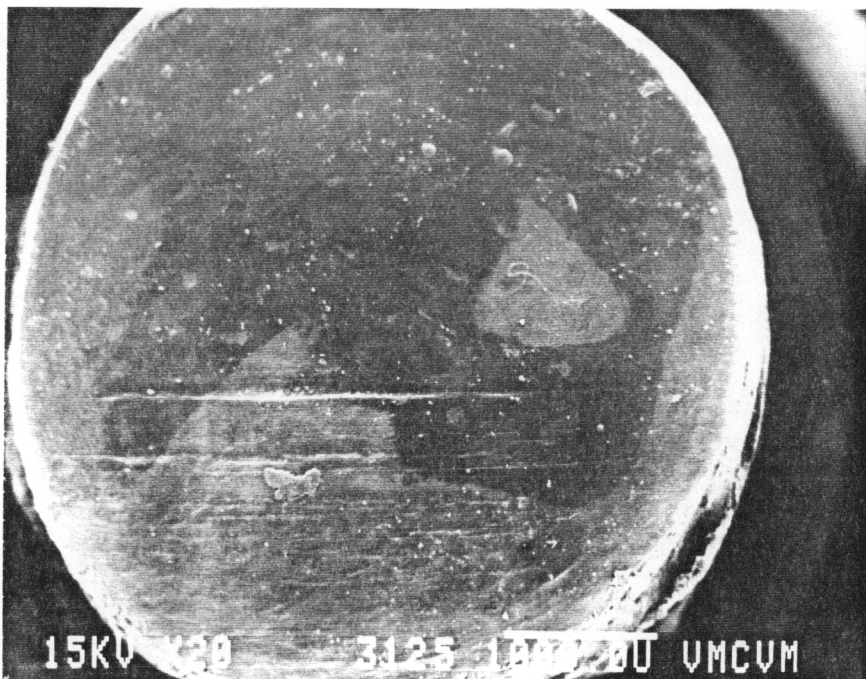


Figure 4.38 SEM Photograph of a Top Plug from a Three-Hour Saline Test (test 9; 20X magnification)

Figure 4.39 is an SEM photograph of an upper cartilage sample from a three-hour serum test (test 16). It is difficult to see any sign of wear on this plug. However, a large patch of cartilage was removed from the lower plug during the test. The light colored circle in the center of the picture is an artifact of sample preparation (this did not affect the surface topography).

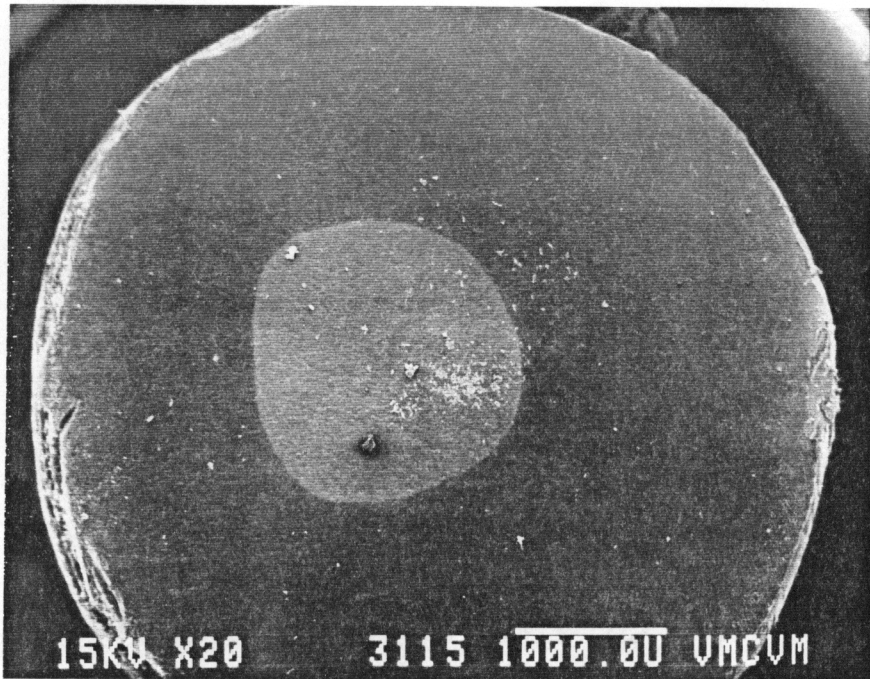


Figure 4.39 SEM Photograph of a Top Plug from a Three-Hour Serum Test (test 16; 20X magnification)

The SEM photograph in Figure 4.40 is of the center of the top plug from the same three-hour serum test as Figure 4.39 (test 16). The higher magnification of this photograph allows the surface detail to be seen more clearly. Again, the direction of sliding is horizontal in this picture. The smooth appearing cartilage of Figure 4.39 is shown here to be really quite rough (also rougher than the unworn cartilage in figure 4.37) on the microscopic level.

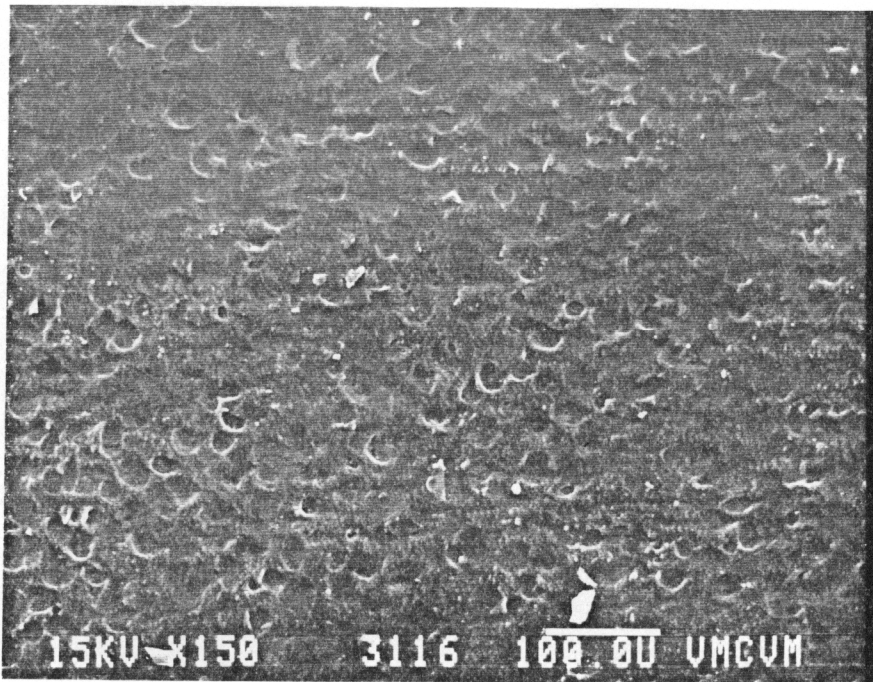


Figure 4.40 SEM Photograph of a Top Plug from a Three-Hour Serum Test (test 16; 150X magnification)

Figure 4.41 is an SEM photograph from the same three-hour serum test top plug center region as Figures 4.39 and 4.40 (test 16). The magnification is increased to 300X in this picture to give detail to the circular depressions first seen in Figure 4.40. Microscopic cracks in the cartilage are now visible and the undulations of the surface are apparent. Even at this high level of magnification there is still no evidence of surface scratches to the top plug (horizontal sliding). However, the surface is rougher than unworn cartilage; there small flaps visible near underlying cells.

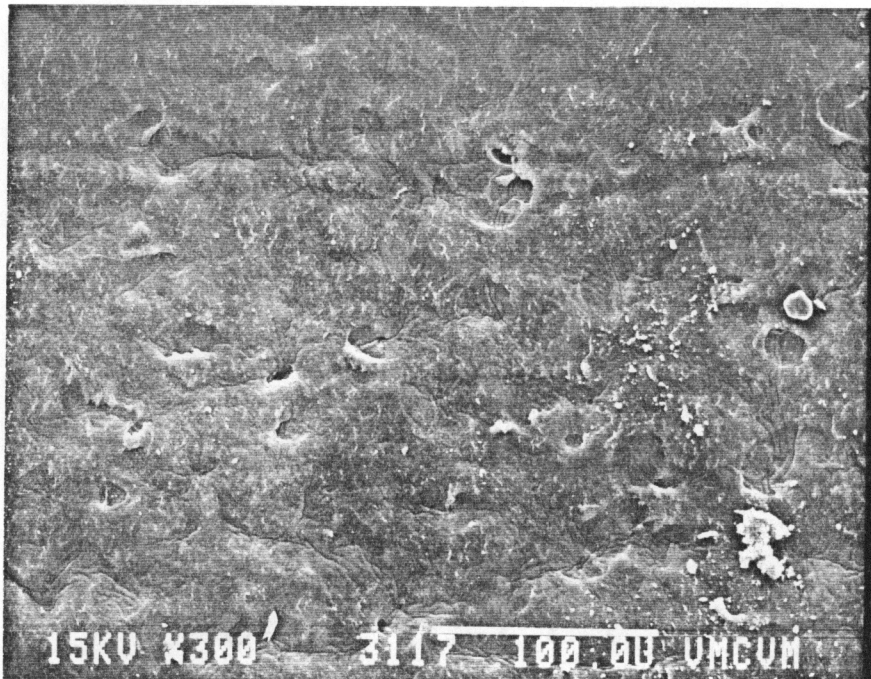


Figure 4.41 SEM Photograph of a Top Plug from a Three-Hour Serum Test (test 16; 300X magnification)

An SEM photograph of a top plug from a high wear three-hour synovial fluid test (test 15) is shown in Figure 4.42. This photograph shows that on the left side of the plug, a surface layer of cartilage was removed during the test. However, no damage is visible on the rest of the plug surface. This plug was also photographed in the photomicroscope (see Figure 4.45). Other top plugs were viewed in the SEM and photographed. Even in other high wear tests, there was remarkably little damage to the top plugs. No wear tracks or damage could be seen on these specimens.

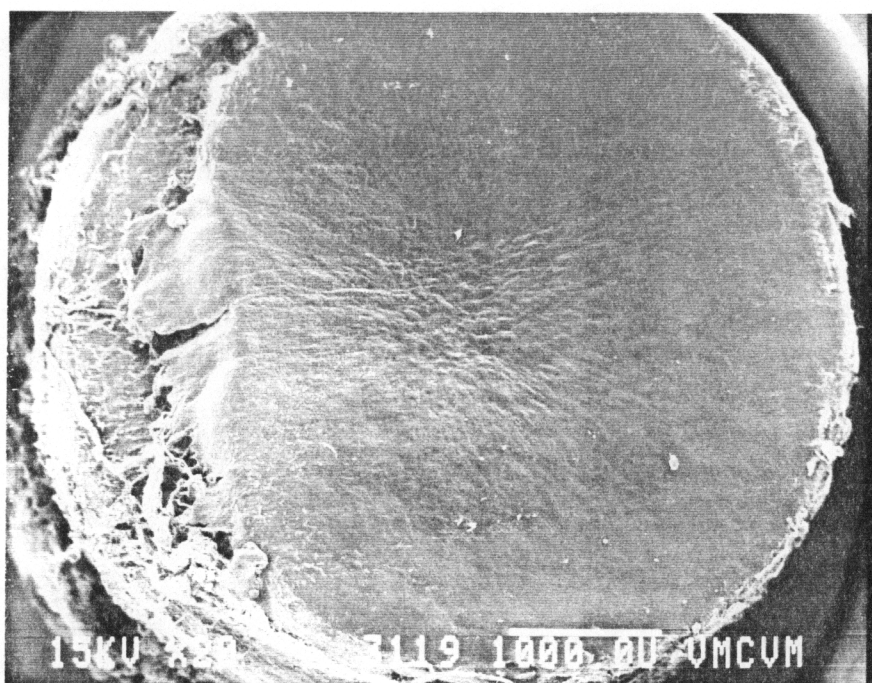


Figure 4.42 SEM Photograph of a Top Plug from the Three-Hour High Wear Synovial Fluid Test (test 15; 20X magnification)

4.4 OPTICAL MICROSCOPE FINDINGS

All of the upper and lower cartilage specimens were viewed before and after testing using the Wild-Heerbrugg photomicroscope. Photomicrographs of the cartilage surfaces were taken of nearly every sample. However, only representative or interesting examples are included and described in section 4.4.1. Cross-sectional slides were prepared from the lower test specimens as described in section 3.5.3. These slides were viewed and photographed at high levels of magnification. A representative selection of these photographs is included and described in section 4.4.2.

4.4.1 Photomicrography

Photomicrographs were taken using mainly side lighting with a small amount of overhead illumination. To gain the best contrast, each sample was tilted until the most detail was visible. Also, any water on the surface of the specimens was allowed to evaporate before useful pictures could be taken. Figure 4.43 is a photomicroscopic picture of the top plug from a three-hour saline test (test 9). Several large horizontal wear scars are visible near the middle of the plug. These scars are in the direction of sliding. This plug was also viewed in the SEM and the same wear scars were visible (see Figure 4.38).

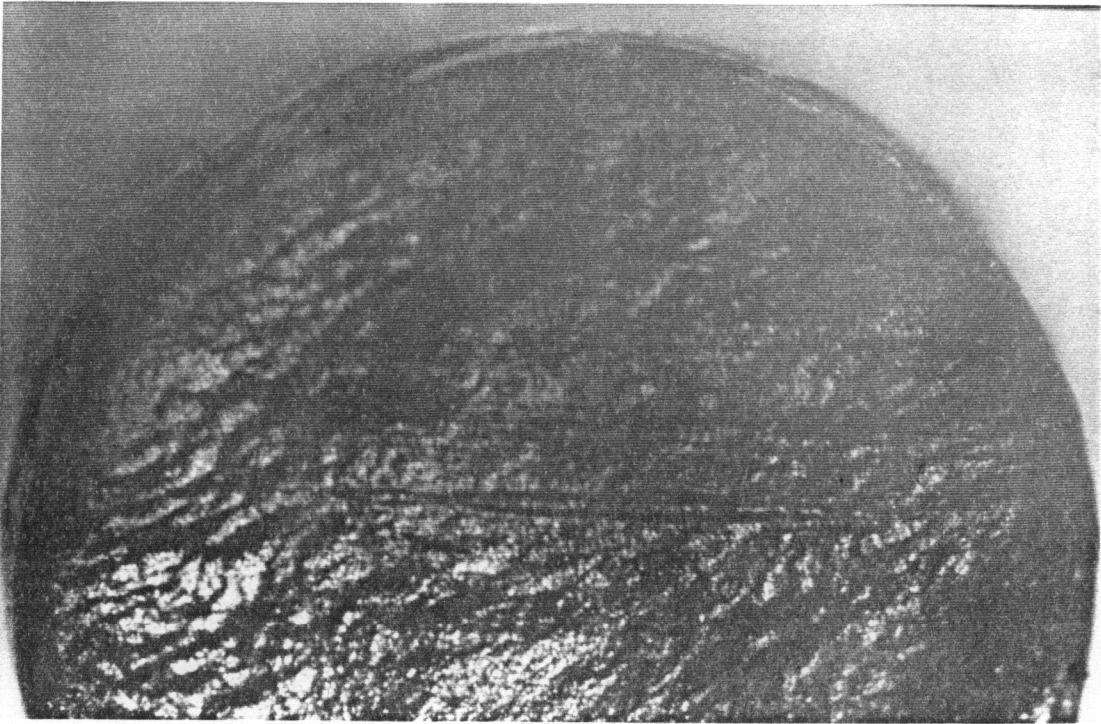


Figure 4.43 Photomicrograph of the Top Plug from a Three-Hour Saline Test (test 9; 16.25X magnification)

The picture in Figure 4.44 is a photomacrograph from a top plug of a three-hour serum test (test 17). A number of fine wear scars are visible near the upper edge of the plug. The center of the plug remained free of scratches in this test. This grouping of wear and damage was a common occurrence seen when viewing the top plugs macroscopically.

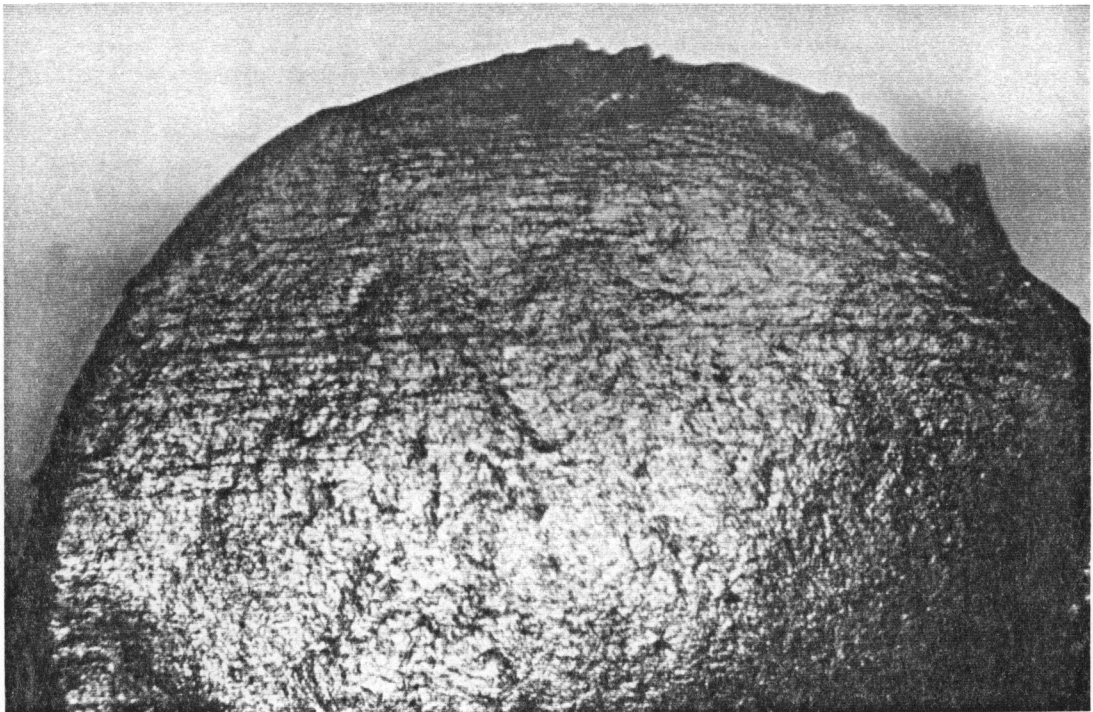


Figure 4.44 Photomacrograph of the Top Plug from a Three-Hour Serum Test (test 17; 16.25X magnification)

Lower plugs were also photographed in the photomicroscope. The bottom plug from a three-hour saline test is presented in Figure 4.45 (test 18). This photograph was taken inside the wear track. Fine horizontal scratches are visible on the left and a large rough area is seen on the right. This plug was severely damaged at the right end of the track where the removal of the top layer of cartilage left a much rougher surface behind. The photomicroscope showed that the damaged top layer was actually still attached and was not collected in the test washings.



Figure 4.45 Photomicrograph of the Bottom Plug from a Three-Hour Saline Test (test 18; 16.25X magnification)

Figure 4.46 is a photomacrograph of a bottom plug from a one-hour synovial fluid test with little damage (test 10). Most of the top portion of this photograph is from the center of the wear track. The area along the bottom of the picture is unworn. Very fine horizontal scratches are visible in the center of the wear track, and a general depression of the entire track compared to the unworn area is apparent.

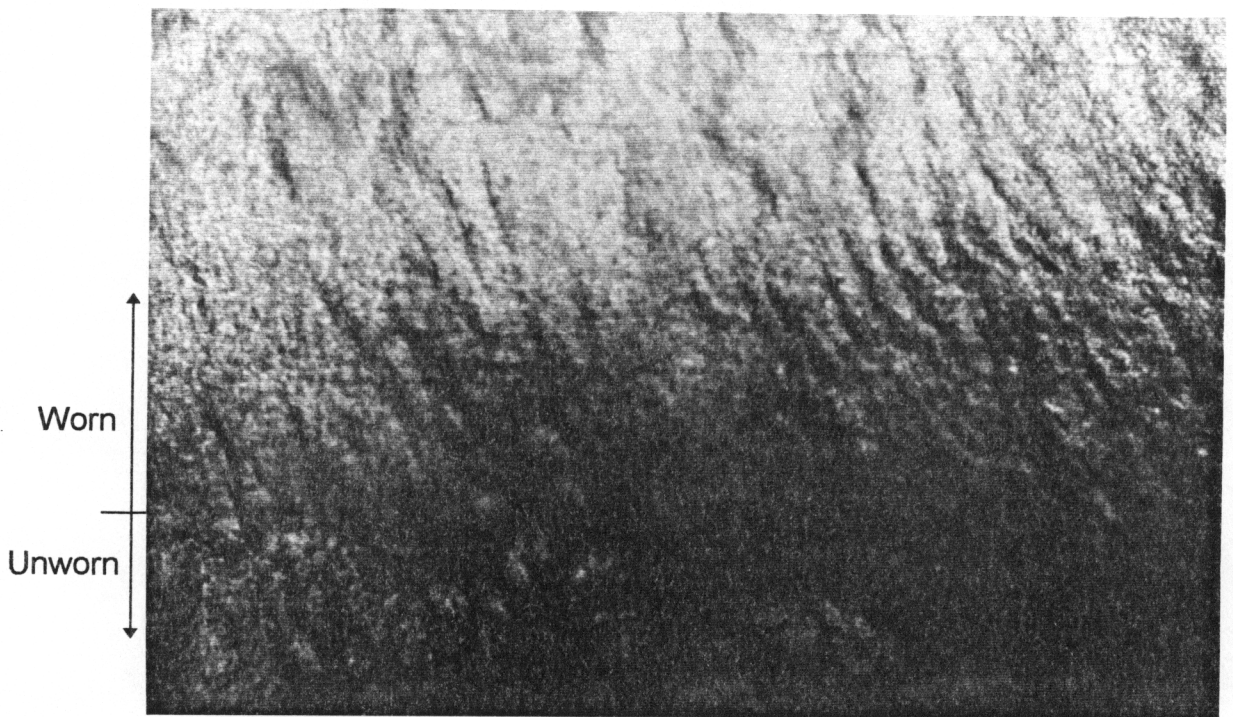


Figure 4.46 Photomacrograph of the Bottom Plug from a One-Hour Synovial Fluid Test (test 10; 16.25X magnification)

The bottom plug from the high wear synovial fluid test is shown in Figure 4.47 (test 15). This test produced damage to the plug very similar to that of the saline test photograph in Figure 4.45 (test 18). Again, a portion of the cartilage surface was removed at the right end of the wear track. Fine horizontal scratches are visible in the less damaged regions of the wear track. This photograph must be used along with results obtained from the LVDT, strain ring, and hydroxyproline testing when drawing any conclusions about the presence or cause of this damage. This test will be discussed in more detail in Chapter 5.

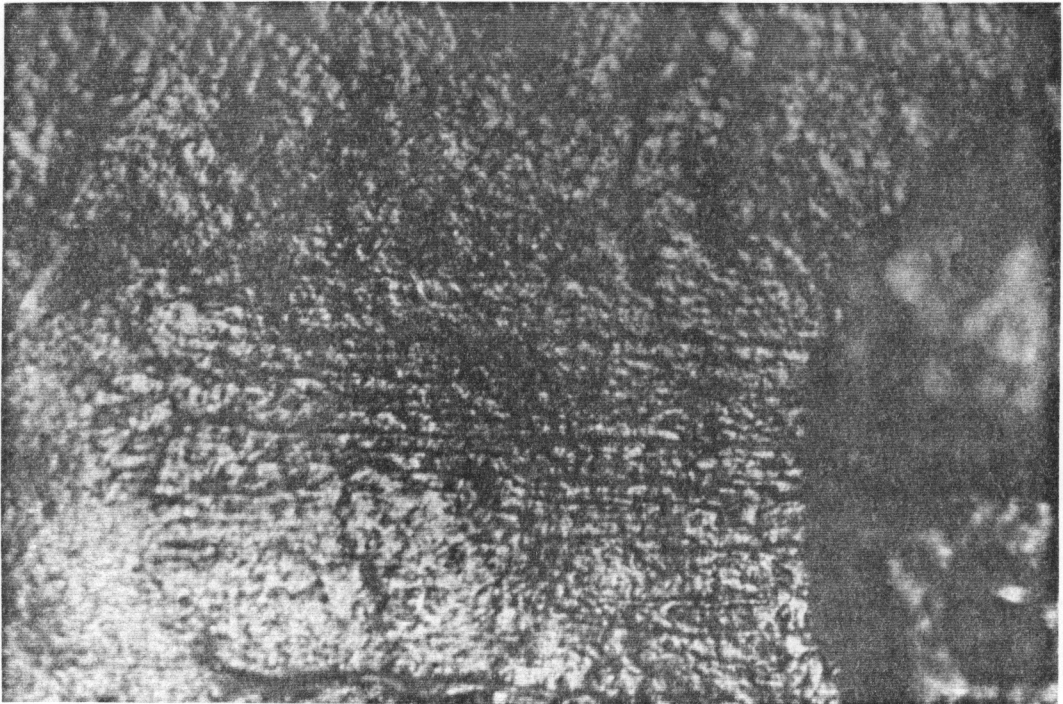


Figure 4.47 Photomicrograph of the Bottom Plug from a Three-Hour High Wear Synovial Fluid Test (test 15; 32.25X magnification)

4.4.2 Stained Slides

Two different stains were used on the cross-sectional slides of lower test specimens. Hemotoxylin and eosin (H&E) was useful for highlighting the collagen fiber bundles while alcian blue emphasized the proteoglycan concentration distribution. The most useful feature of cross-sectional slides was the ability to view subsurface features.

An unworn section of cartilage stained with H&E is shown in Figure 4.48. The small dark spots spread throughout the section are chondrocytes that occupy oval shaped spaces or voids. These voids are termed lacunae and in a living animal, the hydrated cells fill these empty regions. The cells are fairly randomly spaced here near the surface and no empty lacunae are visible. This is the standard appearance of an unworn sample to compare with all other worn sections.

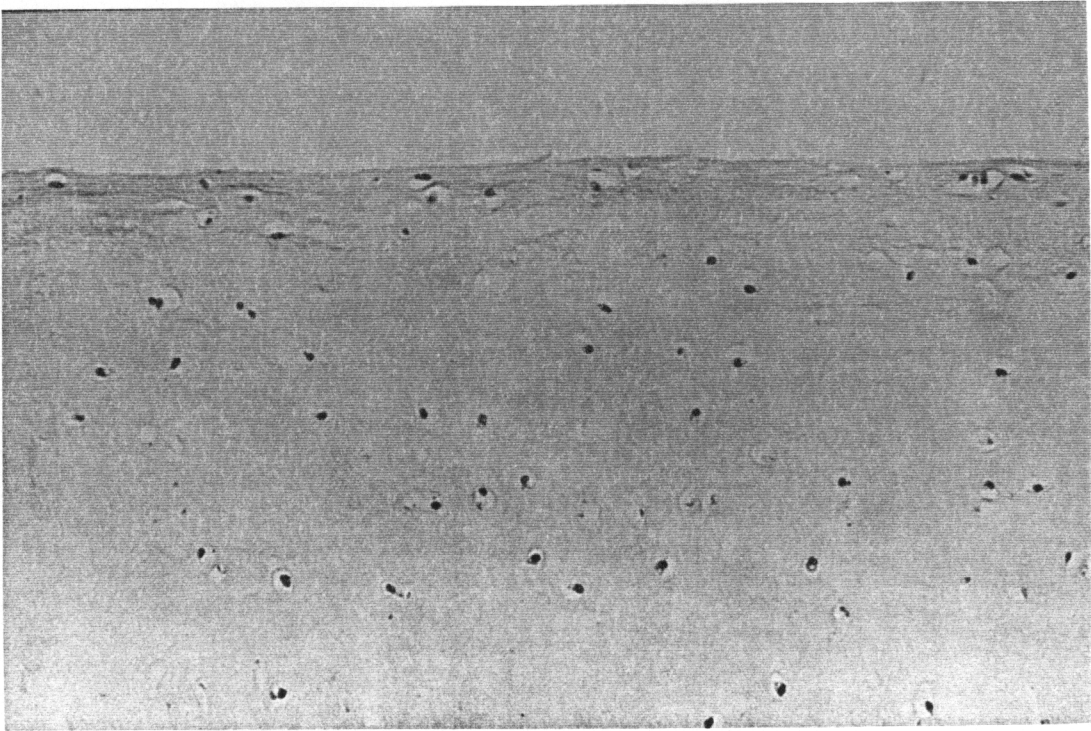


Figure 4.48 H&E Stained Section of Cartilage from Unworn Cartilage (500X magnification)

The photograph in Figure 4.49 is an alcian blue stained cartilage-bone cross section. The zones of the cartilage layer as shown in Figure 2.4 become more visible when stained with alcian blue. About two thirds of the way down through the cartilage layer, a lighter colored horizontal region is visible. This is called the tide mark and separates the top, uncalcified cartilage from the lower, calcified region. The lower-most portion of the photograph is subchondral bone.

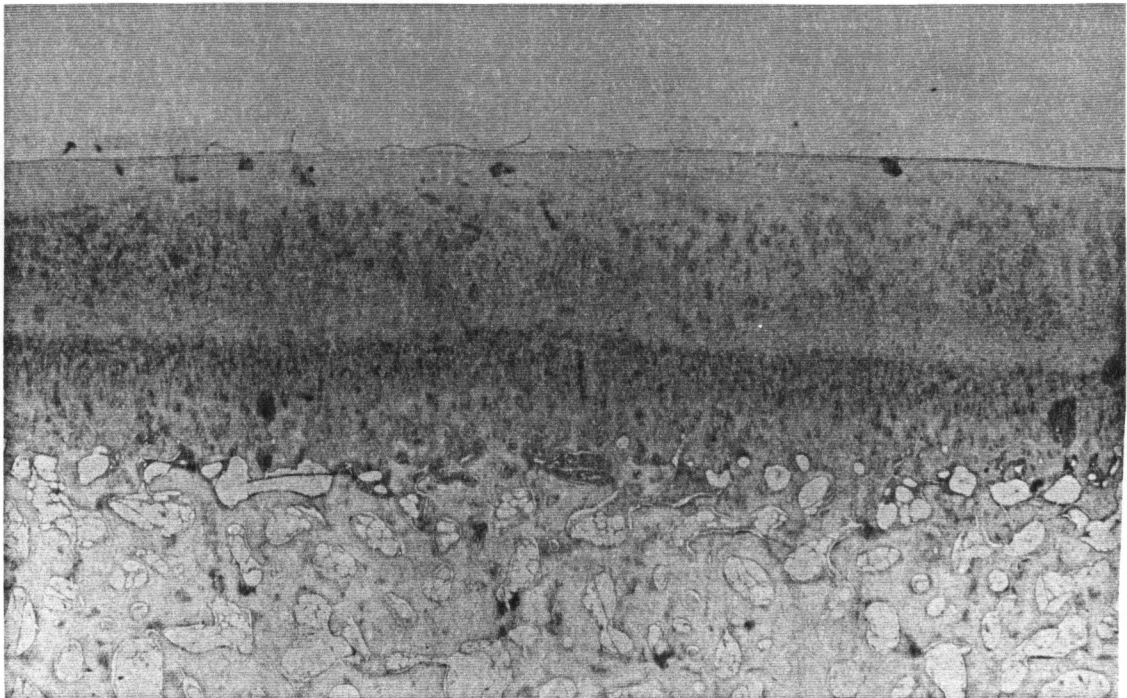


Figure 4.49 Alcian Blue Stained Section of Cartilage Highlighting Zones
(50X magnification)

Figure 4.50 is an H&E stained cartilage and bone cross section. This photograph is included to show how the tough connection between cartilage and bone is created. The subchondral bone surface is very rough and contains deep, irregularly shaped sockets. The lower most cartilage zone grows into these sockets to securely anchor the cartilage layer.

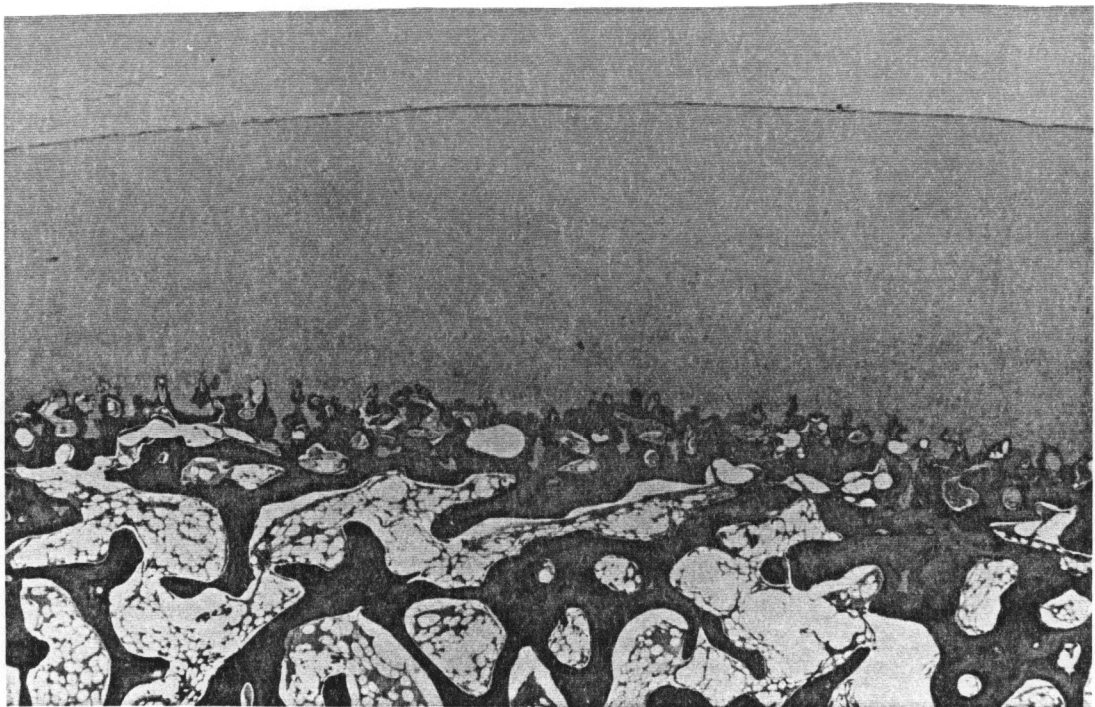


Figure 4.50 H&E Stained Section of Cartilage and Bone Showing Attachment to Subchondral Bone (50X magnification)

A partially worn section of cartilage from a lower plug is shown in Figure 4.51. This section was stained with alcian blue to highlight proteoglycan concentrations. The darker region to the right contains a higher concentration of proteoglycan molecules and is under the unworn area of the specimen. The lighter colored region on the left side of the photograph is under the wear track and shows a lower proteoglycan concentration. Most of the cross-sectional slides gave similar results, showing that tribological contact changed the proteoglycan organization or concentration in some way.

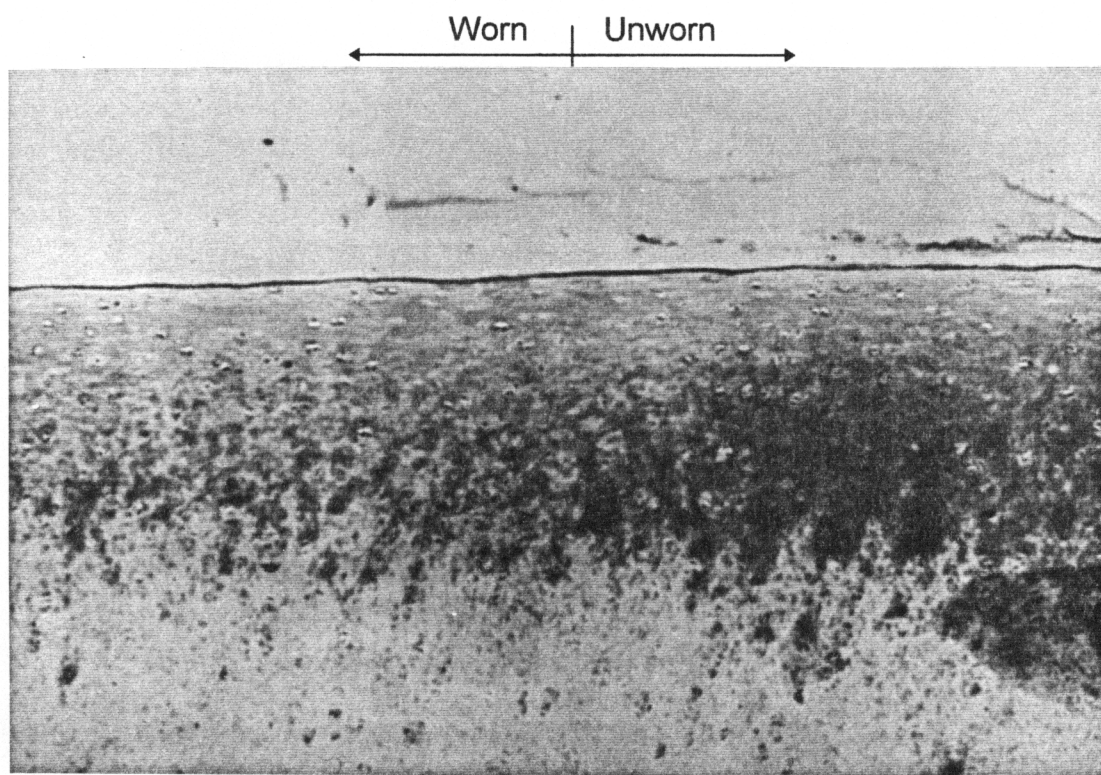


Figure 4.51 Alcian Blue Stained Section of Cartilage Showing Worn and Unworn Areas (100X magnification)

The alcian blue stained section of Figure 4.52 is from a worn region of a one-hour saline test (test 7). The surface of the cartilage contains a subsurface void that is much larger than the chondrocyte voids. This partially detached surface layer may be a precursor to the loose flaps seen at the upper left. The loose cartilage flaps seen on the left might have started as subsurface delamination and then eventually broken down creating loose fibers.

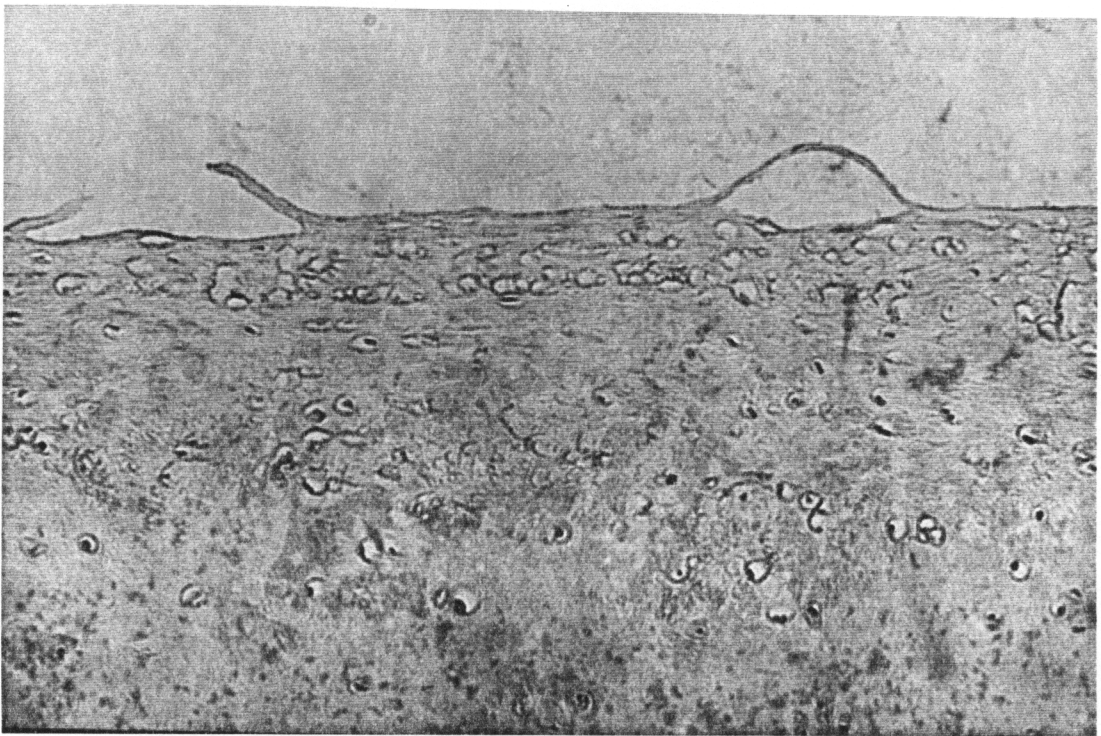


Figure 4.52 Alcian Blue Stained Section of Cartilage from a Worn Region of a One-Hour Saline Test Showing Pre-Flap Conditions (test 7; 500X magnification)

Figure 4.53 is a cross-sectional photograph of a worn section of cartilage from a three-hour saline test (test 9). A large cartilage flap has formed and loose fibers are visible. This damage has not become extreme enough to detach the cartilage flap. Therefore, hydroxyproline analysis will not show this as wear. The flap is of fairly uniform thickness and has grown by tearing through several of the lacunae. Exposed cells are seen within the crack.

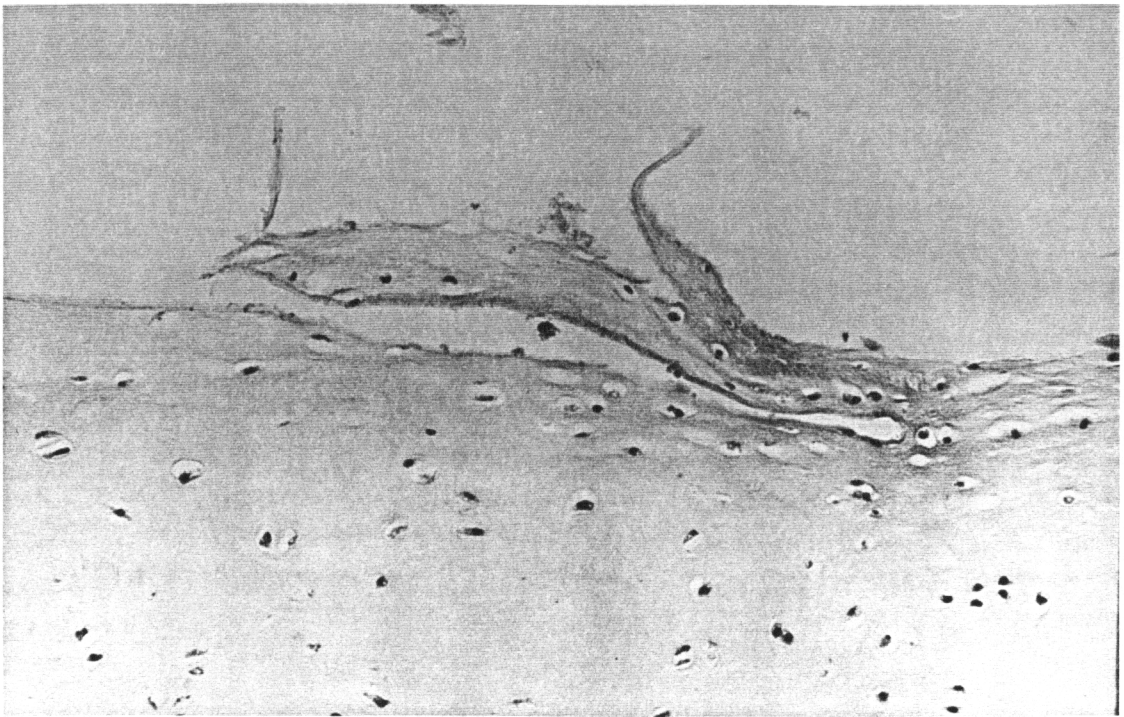


Figure 4.53 H&E Stained Section of Cartilage from a Three-Hour Saline Test Showing a Loose Flap (test 9; 500X magnification)

A cross section from another three-hour saline test is shown in Figure 4.54 (test 18). This test produced higher wear as is evident from the larger cartilage flap created. This flap is still connected to the cartilage surface at the right, but the free end of the flap shows severe deterioration. The area to the left is now the new cartilage surface and does not have the same appearance or properties as the original surface.

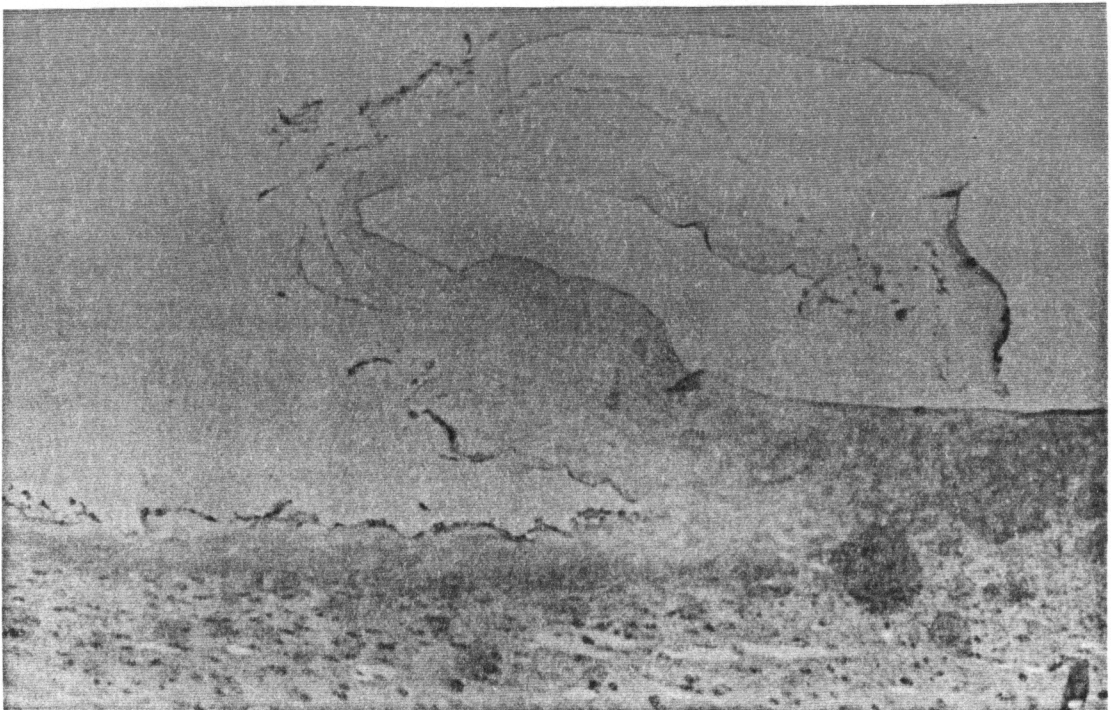


Figure 4.54 Alcian Blue Stained Section of Cartilage from a Three-Hour Saline Test Showing a Very Large Flap (test 18; 100X magnification)

The picture in Figure 4.55 was taken from within the worn region shown on the left of the previous photograph (Figure 4.54). The newly exposed surface is quite rough and loose fibers are seen. This region of cartilage contains collagen fibers that are randomly oriented instead having a horizontal arrangement as those found at the outer-most layer [9].

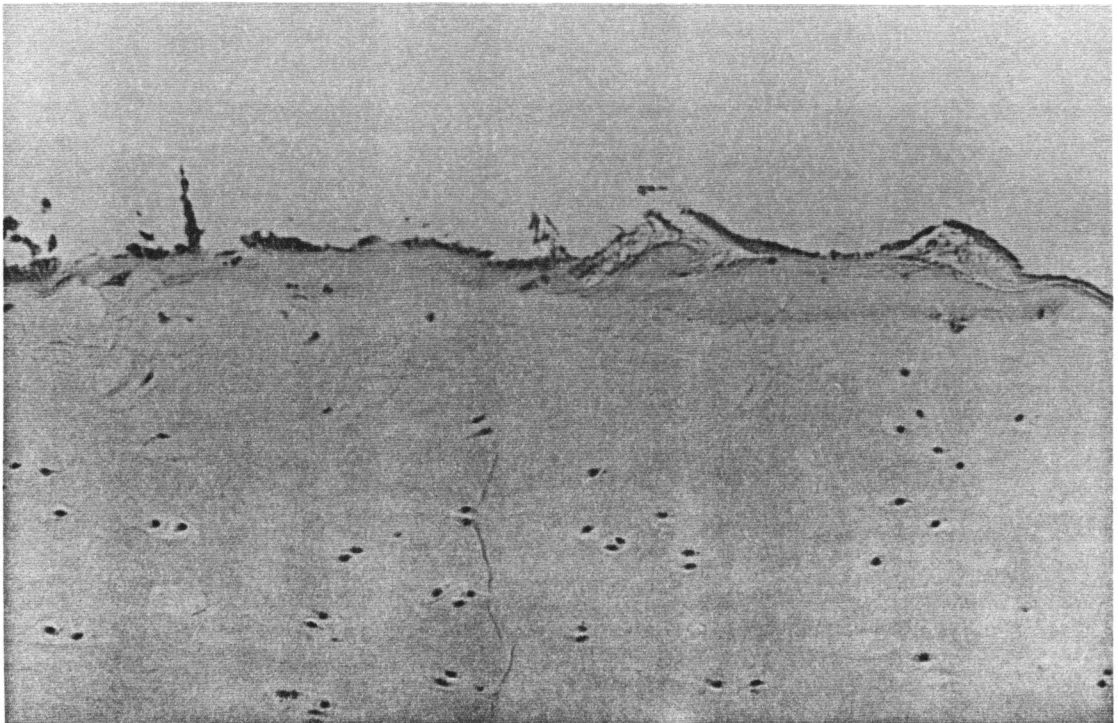


Figure 4.55 Alcian Blue Stained Section of Cartilage from Within the Worn Region of a Three-Hour Saline Test (test 18; 500X magnification)

Figure 4.56 is a photograph of the worn area from a three-hour serum test (test 17). Fine scratches were seen on the surface with the optical microscope. Very minor surface damage is visible in this cross section. Only a few partially detached collagen fibers were found. The lacunae appear to be flatter in shape than those found in untested regions. This change from a more rounded shape may be due to the compressive and shear forces placed on the cartilage under the wear track.

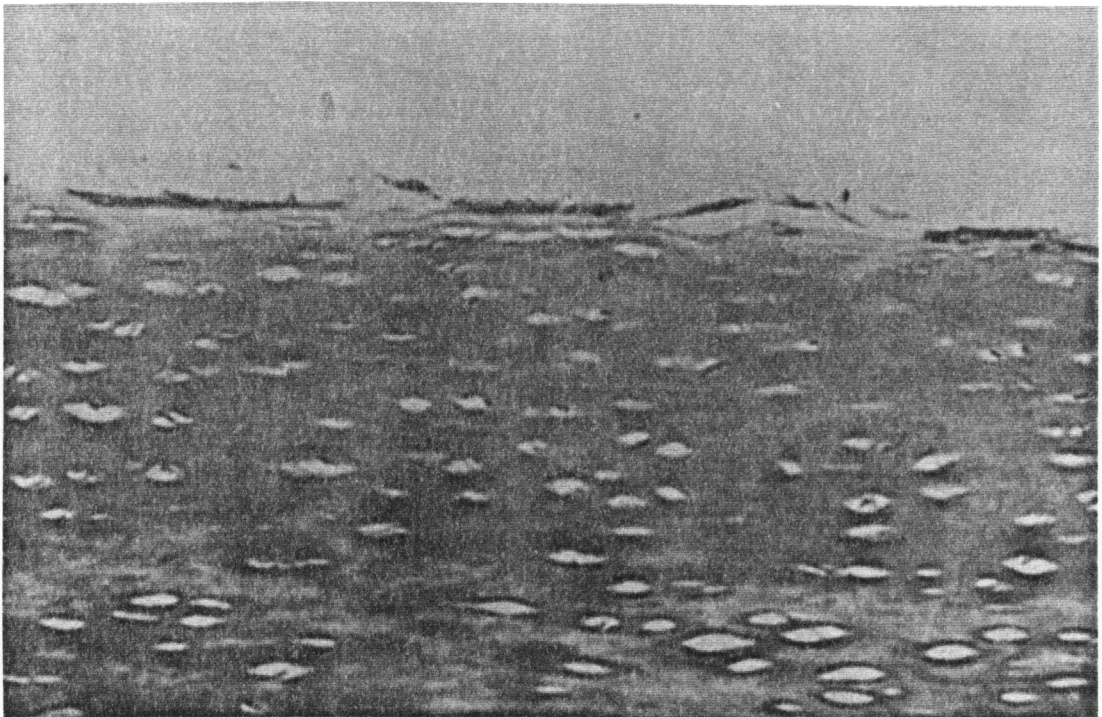


Figure 4.56 Alcian Blue Stained Section of Cartilage from a Low Damage Three-Hour Serum Test (test 17; 500X magnification)

A picture from a worn area of a three-hour synovial fluid test is presented in Figure 4.57 (test 14). This was the low wear synovial fluid test as determined by hydroxyproline assay. Optical microscopy did not show any damage. However, this photograph presents evidence of subsurface changes as a result of the test. Cracks are visible just below the surface. These may be on the way to forming larger voids and eventually creating cartilage flaps. As in Figure 4.56, the lacunae are flattened in this worn area. Also, the chondrocytes in the uppermost layer now completely fill their spaces.

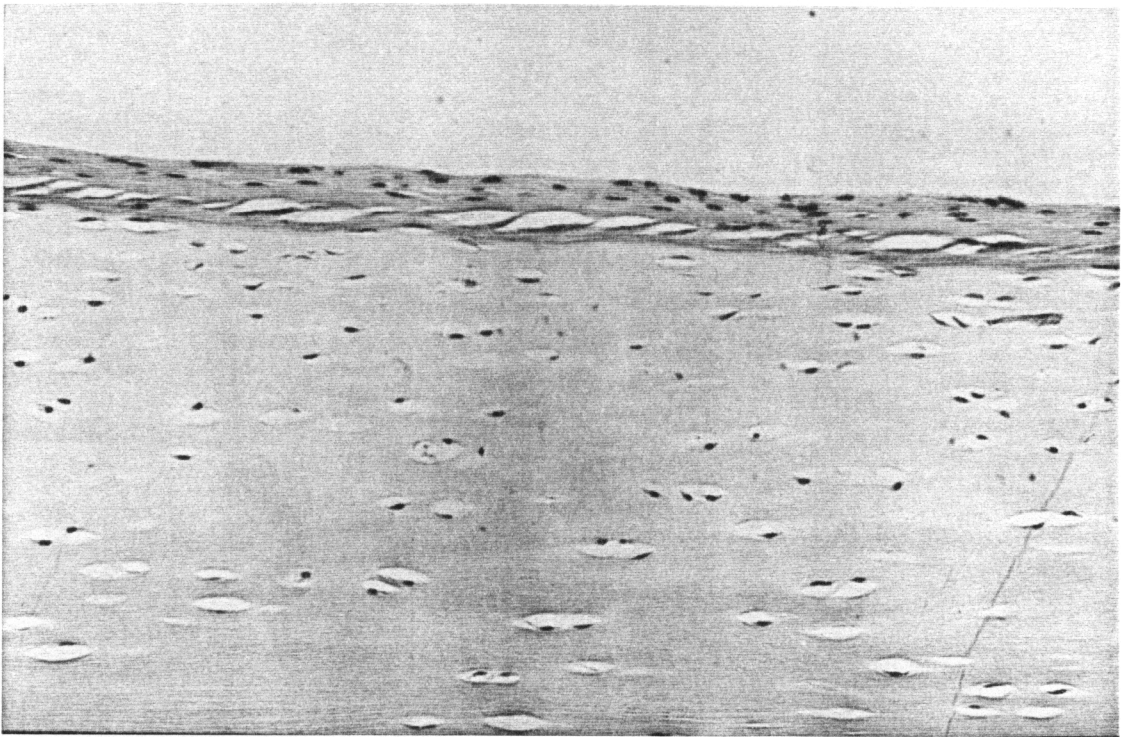


Figure 4.57 H&E Stained Section of Cartilage from a Low Wear Three-Hour Synovial Fluid Test (test 14; 500X magnification)

The photograph in Figure 4.58 is from a worn region of a high wear three-hour synovial fluid test (test 15). As with other high wear tests, a cartilage flap has partially detached from the surface. The left side of the flap is still firmly attached to the cartilage plug and therefore will not be counted as wear in hydroxyproline analysis of washings. The newly exposed surface from beneath the flap is rough and contains exposed chondrocytes as shown previously in Figures 4.44 and 4.53.

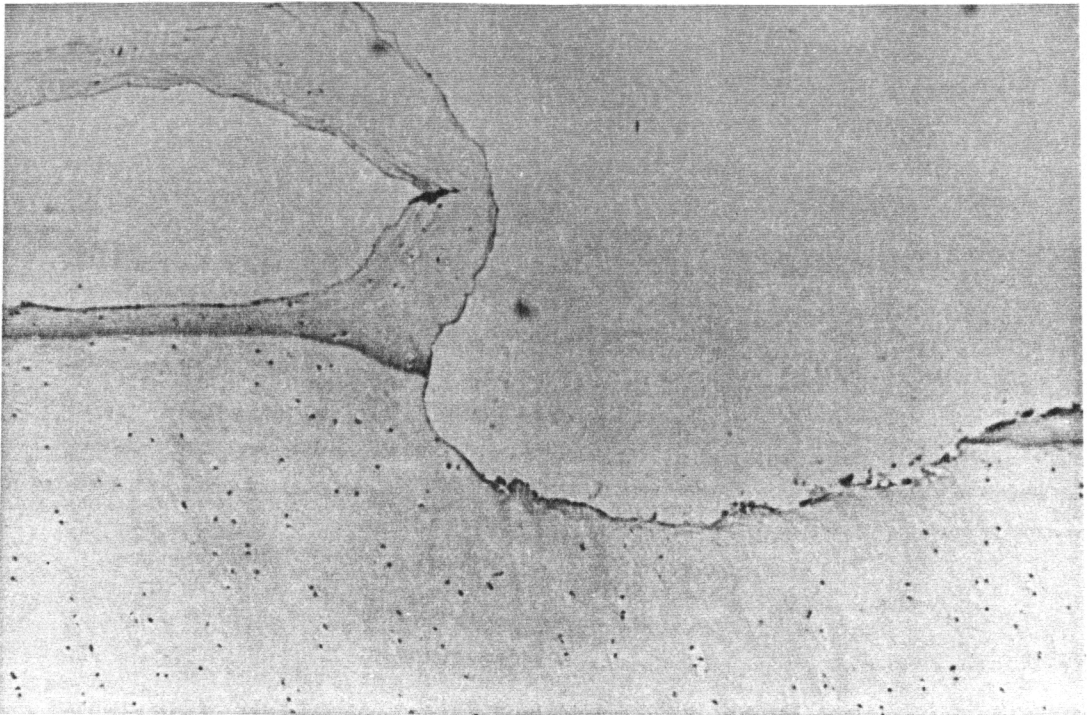


Figure 4.58 H&E Stained Section of Cartilage from a High Wear Three-Hour Synovial Fluid Test (test 15; 200X magnification)

A photograph of an H&E stained section of unworn cartilage is shown in Figure 4.59. Cartilage flaps are visible along this untested surface. This is presented to show that some joints have natural defects. The flaps are smoother than those produced in the wear tests and no exposed chondrocytes are visible.

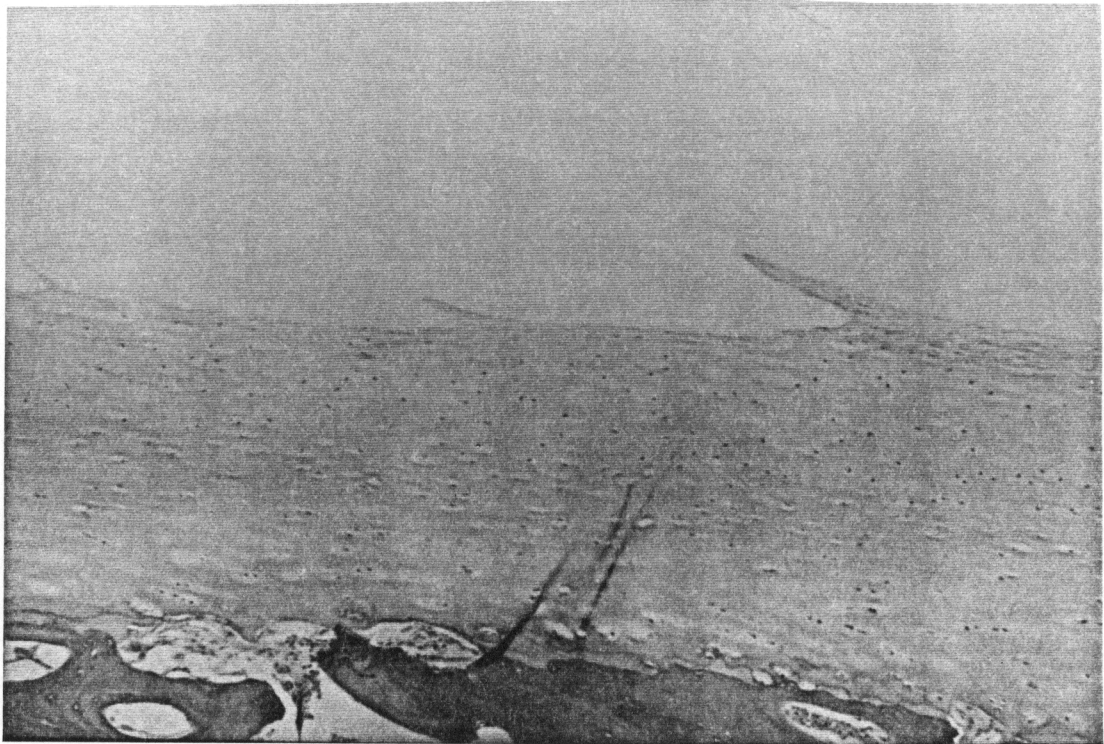


Figure 4.59 H&E Stained Section of Cartilage from an Unworn Region Showing a Rough Surface (500X magnification)

CHAPTER 5

DISCUSSION

5.1 OVERVIEW OF RESULTS

This study resulted in the formation of a standard plan of specimen treatment and testing. Initial tests were run to demonstrate the usefulness of a large variety of equipment and procedures available for analyzing *in vitro* cartilage-on-cartilage tests. Several trends were discovered in the test results and are discussed here.

A general observation was that the buffered saline protected very poorly against wear and damage to the cartilage compared to serum and synovial fluid. Every saline test resulted in measurable wear and damage and significantly increased friction over time. Future tests may be carried out with buffered saline as a base fluid with the addition of possible wear-reducing constituents of synovial fluid.

The use of bovine serum produced less damage and measurable wear than buffered saline. However, several tests did have significant wear and damage. After looking at the LVDT data, this damage could not always be explained by uneven surfaces. Damage to the cartilage was evident in two of the serum tests even with a very flat and relatively level lower plug.

Serum and synovial fluid compositions are very similar when looking at the major components. Synovial fluid is a dialyzate of blood plasma (high molecular weight components removed), but with a greater amount of hyaluronic acid [43]. Serum is blood plasma with the fibrinogen removed. Therefore, serum and synovial fluid are both approximately 90% water and 8% proteins. There are also salts, glucose, fats, and amino acids [44]. Although the proteins make up only a small percentage of the composition in each of these fluids, one source of the greater cartilage protection by synovial fluid may be due to differences in the proteins. Certain wear reducing proteins may be present in synovial fluid that are absent in serum. Future research in biochemistry and *in vitro* testing may eventually lead to the isolation of such a component.

Synovial fluid as a lubricant gave the greatest protection from wear and damage (there was no measurable wear in three of the four synovial fluid tests). In addition, the lowest coefficients of friction were produced by synovial fluid; in several cases, the friction became even lower as the test went on. The one high wear synovial test was analyzed carefully to determine a possible explanation for the extensive damage. As discussed further below, this test was run with a lower specimen that had a sharp change in surface height across the wear track. This caused very large forces to be placed on the leading edge of the upper specimen as it was forced to climb the steep slope of the lower surface. A patch of cartilage was eventually removed from the lower specimen at the peak of the

wear track, leading to a high level of hydroxyproline in the wear debris. This poorly profiled lower specimen proved that even synovial fluid was not capable of protecting the joint from damage under extreme conditions. Other than this one irregular test, the synovial fluid tests consistently produced the fewest number of scratches on the cartilage surfaces with very little damage seen in three hours of testing.

The results presented in Chapter 4 should preferably be analyzed as a group, not individually. For example, very misleading conclusions can be drawn by studying the hydroxyproline results alone. Each analytical technique adds vital information to what occurred during the tests. The hydroxyproline assay results from the three-hour tests are presented in Figure 5.1. These wear results must be viewed along with the friction force data, LVDT data, and microscopic observations before conclusions can be drawn. The high wear in test 15 with synovial fluid D was most likely due to the uneven surface of the lower specimen. Figure 5.1 contains two results from three-hour serum tests (tests 16,17). Again, these hydroxyproline results are misleading if studied separately. The first serum test showing no measurable cartilage wear actually had significant damage during the test. However, the damage was in the form of a cartilage flap that never completely detached from the lower cartilage surface. Therefore, hydroxyproline analysis to determine cartilage wear was not useful in this situation. Microscopic techniques showed that a top layer of cartilage was

partially torn from one end of the wear track. Although the surface was severely damaged, the friction measurements did not show a large increase.

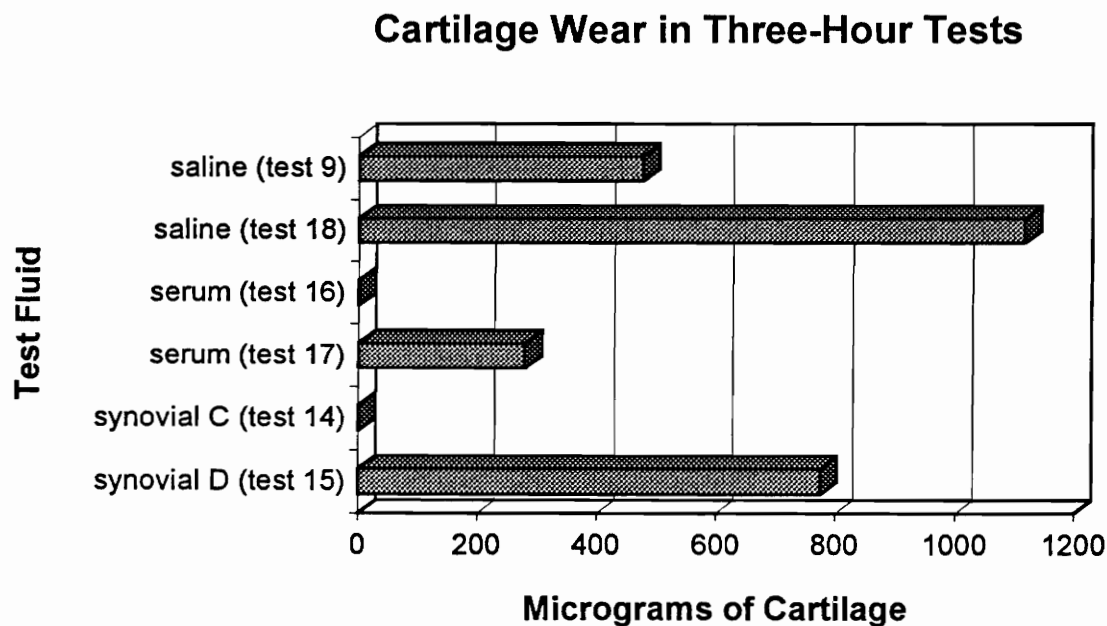


Figure 5.1 Cartilage Wear in Three-Hour Tests as Measured by Hydroxyproline Assay

Figure 5.2 is a plot of the LVDT data from the high wear synovial fluid test (test 15) and another synovial fluid test that produced low wear (test 14). The low wear LVDT plot shows a flatter surface contour that would not create problems as the top plug slides across the surface. The large (0.6 mm) change in height along the surface of the high wear test was greater than in any other experiment.

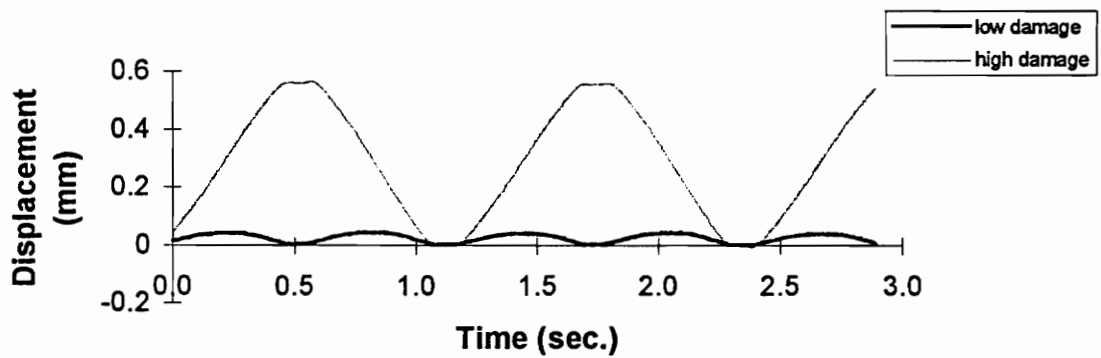


Figure 5.2 LVDT Plot from the Start of Low and High Wear Synovial Fluid Tests (tests 14,15)

As the photomicroscope and SEM pictures showed, the wear in test 15 (synovial fluid D) occurred mainly at one end of the wear track on the high end of the lower test specimen. The displacement plot indicates a tilted lower specimen with a resulting wear track at an average angle of 5.1 degrees. There was a removal of a top layer of cartilage from the high point that created a more even surface as shown in Figure 5.3 with an average angle of 1.6 degrees.

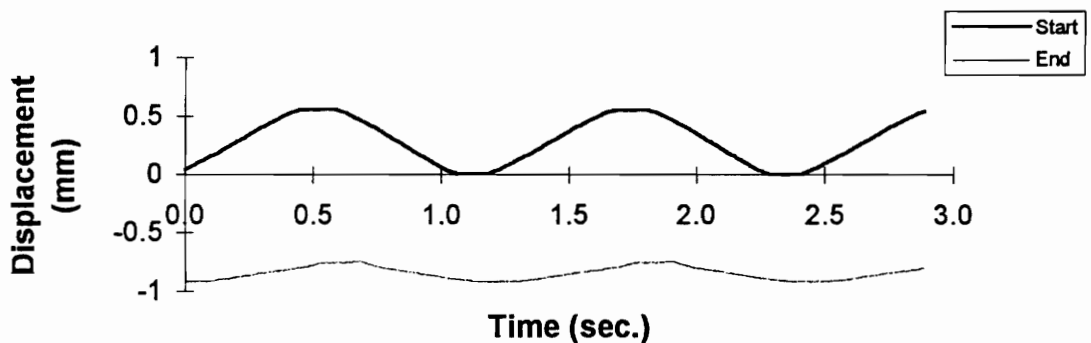


Figure 5.3 LVDT Data from the Start and End of the High Wear Synovial Fluid Test (test 15)

This change in surface contour was only associated with the creation of a surface flap and was absent in low wear tests. A low damage LVDT plot at the end of a test shows a very similar contour to the plot from the beginning of the test. The only major difference is that LVDT displacement has occurred relatively evenly over the length of the test. Figure 5.4 is an example of this displacement without visible surface damage.

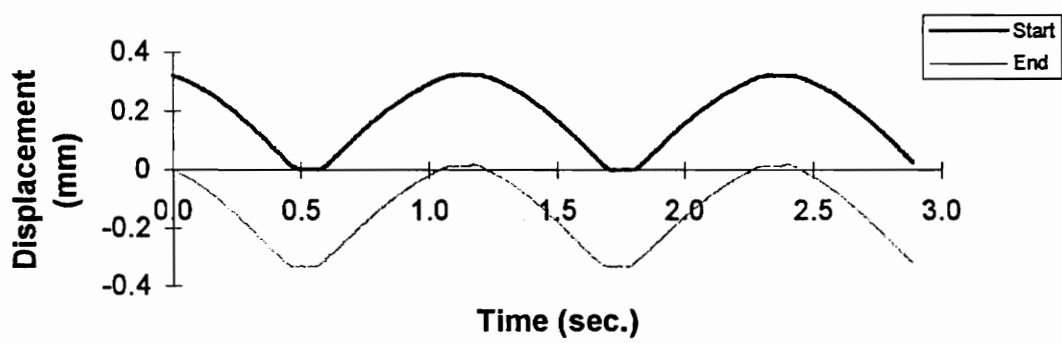


Figure 5.4 LVDT from Start and End of Low Damage Serum Test Showing Displacement (test 17)

Every saline test produced measurable wear even when the lower test plugs were nearly perfectly flat and horizontal. Surface damage to both top and bottom plugs was visible by eye in both three-hour saline tests. The friction measurements during saline tests showed that even when the tests started out with low friction, this value increased throughout the test. The low initial frictional forces may be due to residual lubricating films on the upper and lower

test plugs or lubricant squeezed from the top layers of cartilage. As the residual lubricant is depleted, higher friction values are recorded.

Several factors may be responsible for the vertical LVDT displacement recorded during each test. These mechanisms include elastic deformation, plastic deformation, loss of cartilage from the top plug, and loss of cartilage from the bottom plug. The measured displacement may be due to a combination of several of these mechanisms.

Figure 5.5 is a simplified diagram of top and bottom cartilage-bone plugs as they appear before a test. This diagram is also a model of completely elastic deformation allowing a full recovery after the load (W) is removed. In this case the deformation during testing is a function of load and is reversible. Tests showed that this recovery actually takes place over time and is not complete.

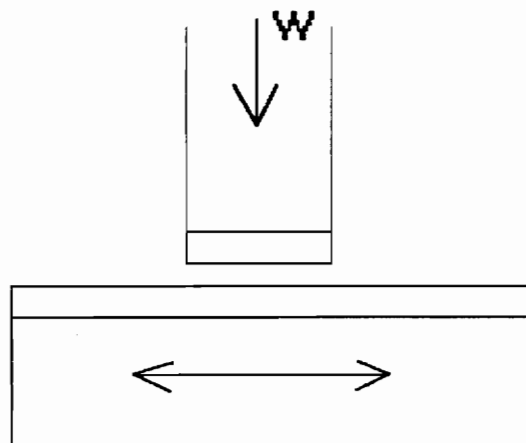


Figure 5.5 Elastic Deformation and Complete Recovery of Cartilage

Permanent plastic deformation could occur during cartilage-on-cartilage tests as shown in Figure 5.6. Even after the load (W) is removed, the cartilage surfaces would remain compressed and LVDT readings would remain the same as with the load applied (with purely plastic deformation). Both the top and bottom plugs would have thinner cartilage layers where tribological contact occurred. This irreversible deformation is a function of the load.

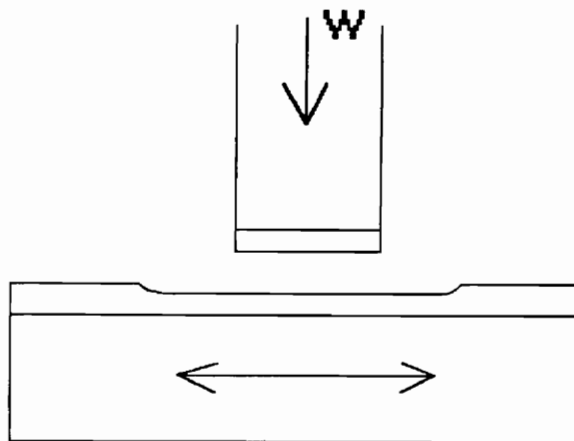


Figure 5.6 Plastic Deformation of Cartilage Surface

Figures 5.7 and 5.8 depict loss of cartilage from the top and bottom plugs respectively. This loss of cartilage can be measured by hydroxyproline analysis. The removal of cartilage leads to surface roughness and wear tracks on the worn specimen. This means that even after the load (W) is removed, the cartilage is thinner on the worn sample and the LVDT would not indicate recovery. The LVDT reading would change throughout the test as successive layers of cartilage were removed.

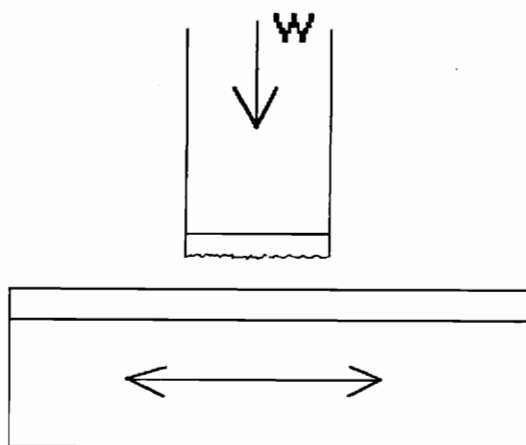


Figure 5.7 Loss of Cartilage from Top Plug Only

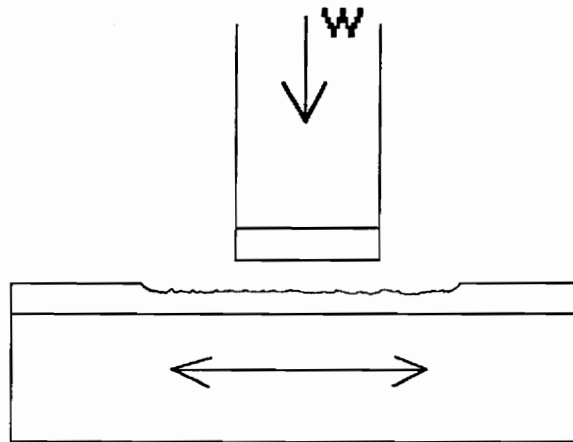


Figure 5.8 Loss of Cartilage from Bottom Plug Only

Another factor which must be considered with imperfect (realistic) samples is that of tilted or uneven cartilage surfaces. Figure 5.9 is an exaggerated example of a tilted lower plug and the plowing that may occur by the leading edge of the upper plug. As described previously, this is the likely cause of high wear in synovial test 15. This model shows that a high coefficient of friction could be expected in one direction of sliding but not in the other.

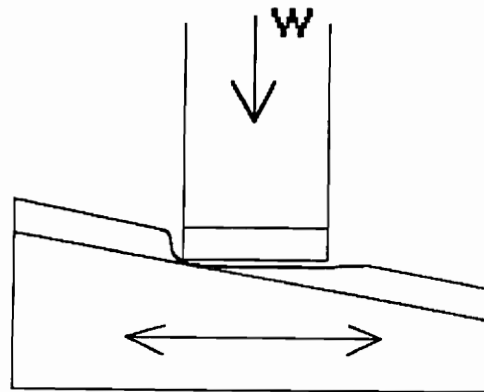


Figure 5.9 Diagram of the Exaggerated Tilt of a Lower Specimen

It is likely that the real source of the LVDT displacement in these tests is a combination of all of these mechanisms. Figure 5.10 is a diagram showing what is believed to be a more realistic depiction of a tested plug. There is a mix of plastic deformation, elastic deformation, wear, and damage. Calculations suggest that nearly all of the displacement in tests is due to elastic and plastic deformation -- not wear. As an example, in the high wear three-hour serum test (test 17) only 3% of the total displacement could have been due to wear. This calculation assumed that all of the wear occurred on the top plug in order to maximize the LVDT change. Therefore, most of the displacement must be

elastic or plastic. It is difficult to separate the two using the present equipment. Future static steel-on-cartilage or cartilage-on-steel compression tests could be performed to study the two types of deformation and to determine their individual impacts on LVDT data.

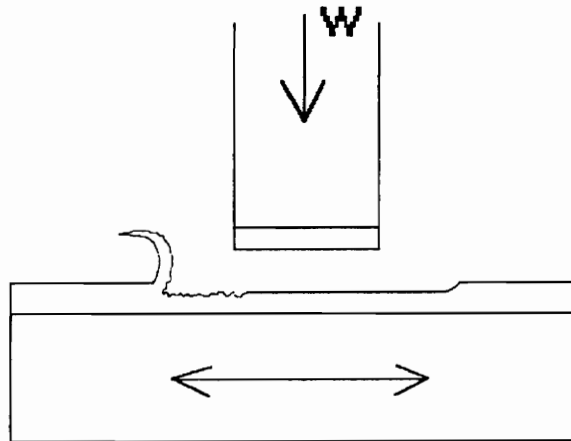


Figure 5.10 Combination of Elastic Deformation, Plastic Deformation, Wear, and Damage

5.2 ANALYTICAL TECHNIQUES

Each analytical technique made specific contributions to the overall comparison of lubricant effectiveness. The computer data, hydroxyproline assays, photomicroscope pictures, and electron microscope pictures also produced many potentially misleading results. It should be emphasized that each method of analysis must be looked at along with all of the other information from a test before drawing conclusions.

DISCUSSION

5.2.1 Computer Data Acquisition

The data obtained from the strain ring and LVDT was useful for analyzing changes in surface contour, deformation of cartilage during a test, and changes in frictional forces during a test and within a single test cycle. The LVDT data can be viewed in conjunction with macroscopic photographs to separate wear from cartilage compression. Figure 5.11 is a graph of LVDT changes from the beginning to the end of a test. These measurements were taken at the same location at one end of the wear track with no applied pressure from the air cylinder; only the shaft weight (6.72 N) was present. These results show that the permanent LVDT displacement resulting from a test ranged from 0.61 to 1.5 mm. Several of the saline tests appear to have some of the largest displacement changes, but this could be coincidental. The most interesting feature of this plot is that there is no large difference in displacement between one-hour and three-hour tests.

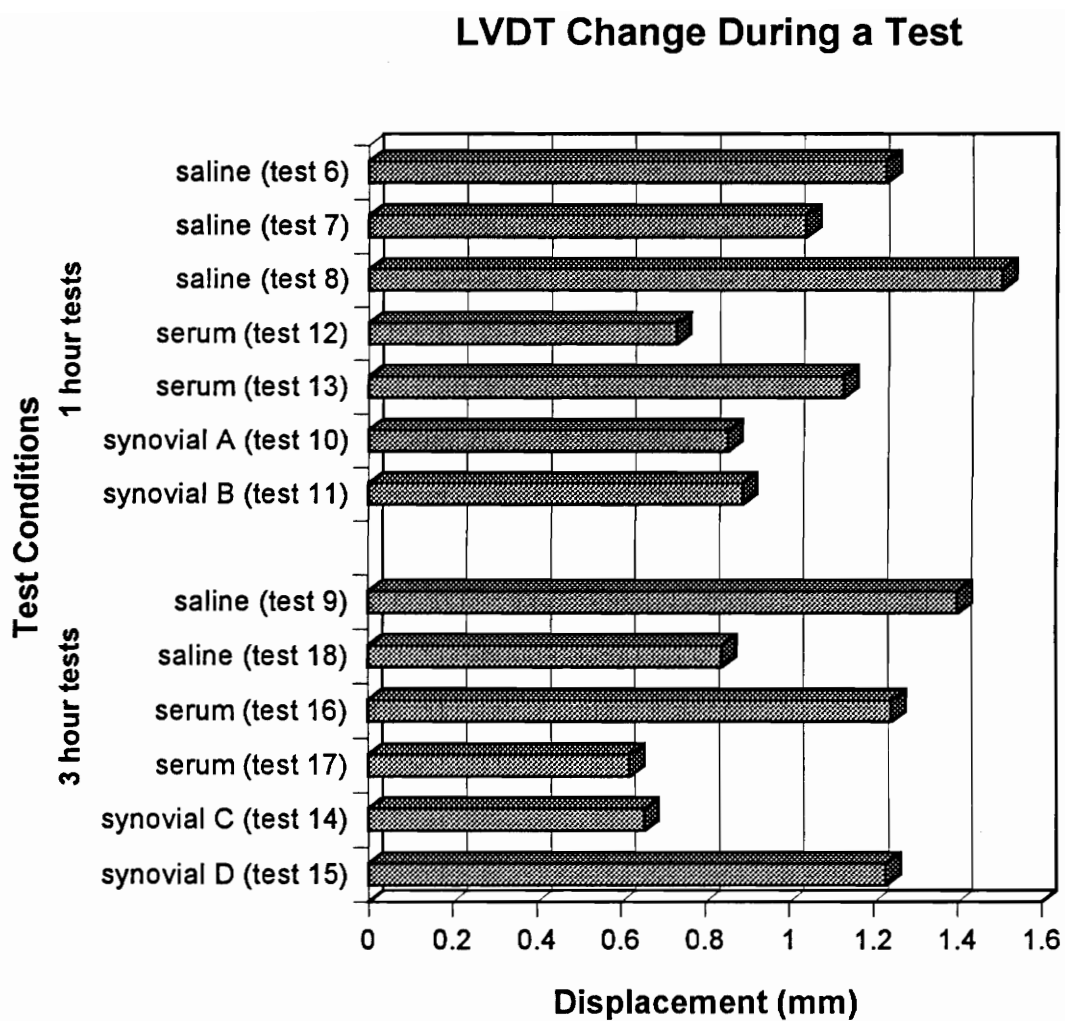


Figure 5.11 LVDT Change from Start to End of Each Test (6.72 N shaft weight)

Friction measurements from the strain ring data were looked at along with microscopic examination of the plug surfaces. Generally, it was found that a sharp increase in friction over one cycle of a test corresponded with the removal of a cartilage flap. It was interesting to note that this sharp peak in friction was usually observed in only one direction (which varied from test to test) of the test cycle.

5.2.2 HYDROXYPROLINE ANALYSIS OF CARTILAGE WEAR

Hydroxyproline assay of the test washings is a very accurate way of measuring particles of cartilage removed from the surface. However, many of the lower test specimens in longer tests produced severe damage without removal of cartilage. This damage in the form of cartilage flaps exposed subsurface cartilage with a different structure. This usually resulted in a large amount of measurable wear. However, the nearly detached cartilage flaps would of course not be detected by hydroxyproline analysis of the washings.

5.2.3 MICROSCOPIC SURFACE ANALYSIS

Use of the photomicroscope and scanning electron microscope gave insight to the type and severity of surface damage from each test. The photomicroscope was used to view each specimen before and after testing to

document qualitative changes in the surfaces. Fine randomly oriented scratches were often observed on test specimens that were created naturally *in vivo*. Severe scratches were avoided when deciding where to position the wear track. Observations from the microscopes combined with friction and displacement data can help create a more complete picture of the type of damage occurring during a test. Often a cartilage flap was seen still attached to the edge of the wear track, thus adding another factor to the quantitative measure of wear by hydroxyproline analysis. This only emphasizes that all available data and observations must be considered when drawing conclusions.

5.2.4 Slides of Cartilage Cross Sections

Slides of cartilage cross sections of every lower test specimen allowed detailed examination of the surface flaps and subsurface damage. Almost all tests showed some change in appearance under the wear track. In the lower wear tests, this change was in the form of compressed chondrocytes and minor subsurface cracks. In the high wear tests, cartilage flaps and their various stages of formation were seen. Staining by alcian blue allowed proteoglycan concentrations to be analyzed showing lower amounts of staining under wear tracks. This shows that tribological contact can change the biochemistry of cartilage. The greatest contribution by cross-sectional analysis was its

usefulness in showing damage well below the surface -- something that no other test indicated.

5.3 WEAR AND DAMAGE

There are several means by which damage to and wear of articular cartilage can occur. These include adhesive wear, fibrillation, delamination, plowing, and third body abrasion. Several of these types of wear were seen in the *in vitro* tests of this study.

Most of the damage in the one-hour tests was on the surface in the form of scratches. Microscopic study of these scratches led to the assumption that some material was removed from the surface, while some was simply pushed to the edges of the scratch (plowing). All of the longer, three-hour tests produced lower test plugs with subsurface cracks or at least severe deformation of the chondrocytes. At times, the subsurface damage was accompanied by small collagen bundles breaking free at the surface. Much of this form of damage did not result in wear detected by the hydroxyproline method. In the tests in which a cartilage flap was created, the subsurface cracks had grown to reach through the upper layer of cartilage. In the tests with the highest amount of wear, portions of the cartilage flaps had broken loose and were gathered in the test washings.

5.4 SUMMARY

This study has helped to form a foundation for future research in biotribology at Virginia Tech. The sample preparation and test procedures developed and outlined in Chapter 3 were followed successfully to carry out useful cartilage-on-cartilage tests. The data acquisition system and various forms of microscopy were used along with hydroxyproline assays to effectively study cartilage-on-cartilage lubrication with saline, serum, and synovial fluid. Tangential and normal force data values were successfully combined to study friction forces over single cycles during a test. This friction analysis was studied along with LVDT displacement data to determine relationships between changes in the cartilage surface and frictional forces. The microscopy work using a scanning electron microscope, environmental scanning electron microscope, and a photomicroscope was useful in studying the surface damage produced during each test. Other extremely important microscopic findings were of subsurface damage as seen in cartilage cross sections. The hydroxyproline analysis of the test washings showed that cartilage damage and wear are related; however, damage does not always result in wear. Also, hydroxyproline analysis of the test fluids indicated significant amounts of hydroxyproline may be present in the original synovial fluid and serum. This study showed that the biochemistry of the test fluid can significantly influence wear and damage in an

in vitro cartilage-on-cartilage test. This finding is consistent with the work of Furey [4] in which bovine articular cartilage was in reciprocating sliding contact against stainless steel. Synovial fluid protected against cartilage wear and damage much more effectively than serum or buffered saline. Future work can now be carried out and compared to the base results obtained in this project. Using the techniques described in this study along with recommendations described in Chapter 7, future tests can be analyzed and lubricant biochemistry effects can be classified.

CHAPTER 6

CONCLUSIONS

Bovine cartilage-on-cartilage *in vitro* tests were successfully carried out with lubricants of buffered saline, serum, and synovial fluid. The results of these tests and the reported procedures should be useful in the continuing study of the wear and lubrication of synovial joints being carried out at Virginia Tech.

1. Approximately 90 bovine stifle and shoulder joints from a separate controlled study were collected and frozen at -25°C. This was accomplished with the help of Dr. Hugo Veit, Ms. Heather Hughes, Mr. Ben Tritt, Mr. Mark Freeman, Mr. Ed Lee, and Mr. Michael Owellen.
2. A detailed procedure for cutting upper and lower test specimens was successfully developed and tested.
3. A computer data acquisition system was added to the original test device and a computer program was developed (with the help of Mr. Michael Owellen) to control the oscillating motion of the lower test specimen.
4. The first *in vitro* cartilage-on-cartilage tests measuring friction, wear, and deformation were successfully carried out. The new data acquisition system made it possible to carry out detailed analysis of load, deformation, and friction during a single cycle.

5. A successful procedure for collecting tested fluids and wear debris was developed and tested. These fluids were analyzed to give a quantitative measure of cartilage wear using hydroxyproline analysis. This work was carried out under the direction of Dr. E. M. Gregory. Serum and synovial fluid may contain significant amounts of hydroxyproline. Therefore, these fluids should be tested to determine the initial concentration of hydroxyproline before using them as lubricants.
6. Photomacrographs, SEM photographs, and ESEM photographs were taken of worn and unworn cartilage specimens. The photomacrography and SEM photographs were the most helpful in studying surface wear and damage.
7. Cartilage sectioning and staining was carried out with the help of Dr. Hugo Veit and Ms. Heather Hughes. Hemotoxylin and eosin stain (H&E) was very useful for highlighting subsurface damage and changes to chondrocytes. Alcian blue stain successfully highlighted proteoglycans and indicated varied organization or lower concentrations under worn areas.
8. Preliminary cartilage-on-cartilage tests were successfully carried out using lubricants of buffered saline solution, bovine serum, and bovine synovial fluid. The results of these tests were analyzed and observations of unusual phenomena were recorded. Recommended future changes in the test procedure and machine design were detailed to avoid problems encountered in these preliminary tests. These changes include paying

close attention to the tilt of the lower test specimen in order to ensure a level wear track for more repeatable tests.

9. The findings from this preliminary study should be useful in future research in biotribology at Virginia Tech. New students who will carry out this work have been trained in the techniques developed and reported on in this study.
10. Several important discoveries were made in this preliminary work:
 - (a) The biochemistry of synovial fluid plays an important role in the reduction of wear and damage of cartilage. This was shown by comparing synovial fluid test results with results from serum and buffered saline tests.
 - (c) Saline produced the most damage and wear. Also, the highest friction forces were recorded in the saline tests.
 - (d) Serum generally produced lower wear and damage than saline; however the results were not as consistent as those obtained with the other fluids.
 - (e) Synovial fluid produced lower damage, wear, and friction than buffered saline or serum. This could mean that synovial fluid contains specific wear and friction reducing compounds that are missing in serum and buffered saline.
 - (g) Friction and wear of articular cartilage are not simply related. However, severe damage was consistently accompanied by an increase in friction.

- (h) Several types of wear took place in these tests. Scratches were formed on the surfaces of both the top and bottom plugs. This may have been due to microscopic abrasive material in the test fluids (third body abrasive wear) or abrasion by the opposing surface. The combination of shearing and compressive forces produced subsurface cracks. In severe cases these cracks reached the joint surface and cartilage flaps were produced.
- (i) Damage without cartilage removal or debris formation is possible -- cartilage flaps can stay attached to the surface.

CHAPTER 7

RECOMMENDATIONS

MACHINE MODIFICATIONS

Several modifications were designed to improve the performance of the cartilage-on-cartilage test device. Appendix A contains the designs for these changes. The changes are designed so that when all of the new parts are machined, they can be easily attached to the existing device. The new vertical shaft with ball bearings is expected to reduce the sideways play of the shaft while also reducing shaft sliding friction.

TEST SETUP

The plug cutting procedure described in Section 3.2 may be modified in the future to keep track of cartilage plug orientation. Both the top and bottom plugs could be marked on the bone as they are cut in order to align the cartilage surfaces in a specific direction. It could be interesting to run one set of tests with the top plug turned 90 degrees from the natural sliding direction.

RECOMMENDATIONS

Before each test is run, the lower plug tilt must be checked. An extreme difference in height from one end of the wear track to the other can produce increased wear and damage. The height difference could be checked by lowering the upper plug carefully at each end of the wear track before the test. The change in the LVDT reading will indicate the tilt of the surface. If too large a tilt is found, thin spacers could be placed under one edge of the lower specimen holder to create a more level surface.

PARTICLE CHARACTERIZATION

Particle size and shape information may be useful when comparing different test results. Several methods for determining particle size are available including optical microscopy, scanning electron microscopy, and filtration. There are questions of how cartilage hydration will affect these results and a standard procedure will be needed. It would be interesting to study the cartilage particles in both the test washings and in normal and arthritic synovial fluid.

BIOCHEMISTRY

Possible changes in the biochemistry of tested synovial fluid and cartilage should be studied further. These changes may point the way toward specific constituents of synovial fluid that are partially responsible for the low friction and wear of articular cartilage. Biochemical techniques could be used to isolate

RECOMMENDATIONS

these constituents which could then be added to buffered saline and used as lubricants. Also, any changes in the biochemistry of tested cartilage could provide information about the reduced wear resistance that occurs over the length of a test.

STAINING

Stains other than H&E and alcian blue for the cartilage cross sections should be tested. There could be different stains that highlight various changes that occur in the cartilage during testing. These stains should be useful when comparing tests run with different lubricants.

TEST FLUIDS

The synovial fluid from several joints could be pooled to form a large uniform batch to be used in future tests. This fluid should be centrifuged to remove large pieces of floating debris. Before tests are run with this synovial fluid, a hydroxyproline assay and other biochemical tests should be run. This will give a base line value for hydroxyproline in the synovial fluid and also allow measurement of the changes in the biochemistry of the tested fluid.

Various constituents of synovial fluid may be isolated and added to the buffered saline reference fluid. This would allow testing of these biochemical compounds to find what individual roles they play in the reduction of wear and

RECOMMENDATIONS

damage of cartilage. This would repeat the work of Furey [4] only using cartilage-on-cartilage. Also, artificially degraded or arthritic synovial fluid could be used as a lubricant and compared to tests with normal synovial fluid.

FUTURE TESTS

Several ideas for future tests have been discussed. Some of the possible variations include changing the load, test length, specimen material, speed, sliding distance, and temperature.

The upper and lower plug materials can be changed to test configurations other than cartilage-on-cartilage. Lower plugs made of polished stainless steel could be tested with upper plugs of cartilage to compare with past cartilage-on-steel tests by Furey [2]. This type of test would also be similar to conditions present in half joint replacements.

Future studies could use degraded or arthritic cartilage plugs that are hypothesized to have a reduced wear resistance. These *in vitro* tests could determine if new or different wear mechanisms occur in cases with previously damaged cartilage.

RECOMMENDATIONS

REFERENCES

1. Furey, M. J., "Biotribology: Friction, Wear, and Lubrication of Natural Synovial Joints," Paper, 4th International Tribology Conference, AUSTRIB '94, Perth, Western Australia, Dec. 5-8, 1994.
2. Furey, M. J., "Joint Lubrication," Chapter 23, pp. 333-351, *Biomedical Engineering Handbook*, 1995 by CRC Press, Inc.
3. Furey, M. J., "Biotribology: Possible Connections Between Tribology and Osteoarthritis," Proceedings, 4th International Tribology Conference (AUSTRIB '94), Dec. 5-8, 1994, Perth, Western Australia, Vol. 1, pp. 363-368.
4. Furey, M. J., "Biotribology: Cartilage Lubrication and Wear," 6th International Congress on Tribology, EUROTRIB '93, Budapest, Hungary, Aug. 30 - Sept. 2, 1993.
5. Furey, M. J., "Biochemical Aspects of Synovial Joint Lubrication and Cartilage Wear," European Society of Osteoarthrology Symposium on "Joint Destruction in Arthritis and Osteoarthritis," Noordwijkerhout, The Netherlands, May 24-27, 1992.
6. Burkhardt, B. M., "Development and Design of a Test Device for Cartilage Wear Studies," M.S. thesis, Mechanical Engineering, Virginia Polytechnic Institute & State University, Blacksburg, VA, Dec. 1988.
7. Discussions with Dr. M. J. Furey, Virginia Tech, January 1995.
8. Stockwell, R. A., *Biology of Cartilage Cells*, Cambridge Univ. Press, Cambridge, 1979.
9. Freeman, M. A. R. (editor), *Adult Articular Cartilage*, Pitman Medical Publishing Co., Ltd., Tunbridge Wells, Kent, England, 2nd ed., 1979.
10. Mankin, H. J., and Brandt, K.D., in *Osteoarthritis: Diagnosis and Management* (Moskowitz, R. W., Howell, D. S., Goldberg, V. M., and Mankin, H. J., Eds.) pp. 43-79, Saunders, Philadelphia, 1984.
11. Buckwalter, J.A., "Cartilage," in *Encyclopedia of Human Biology*, Volume II pp. 201-215.

12. Muir, H., Hirohata, K., Shichikawa, K.(editors), *Mechanisms of Articular Cartilage Damage and Repair in Osteoarthritis*, Hogrefe and Huber Publishers, Toronto, 1990.
13. Bergman and Loxley, *Analytical Chemistry*, 35: 1961-1965, 1963.
14. Lipshitz, H., and Etheredge, R., III, "'In Vitro' Wear of Articular Cartilage," *J. Bone Joint Surgery.*, Vol. 57-A, June 1975, pp. 527-534.
15. Lipshitz, H., and Glimcher, M. J., "'In Vitro' Studies of Wear of Articular Cartilage, II. Characteristics of the Wear of Articular Cartilage when Worn Against Stainless Steel Plates Having Characterized Surfaces," *Wear*, Vol. 52, pp. 297-337, 1979.
16. Hou, J. S., Mow, V. C., Lai, W. M., Holmes, M. H., "An Analysis of the Squeeze-film Lubrication Mechanism for Articular Cartilage," *J. Biomechanics.*, Vol. 25, No. 3, pp. 247-259, 1992.
17. Swanson, S. A. V., "Friction, Wear and Lubrication," Chapter 7 in *Adult Articular Cartilage*, ed. by M. A. R. Freeman, Pitman Medical Publishing Co., Ltd., Tunbridge Wells, Kent, England, 2nd ed., pp. 415-460, 1979.
18. Higginson, G. R., and Unsworth, T., "The Lubrication of Natural Joints," Chapter 3 in *Tribology of Natural and Artificial Joints* by J. H. Dumbleton, Elsevier Scientific Publishing Co., Amsterdam and New York, pp. 47-73, 1981.
19. Droogendijk, L., "On the Lubrication of Synovial Joints," Ph.D. thesis, Twente University of Technology, The Netherlands, 1984.
20. Hayes, A., Harris, B., Dieppe, P.A., Clift, S.E., "Wear of Articular Cartilage: the Effect of Crystals," *IMechE*, pp.41-58, 1993.
21. Stachowiak, G. W., Batchelor, A. W., and Griffiths, L. J., "Friction and Wear Changes in Synovial Joints," *Wear*, Vol. 171, pp. 135-142, 1994.
22. Hollander, A. P., et al., "Increased Damage to Type II Collagen in Osteoarthritic Articular Cartilage Detected by a New Immunoassay," *J. Clinical Investigation*, Vol. 93, pp. 1722-1732, April 1994.
23. Beltran, J., et al., "Joint Effusions: MR Imaging," *Radiology*, Volume 158, No.1, pp. 133-137, 1986.

24. Hayes, A., Swan, A.J., and Dieppe, P.A., "Crystals in Equine Articular Cartilage," *Research in Veterinary Science*, Vol. 57, pp.106-109, 1994.
25. Meachim, G. and Brooke, G., in *Osteoarthritis: Diagnosis and Management* (Moskowitz, R. W., Howell, D. S., Goldberg, V. M., and Mankin, H. J. Eds.) pp. 29-42, Saunders, Philadelphia, 1984.
26. Verbruggen, G., and Veyes, E. M.(editors), *Degenerative Joints: Test Tubes, Tissues, Models, and Man*, Proc. First Conf. on Degenerative Joint Diseases, Ghent, Oct. 10-11, 1980; Excerpta Medica, Amsterdam-Oxford-Princeton, 1982.
27. Brittberg, M., et al., "Treatment of Deep Cartilage Defects in the Knee with Autologous Chondrocyte Transplantation," *The New England Journal of Medicine*, Volume 331, No. 14, October 6, 1994, pp. 889-895.
28. Saikko, V., "Wear and Friction Properties of Prosthetic Joint Materials Evaluated on a Reciprocating Pin-on-Flat Apparatus," *Wear*, Vol. 166 (1993), pp.169-178.
29. Corkhill, P. H., Trevett, A. S., Tighe, B. J., "The Potential of Hydrogels as Synthetic Articular Cartilage," *Proc. Instn. Mech. Engs., Part H: Journal of Engineering in Medicine*, Vol. 204 (1990), pp. 147-155.
30. Moskowitz, R. W., Howell, D. S., Goldberg, V. M., Mankin, H. J., *Osteoarthritis Diagnosis and Management*, p. 433, W. B. Saunders Company, Philadelphia, 1984.
31. Peterson, L., Menche, D., and Grande, D., et al., "Chondrocyte Transplantation – An Experimental Model in the Rabbit." in *Transactions from the 30th Annual Orthopedic Research Society*, Atlanta, February 7-9, 1984. palatine, Ill.: Orthopedic Research Society, 1984:218.
32. Discussions with Dr. Hugo Veit, Virginia Tech, 1993-1995.
33. Amiel, D. et al. "A Histological and Biochemical Assessment of the Cartilage Matrix Obtained from *In Vitro* Storage of Osteochondral Allografts," *Connective Tissue Research*, Vol. 23, pp.89-99, 1989.
34. Kwan, M. K. et al. "Histological and Biomechanical Assessment of Articular Cartilage from Stored Osteochondral Shell Allografts," *Journal of Orthopaedic Research*, Vol. 7, no.5, pp.637-644, 1989.

35. Wayne, J.S. et al., "Long-term Storage Effects on Canine Osteochondral Allografts," *Acta Orthop Scand* 1990, vol. 61, no. 6, pp.539-545.
36. Schachar, N.S. et al., "Metabolic Activity of Bovine Articular Cartilage During Refrigerated Storage," *Journal of Orthopaedic Research*, Vol. 12, no. 1, 1994.
37. Sambrook, J., Fritsch, E. F., and Maniatis, T., *Molecular Cloning. A Laboratory Manual*. Appendix B, p. 12. Cold Spring Harbor Press, 1987.
38. Beverlander, G. and Ramaley, J.A., *Essentials of Histology*, The C.V. Mosby Company, St. Louis, 1979.
39. Minns, R.J. and Steven, F.S., "The Collagen Fibril Organization in Human Articular Cartilage," *Journal of Anatomy*, Vol. 123, no. 2, pp.437-457, 1977.
40. Clark, J.M. "Variation of Collagen Fiber Alignment in a Joint Surface: A Scanning Electron Microscope Study of the Tibial Plateau in Dog, Rabbit, and Man," *Journal of Orthopaedic Research*, Vol. 9, pp.246-257, 1991.
41. Cameron, R.E. "Environmental SEM: Principles and Applications," *USA Microscopy and Analysis*, pp. 17-19, May 1994.
42. Clarke, I.C. "In Vivo and in Vitro Comparative Studies of Animal Articular Surfaces," *Annals of Biomedical Engineering*, Vol.3, pp. 100-110, 1975.
43. McHenry, R. (editor), *The New Encyclopedia Britannica*, Vol. 28, p.311, 1992.
44. McHenry, R. (editor), *The New Encyclopedia Britannica*, Vol. 2, p. 290, 1992.

APPENDIX A

Modifications Designed for Cartilage Testing Machine

Several improvements to the machine were thought of during the course of running tests and designing a test procedure. The direction of motion was changed to 90 degrees from the LVDT arm instead of being in-line with the arm. This helped eliminate extraneous LVDT readings due to rocking of the vertical shaft during testing. Other improvements included attaching an IBM computer running the data acquisition program Global Lab, and adding a digital multimeter to read any of the three data channels during a test or for pre-test calibration.

A new vertical shaft was purchased from Nook Industries to reduce rocking during testing. This new shaft is a Power Trax ball spline and consists of a hardened steel shaft with races that slides inside an outer housing containing precision ball bearings. This new shaft will be held to the top plate using a machined aluminum housing as shown in Figure A1. A new top plate (Figure A2) will be made with four additional holes to attach the new shaft holder (Figure A3). Also, a new coupler between the shaft and the strain ring was designed as shown in Figure A4. The redesigned machine will appear as shown in Figure A5. This new shaft configuration should significantly reduce shaft rocking which can contribute to errors in the LVDT and strain ring outputs.

ALL DIMENSIONS IN INCHES

Technical drawing of a mechanical assembly, likely a valve or actuator, showing a cross-section. The drawing includes the following dimensions:

- Overall width: 6.92
- Overall height: 3.51
- Top horizontal dimension: .25
- Top horizontal dimension: .72
- Top horizontal dimension: .25
- Left horizontal dimension: 2.42
- Left horizontal dimension: .63
- Left horizontal dimension: .25
- Bottom horizontal dimension: 1.00
- Bottom horizontal dimension: 1.53

The drawing shows a central vertical component with a flange at the top and a tapered bottom. Two horizontal arms extend from the central body, each with a hatched section. The dimensions are provided in inches.

Figure A1 New Shaft Attached to Redesigned Top Plate (by Mark Freeman)

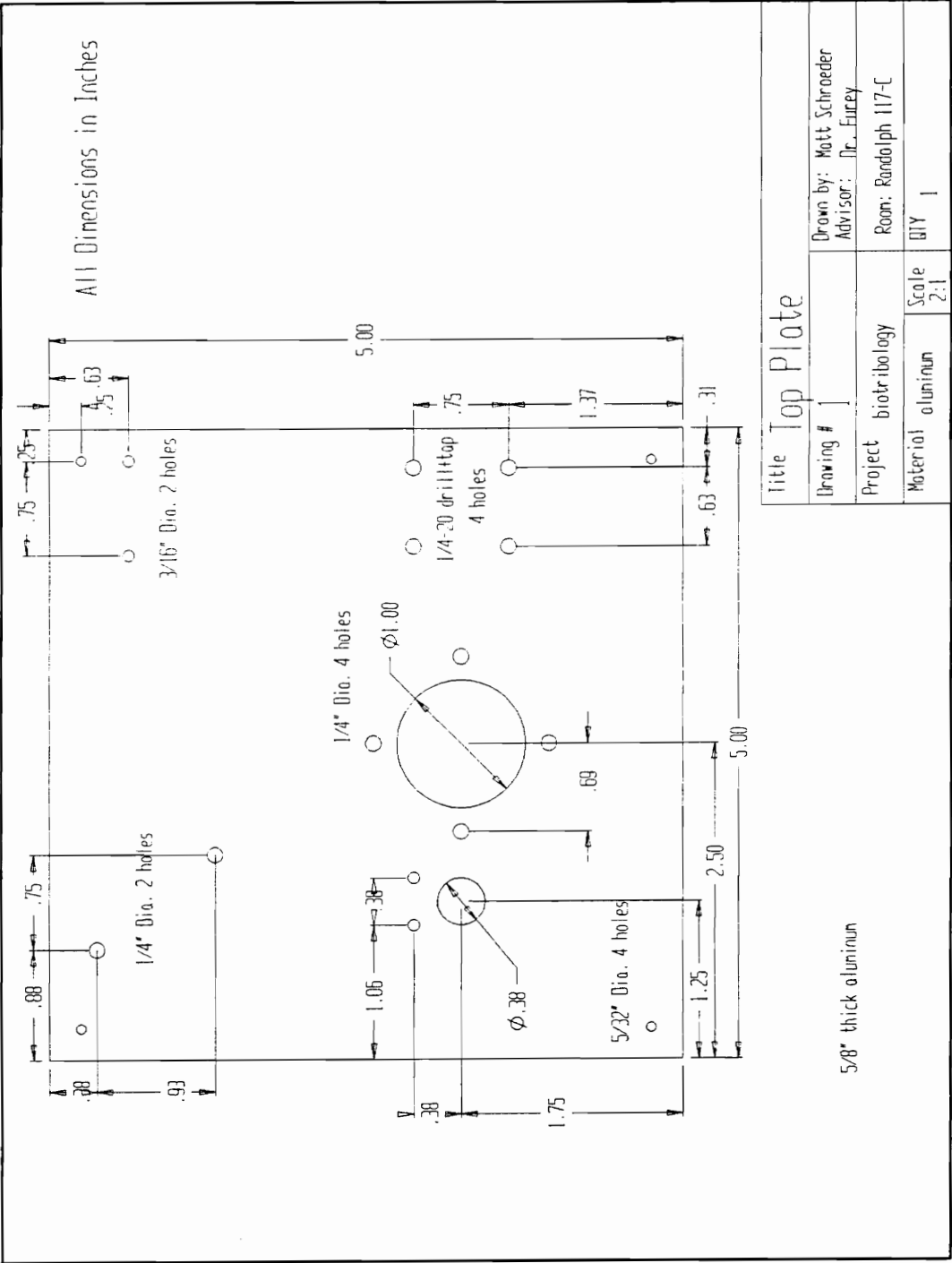


Figure A2 Redesigned Top Plate

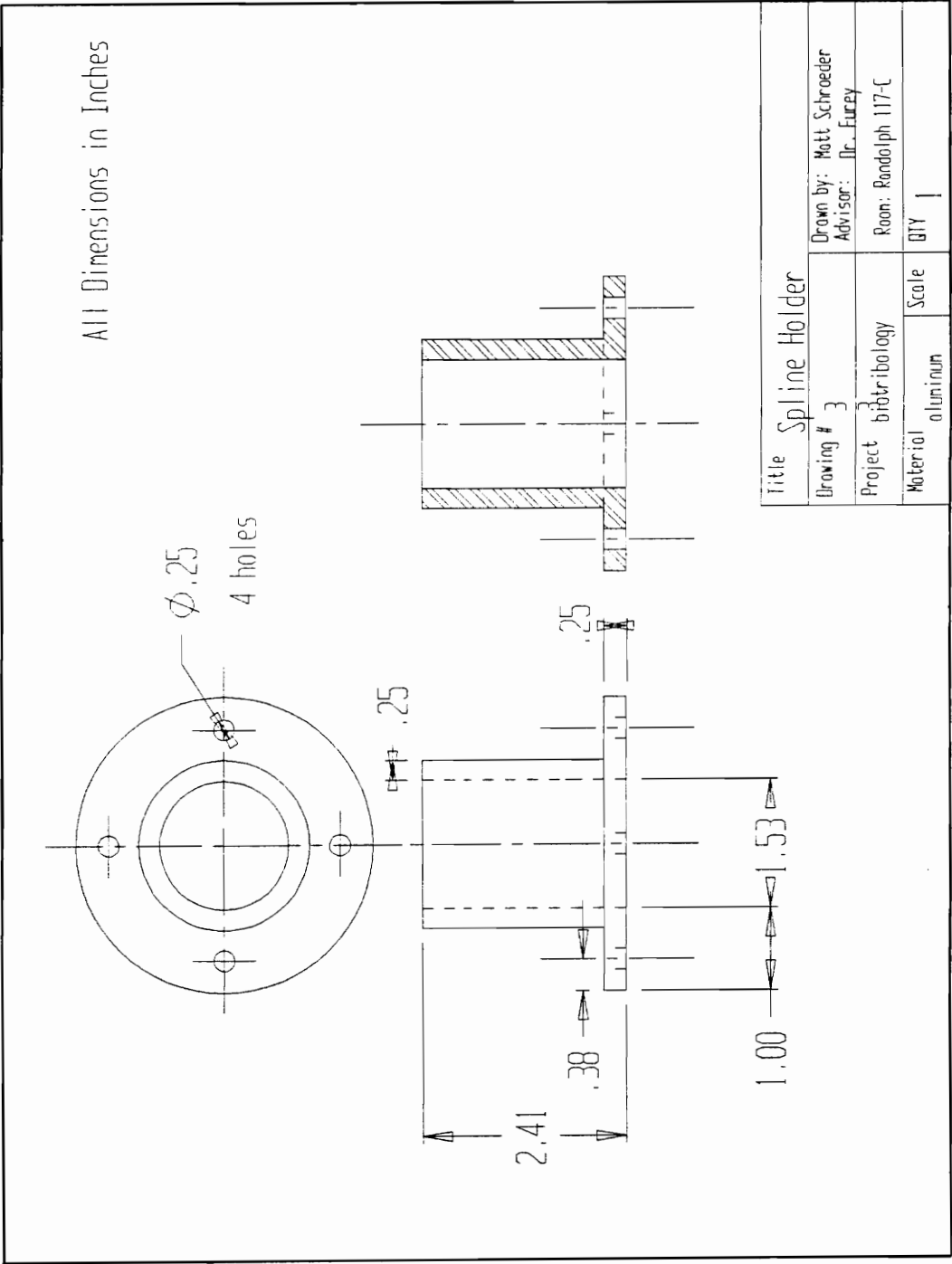


Figure A3 New Shaft Holder

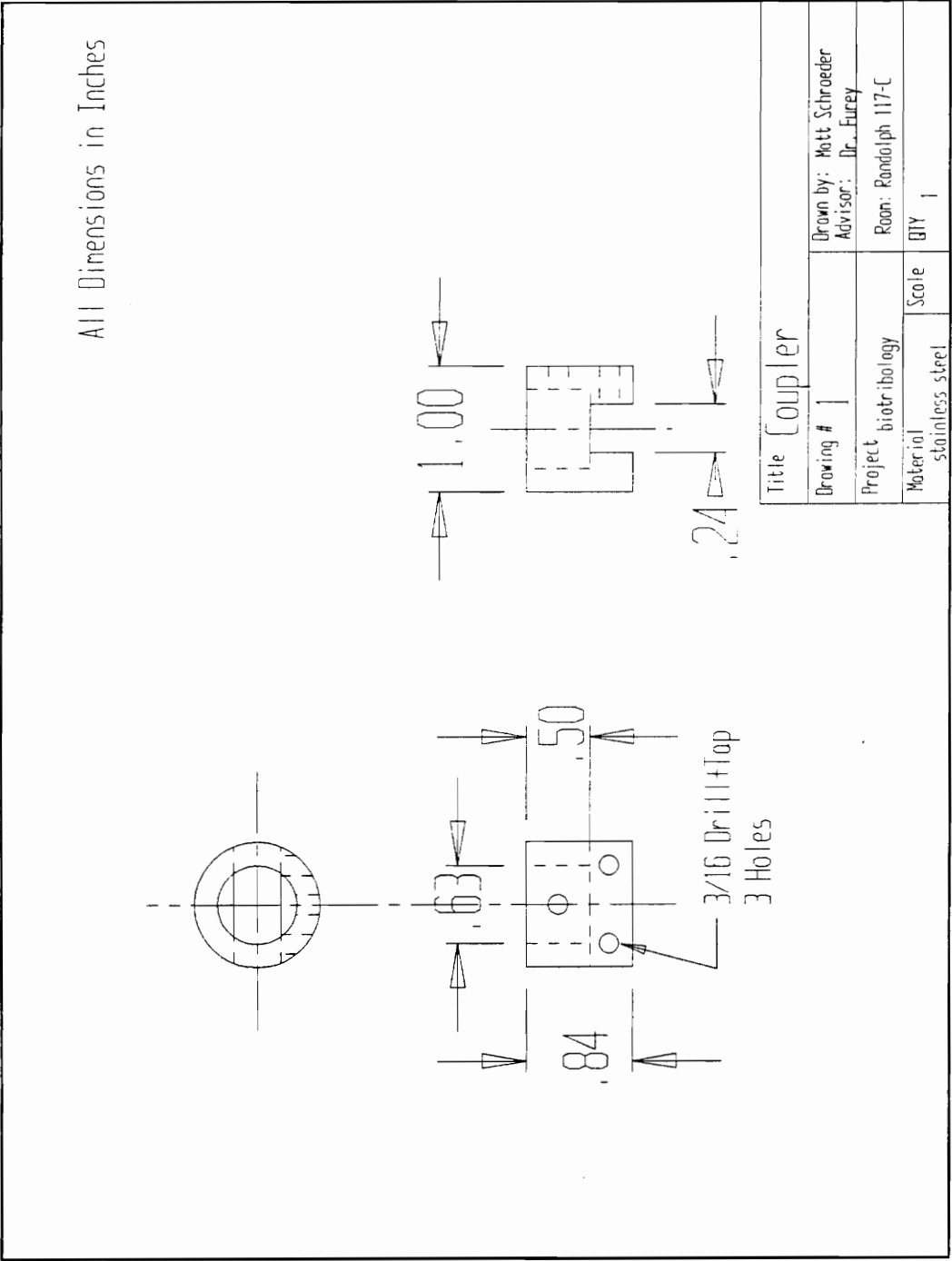


Figure A4 Coupler Between Shaft and Strain Ring

APPENDIX B

BASIC Program Used in All Wear Tests

```
5 REM Test Program for NEAT-310 Motion Controller
6 REM by Michael Owellen, Matt Schroeder
7 CLS
10 PRINT "To avoid damage to the apparatus, please make sure that the upper"
11 PRINT "sample holder is in its uppermost position."
12 PRINT "Hit any key when ready..."
15 GOSUB 20
20 WHILE INKEY$=""
22 WEND
30 OPEN "COM1:4800,N,8,1,RS,CS,DS,CD" FOR RANDOM AS #1 'open serial
    port
40 PRINT #1, "MED" 'make sure mnemonics are disabled
50 GOSUB 180 'wait until asterisk is returned
60 PRINT #1, "MFE" 'make sure move finished is enabled
61 GOSUB 180 'and wait for asterisk
63 PRINT #1, "MH-"
64 GOSUB 150
66 PRINT #1, "MR2000"
69 GOSUB 300
71 PRINT "Lower the sample holder and apply pressure now."
72 PRINT "Hit ENTER to continue."
73 INPUT X
78 PRINT "Enter the number of cycles for the complete test."
79 INPUT NUM
80 FOR I = 1 to NUM 'for-next loop; "num" iterations
81 GOTO 90
82 PERCENT=INT((I/NUM)*100)
83 CLS
84 PRINT "Hit F1 to pause the test for repositioning."
85 PRINT I; "cycles completed."
86 PRINT PERCENT;"% done."
90 PRINT #1, "MR253" '+253 step move
100 GOSUB 150 'wait until motor has stopped
110 PRINT #1, "MR-253" '-253 step move
115 ON KEY(1) GOSUB 300
116 KEY(1) ON
117 KEY(1) ON
120 GOSUB 150
```

```

130 NEXT I
140 END
150 IF INPUT$(1,#1)="F" THEN RETURN 'wait until an "F" arrives
170 GOTO 150 'exit subroutine
180 IF INPUT$(1,#1)="*" THEN RETURN 'wait until 310 ready (sends "**")
190 GOTO 180 'loop per above
300 PRINT "Use arrow keys to reposition sample."
301 PRINT "Type 'R' when the sample is in position, or 'Q' to quit."
310 A$=INKEY$: IF A$="" THEN 310
340 IF LEN(A$)>1 THEN A$=RIGHT$(A$,1)
345 IF ASC(A$)=75 THEN 400
347 IF ASC(A$)=77 THEN 410
350 IF A$="R" OR A$="r" THEN RETURN
355 IF A$="Q" OR A$="q" THEN GOTO 140
370 GOTO 310
400 PRINT #1, "MR-10" : GOSUB 150 : GOTO 310
410 PRINT #1, "MR10" : GOSUB 150 : GOTO 310

```

APPENDIX C

Calibration of Instrumentation

All instrumentation was calibrated before testing began. These calibrations were repeated several times and found to be consistent. The LVDT was calibrated using feeler gages of various thickness to obtain a calibration curve that covered displacements of up to 2 mm. An example of the LVDT calibration is shown in Figure C1. The equation of the line is:

$$\text{Displacement (mm)} = 0.13666 * \text{Voltage(V)}$$

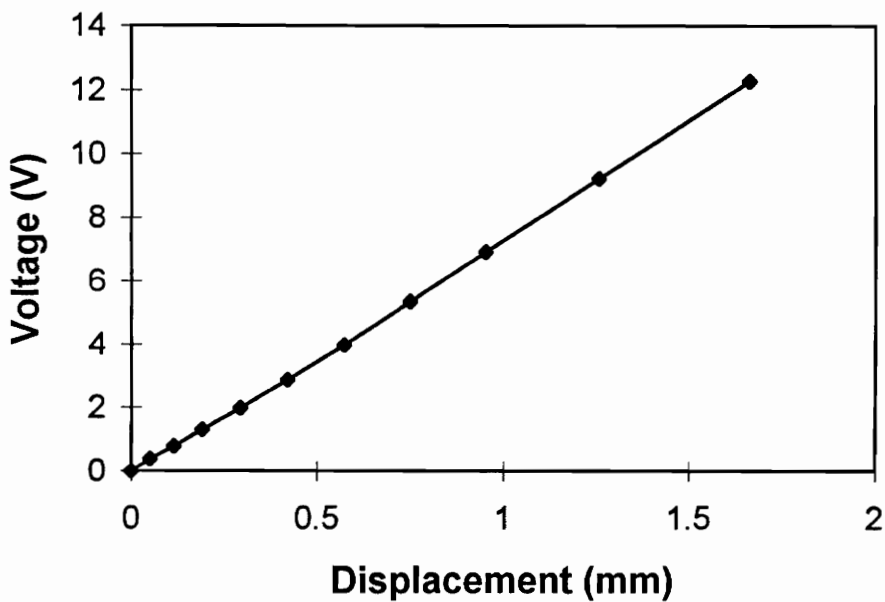


Figure C1 LVDT Calibration Curve

The tangential load was calibrated using weights and a specially designed pulley. The strain ring was calibrated in both directions and found to give an almost perfectly linear response. The tangential readings were calibrated for loads up to 14 N in either direction. The equation of the tangential calibration line was found to be:

$$\text{Force(N)} = -21.771 * \text{Voltage(V)} + 7.0339$$

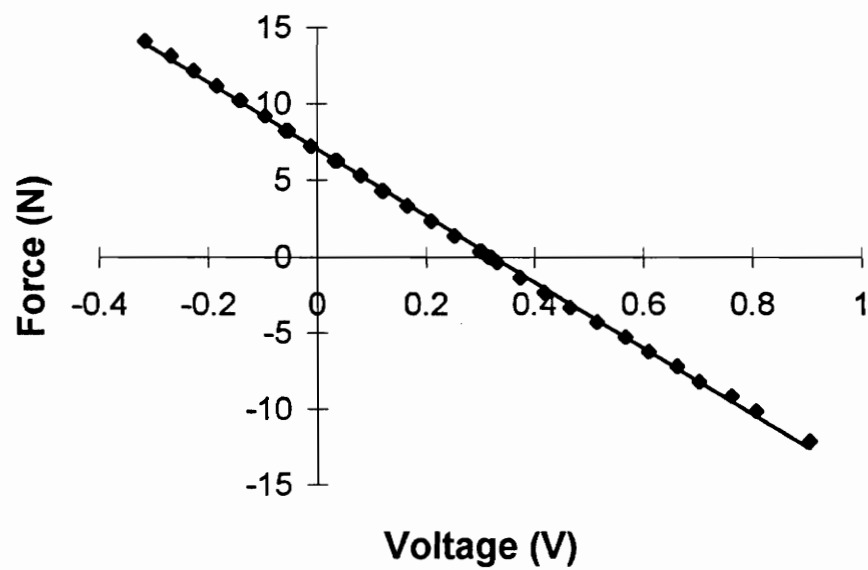


Figure C2 Tangential Calibration Curve

Two separate calibrations were needed for the normal load. First, the strain ring was calibrated up to a load of 92 N. Next, the pressure gage was calibrated up to a pressure of 55 kPa. This way the pressure gage could be used to dial in the required load for each test. Figure C3 is the normal load calibration performed with weights. The actual normal load fluctuated around the average load (63.8 N) during the tests. This fluctuation may have been due to the rocking of the vertical shaft. Minimal cross talk was seen in these calibrations (approx. 2 N for normal and tangential readings). The equation of the calibration line was linear for the values of 20 N to 80 N and was found to be:

$$\text{Load(N)} = 49.394 * \text{Voltage(V)} + 73.032$$

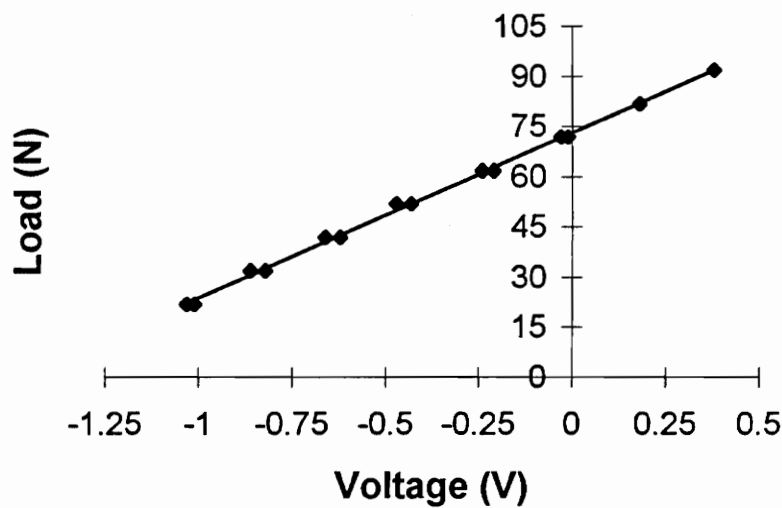


Figure C3 Normal Calibration Using Weights

The gage pressure and strain ring output were calibrated up to 55 kPa.

Figure C4 is a plot of this calibration. The equation of this line is:

$$\text{Voltage (V)} = 0.0521 * \text{Pressure (kPa)} - 2.2375$$

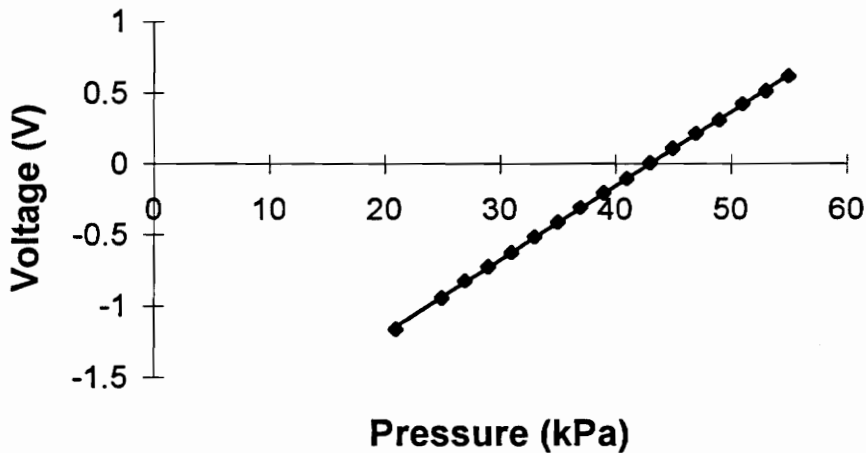


Figure C4 Voltage vs. Pressure Calibration

Finally, pressure and load were related by combining the calibration equations of load vs. voltage and pressure vs. voltage. This resulted in the pressure vs. load relation of:

$$P_g(\text{kPa}) = 0.385 * \text{Load}(\text{N}) + 14.992$$

This equation (valid from 20 to 80 N) is useful for determining the gage reading to achieve a desired load during a test. It should be noted that approximately 20 kPa of gage pressure is required before the cylinder applies pressure to the specimen.

APPENDIX D

Table D.1 contains a description of each test and the corresponding joint that produced the cartilage-bone plugs.

Table D.1 Test Listing

Test	Description	Joint	Wear
6	1 hour saline	P1LK	high
7	1 hour saline	O13LK	high
8	1 hour saline	G14LK	high
9	3 hour saline	O13RK	high
10	1 hour synovial Fluid A	O13LK	low
11	1 hour synovial Fluid B	G14LK	low
12	1 hour serum	O13RK	low
13	1 hour serum	G13LK	high
14	3 hour synovial Fluid C	P7LK	low
15	3 hour synovial Fluid D	G14RK	high
16	3 hour serum	G14RK	low
17	3 hour serum	P1LK	high
18	3 hour saline	G9RK	high

All of the bovine shoulder and stifle joints were obtained from 24 steers on June 16 and 17, 1994. The joints were immediately placed in air tight plastic bags with saline saturated gauze pads and frozen at -25°C. The steers were

designated by ear tag number and color. Each joint was labeled as to type of joint and steer. Shoulder joints were marked with an “S” and stifle joints with a “K”. The letter “R” or “L” indicates right or left leg. The other letters and numbers are the ear tag designations. Table D.2 is a listing of the joints and synovial fluid.

Table D.2 Joint and Synovial Fluid Listing

Steer	Status of Joints	Synovial Fluid
W6	all joints in freezer	freezer
O9	all joints in freezer	freezer
P6	all joints in freezer	freezer
G4	all joints in freezer except RK thrown out	freezer
P12	all joints in freezer except RS thrown out	freezer
W11	all joints in freezer	freezer
O1	all joints in freezer except half of LK	freezer
W1	all joints in freezer	none from RK
G10	all joints in freezer	none from RK
P5	all joints in freezer	none from LK
O12	all joints in freezer	right is extra thick
G13	all joints in freezer except LK used in test	freezer
O10	all joints in freezer	freezer
P7	all joints in freezer except LK used in test	synovial C used in test
G3	all joints in freezer except LS thrown out	freezer
O13	joints used in tests	synovial B used in test
G9	all joints in freezer except RK used in test	freezer
G14	stifles used in tests, shoulders in freezer	synovial A,D used in tests
O2	all joints in freezer	freezer
P14	all joints in freezer	freezer
P1	RK and LK used in tests	thick, in freezer
W12	joints used in preliminary test	mixed with P1 and W9
W9	all joints in freezer	mixed with P1 and W12
W5	all joints in freezer	none

APPENDIX E

Table E.1 contains a description of each test and the corresponding hydroxyproline mass measured from the biochemical assay.

Table E.1 Hydroxyproline Assay Results of Test Washings

Test	Description	Hydroxyproline (µg)
6	1 hour saline	5.29
7	1 hour saline	7.77
8	1 hour saline	10.28
9	3 hour saline	10.00
10	1 hour synovial Fluid A	0.00
11	1 hour synovial Fluid B	0.00
12	1 hour serum	0.00
13	1 hour serum	10.45
14	3 hour synovial Fluid C	0.00
15	3 hour synovial Fluid D	16.27
16	3 hour serum	0.00
17	3 hour serum	5.87
18	3 hour saline	23.42

VITA

The author was born on November 22, 1971 in Bridgeton, New Jersey to Mr. and Mrs. Oskar Schroeder. He graduated Summa Cum Laude with a Bachelor of Science in Mechanical Engineering from the University of Delaware in May of 1993. The following August he began working towards a Master of Science degree in Mechanical Engineering at Virginia Polytechnic Institute and State University. Upon completion of the MS degree, he will work for Medeco Security Locks, Inc. in Salem, Virginia.